

CARDIOVASCULAR MAGNETIC RESONANCE
IN THE PREDICTION OF OUTCOME AFTER
CARDIAC RESYNCHRONISATION THERAPY

by

Dr PAUL WILLIAM XAVIER FOLEY

A thesis submission to University of
Birmingham for the degree of Doctorate
of Medicine

College of Medical and Dental Sciences
The University of Birmingham
June 2011

UNIVERSITY OF
BIRMINGHAM

University of Birmingham Research Archive

e-theses repository

This unpublished thesis/dissertation is copyright of the author and/or third parties. The intellectual property rights of the author or third parties in respect of this work are as defined by The Copyright Designs and Patents Act 1988 or as modified by any successor legislation.

Any use made of information contained in this thesis/dissertation must be in accordance with that legislation and must be properly acknowledged. Further distribution or reproduction in any format is prohibited without the permission of the copyright holder.

ABSTRACT

Contemporary management of patients with heart failure (HF) includes treatment with cardiac resynchronisation therapy (CRT). The benefit of CRT results from several mechanisms, predominantly correction of dyssynchrony. The development of a novel method of measuring left ventricular global dyssynchrony using cardiovascular magnetic resonance (CMR), termed CMR-tissue synchronisation index (CMR-TSI) is described.

A study of 225 patients with HF who underwent CMR-TSI found that HF appears synonymous with dyssynchrony. The importance of myocardial scar is illustrated in a study of 95 patients which revealed a significantly higher mortality in patients undergoing CRT who had postero-lateral (PL) scar on CMR.

A study into the effects of a combination of CMR-TSI and scar imaging found that presence of either CMR-TSI >110 ms or PL scar resulted in a worse outcome, whilst the presence of both was associated with the highest mortality.

A final study in 148 patients allowed the development of a risk score to predict mortality from CRT on the basis of 16 candidate variables. PL scar, dyssynchrony and creatine discriminated between survivors and non-survivors and were used to derive the score.

The score is discussed in the context of data derived from echocardiography and clinical studies.

DEDICATION

I would like to thank the many people who contributed or assisted in this work. Dr Francisco Leyva, Consultant Cardiologist and Reader at the University of Birmingham, for his support, friendship and encouragement throughout. I would also like to thank Dr Russell Smith, Honorary Senior Lecturer at the University of Birmingham for his guidance and wise council.

Dr Shajil Chalil made substantial contributions to the work on cardiovascular magnetic resonance dyssynchrony analysis (CMR-TSI) and was crucial to the development of the CMR-TSI measure. He continued to provide assistance in scan interpretation after he left and has been a good friend throughout my time in research.

Dr Berthold Stegemann, Principle Scientist at the Bakken Research Centre, Maastricht, The Netherlands, I owe a depth of gratitude for his unfailing support and for writing the software which analyses CMR-TSI.

Nick Irwin, Heart Failure nurse at Good Hope Hospital, supported the work throughout and helped with clinical data collection. I would like to thank all the cardiac physiologists at Good Hope, especially Janet Brashaw-Smith, Lisa Ball and Jane Tipping for all their help. The catheter laboratory staff and magnetic resonance radiographers assisted though out with patience and good humour.

Lastly, I would like to thank Helen, my wife, and Ben, my son.

MY CONTRIBUTION

This work was supervised by Dr Francisco Leyva and Professor John Sanderson, Professor of Clinical Cardiology, University of Birmingham. Dr Shajil Chalil was my immediate predecessor as research fellow, and he devised the CMR-TSI technique with Dr Leyva and Dr Stegemann. My work followed on from Dr Chalil's original work and naturally developed from the work already undertaken. Dr Chalil analysed the original 20 controls and 77 patients undergoing CRT. He also devised the database into which patients were entered into the study. My contribution was the recruitment, analysis and clinical follow up of an additional 30 control patients and 148 patients undergoing CRT, whilst continuing the clinical, biochemical and echocardiographic follow up on the original 77 patients. I was involved in the analysis of the CMR scans which were subsequently published. (Chalil et al., 2007a; Chalil et al., 2007b) This Thesis extends the duration of follow up, providing long term data on a substantial cohort of patients undergoing CRT. At the time of writing this is the largest published cohort of patients who have undergone CRT with long term follow up and pre-implant CMR.

The original observations include patchiness of dyssynchrony using radial wall motion bullseyes, relationship between QRS and LV dimensions, the relationship between scar and dyssynchrony, the integration and analysis of CMR-TSI with scar. I obtained the data and was involved in the analysis which resulted in the development of the risk index (DSC) in conjunction with Dr Leyva and Dr Stegemann. The role of pacing scar was confirmed in this larger population over a longer clinical, echocardiographic and events follow up.

TABLE OF CONTENTS

CHAPTER 1. INTRODUCTION	1
1.1.1 Cardiac resynchronisation pacing.....	3
1.2 Clinical studies of CRT.....	5
1.2.1 Baseline characteristics in clinical trials.....	5
1.3 Response to CRT	9
1.3.1 The surface electrocardiogram and CRT.....	11
1.3.2 Role of 12 lead ECG in predicting response to CRT.....	17
1.3.3 Relationship between QRS duration and mechanical dyssynchrony	18
1.3.4 QRS and response to CRT.....	18
1.3.5 Response to CRT in patients with a narrow QRS.....	19
1.4 Diastolic function and diastolic ventricular interaction	20
1.4.1 Reduction of DVI with left ventricular pacing is independent of QRS.....	22
1.5 Echocardiographic assessment of dyssynchrony	23
1.5.1 M-Mode echocardiography	23
1.5.2 Doppler blood pool echocardiography	28
1.5.3 Use of an echocardiographic global measure of dyssynchrony and CRT	29

1.5.4	Tissue Doppler imaging.....	30
1.5.5	Studies of TDI in heart failure patients with narrow QRS	33
1.5.6	Reproducibility of measures of dyssynchrony	33
1.5.7	Predicting response to CRT using TDI.....	34
1.5.8	Studies of CRT in patients with echocardiographic evidence of dyssynchrony regardless of QRS duration.....	34
1.5.9	Prediction of reverse remodelling using TDI	34
1.6	Tissue Doppler strain imaging	37
1.7	Speckle tracking.....	40
1.8	Studies of strain analysis in CRT patients	40
1.8.1	Strain analysis to determine optimal lead position	41
1.8.2	Strain imaging and outcome of CRT	41
1.8.3	Tissue Doppler strain rate compared with tissue velocity imaging.....	41
1.8.4	Echocardiographic Tissue Synchronisation Index.....	45
1.8.5	Real time three dimensional echocardiography (RT3DE).....	45
1.8.6	Echocardiographic studies of dyssynchrony	47
1.8.7	Prospective evaluation of echocardiographic measures of dyssynchrony.....	50
1.8.8	Myocardial Contrast Perfusion Echocardiography.....	51

1.9	Nuclear Imaging – Myocardial Scintigraphy	54
1.9.1	Nuclear Cardiology – Positron Emission Tomography	54
1.10	Endocardial mapping in CRT	55
1.11	Cardiovascular magnetic resonance	56
1.11.1	Myocardial tagging	56
1.11.2	Tagging and Ventricular Interaction.....	71
1.12	Left ventricular torsion analysis.....	75
1.13	Predictors of response	81
1.13.1	Role of dyssynchrony in predicting response	83
1.13.2	Scar Burden on CMR.....	84
1.13.3	B-type natriuretic peptide and response	86
1.14	Summary	87
CHAPTER 2. CARDIOVASCULAR MAGNETIC RESONANCE TISSUE		
SYNCHRONISATION INDEX (CMR-TSI)		
		88
2.1	Introduction.....	89
2.2	Methods.....	91
2.2.1	Cardiovascular magnetic resonance	92
2.3	Figure legends	95

CHAPTER 3. LEFT VENTRICULAR FUNCTION AND RELATION TO
RADIAL DYSSYNCHRONY AND QRS DURATION – A
CARDIOVASCULAR MAGNETIC RESONANCE STUDY 99

3.1 Introduction 100

3.2 Methods 102

 3.2.1 Subjects 102

 3.2.2 Cardiovascular magnetic resonance 102

 3.2.3 Septal to lateral wall motion delay 103

 3.2.4 Spatial Distribution of Dyssynchrony 103

 3.2.5 Scar Imaging 103

 3.2.6 Statistical Analysis 104

3.3 Results 104

 3.3.1 Dyssynchrony and QRS duration 105

 3.3.2 Dyssynchrony and left ventricular function 106

 3.3.3 Spatial distribution of dyssynchrony and QRS duration 107

3.4 Discussion 107

 3.4.1 Left ventricular volumes 108

 3.4.2 Myocardial Scar 108

3.4.3	Relationship between QRS duration and dyssynchrony.....	110
3.4.4	Implications for CRT in narrow QRS.....	112
3.5	FIGURE LEGENDS	114

CHAPTER 4. CMR-TSI PREDICTION OF OUTCOMES AND EVENTS

122

4.1	Introduction.....	123
4.2	Methods.....	124
4.2.1	Subjects.....	124
4.2.2	Echocardiography	124
4.2.3	Cardiovascular Magnetic Resonance.....	125
4.2.4	Device Therapy.....	125
4.2.5	Definition of events	126
4.2.6	Statistics.....	126
4.3	Results.....	127
4.3.1	Baseline Characteristics.....	127
4.3.2	Symptomatic response to therapy	128
4.3.3	Survival after CRT.....	128
4.3.4	Uni-variable and multi-variable predictors of outcome.....	129

4.4	Discussion	129
4.4.1	QRS duration and CMR-TSI	131
4.5	TABLE LEGENDS.....	133
4.6	FIGURE LEGENDS	133
CHAPTER 5. MYOCARDIAL SCAR AND OUTCOME AFTER CRT .		142
5.1	Introduction	143
5.2	Methodology	144
5.2.1	Volume of scar.....	145
5.2.2	Scar location and transmuralit y	145
5.2.3	Device follow up.....	146
5.2.4	Echocardiographic analysis	147
5.2.5	Clinical follow up	147
5.2.6	Determination of site of scar.....	148
5.2.7	Left ventricular lead position.....	148
5.2.8	Determination of effect of pacing scar via the left ventricular lead	151
5.2.9	End points	151
5.2.10	Statistics	152
5.3	Results	152

5.3.1	Effects of PL scar.....	153
5.3.2	Effects of PL scar transmuraliity	154
5.3.3	Effects of pacing PL scar.....	154
5.4	Discussion	155
5.4.1	Pacing PL scar	156
5.4.2	Limitations of the study.....	157
5.5	Table legends:	159
5.6	Figure legends	159
CHAPTER 6. CMR-TSI AND SCAR		170
6.1	Introduction.....	171
6.2	Methods.....	172
6.2.1	Study Design.....	173
6.2.2	Device Therapy.....	173
6.2.3	Cardiovascular Magnetic Resonance.....	174
6.2.4	Tissue Synchronization Index.....	174
6.2.5	Scar Imaging.....	174
6.2.6	Echocardiography	174
6.2.7	Follow up and Endpoints.....	175

6.2.8	Statistical analysis.....	175
6.3	Results	176
6.3.1	Baseline characteristics.....	176
6.3.2	Clinical and echocardiographic data.....	179
6.4	Discussion	179
6.4.1	Dyssynchrony and outcome.....	180
6.4.2	CMR dyssynchrony and outcome – contrast with echocardiographic dyssynchrony	181
6.4.3	Effect of posterolateral scar	181
6.5	TABLE LEGENDS.....	184
6.6	FIGURE LEGENDS	184
 CHAPTER 7. DEVELOPMENT AND VALIDATION OF A CLINICAL INDEX TO PREDICT SURVIVAL AFTER CARDIAC RESYNCHRONISATION THERAPY		
7.1	Introduction.....	196
7.2	Methods.....	197
7.2.1	Patients.....	197
7.2.2	Study design.....	198

7.2.3	Device therapy	198
7.2.4	Cardiovascular magnetic resonance	199
7.2.5	Statistical analysis.....	199
7.2.6	Development of the risk index.....	199
7.2.7	Validation	200
7.2.8	Calculation of the risk index.....	201
7.3	Results	202
7.3.1	Predictor variables	202
7.3.2	Derivation	203
7.3.3	The DSC index	203
7.3.4	Validation	204
7.4	Discussion	204
7.4.1	Role of posterolateral scar	205
7.4.2	Role of dyssynchrony	206
7.4.3	Role of renal function in outcome	206
7.4.4	Limitations of the Study	207
7.5	Summary	208
7.6	Table legends	209

7.7	Figure legend.....	209
CHAPTER 8. CONCLUSIONS.....		218
APPENDIX I. CMR-TSI CALCULATION - WRITTEN BY BERTHOLD STEGEMANN		225
APPENDIX 2: PUBLICATIONS ARISING FROM THESIS		231
LIST OF REFERENCES		232

LIST OF ILLUSTRATIONS

Figure 1-1 Signal averaged ECG from normal patient and patient with dilated cardiomyopathy and left bundle branch block pattern	15
Figure 1-2 Effect of lower body negative pressure on diastolic ventricular interaction	21
Figure 1-3 Measuring septal to posterior wall motion delay	25
Figure 1-4 Kaplan-Meier survival curves for patients with septal to posterior wall motion delay	27
Figure 1-5 Dyssynchrony measured with TDI in patients with narrow and wide QRS HF and controls	32
Figure 1-6 Relationship between dyssynchrony and change in LVESV	36
Figure 1-7 Example of possible error in strain imaging – the impact of angulation on strain rate imaging.	39
Figure 1-8 Typical velocity, strain rate and strain curve from the mid septum in LBBB ...	43
Figure 1-9 Velocity and strain curves before and after CRT	44
Figure 1-10 Contrast echocardiography in the detection of dyssynchrony	53
Figure 1-11 Analysis of a CMR tagged image	58
Figure 1-12 Vertical tags at two time points during the cardiac cycle	59
Figure 1-13 Central slab of the Fourier transform magnitudes taken from Figure 1-12	59
Figure 1-14 Harmonic magnitude images taken from figure 1-13	60
Figure 1-15 Mask derived from the harmonic magnitude images from figure 1-14	60
Figure 1-16 Harmonic phase images (masked).	61
Figure 1-17 Annular mesh style tagged image	62

Figure 1-18 A sequence of Eulerian strain maps from a Canine heart.....	64
Figure 1-19 Mechanical dyssynchrony measured using temporal uniformity of strain, regional variance of strain and regional variance vector (combining strain magnitude and location)	67
Figure 1-20 Mechanical activation maps for atrio-LBBB, atrio-biventricular and atrio-left ventricular pacing.	69
Figure 1-21 Electrical activation map derived from nylon mesh electrode array	70
Figure 1-22 Time-dependent plots of cardiac dyssynchrony and resolution of dyssynchrony	74
Figure 1-23 Myocardial velocity sampling regions and velocity profiles for LV rotation measurements (apical level).	76
Figure 1-24 LV rotation profile by CMR and TDI in representative case.	77
Figure 1-25 Scar imaging and response to CRT.....	85
Figure 2-1 Division of the left ventricular myocardium into slices.....	96
Figure 2-3 Wall motion over time	97
Figure 2-4 Three dimensional representation of the mechanical activation of the left ventricle in control.....	98
Figure 2-5 Three dimensional representation of the mechanical activation of the left ventricle in patient with HF and LBBB.....	98
Figure 3-1 CMR-TSI and QRS duration	117
Figure 3-2 Correlation between CMR-TSI and QRS duration.....	118
Figure 3-3 Regression analyses of CMR-TSI against parameters of left ventricular function	119
Figure 3-4 CMR-TSI in relation to scar size	120

Figure 3-5 Bull's eye maps of radial wall motion	121
Figure 4-1 Kaplan-Meier estimates of the time to the death	141
Figure 5-1 Determination of left ventricular lead position using fluoroscopy	150
Figure 5-2 Kaplan-Meier survival graphs of outcome of transmural PL scar vs non-transmural PL scar	168
Figure 5-3 Kaplan-Meier survival graph of effect of pacing myocardial scar on outcome	169
Figure 6-1 Kaplan-Meier estimates of the time to the various clinical endpoints.....	193
Figure 6-2 Kaplan Meier stratified according to ICM vs NICM.....	194
Figure 7-1 Kaplan-Meier estimates of the time to cardiovascular death.....	214
Figure 7-2 Calibration of predictions of mortality after cardiac resynchronisation therapy	215
Figure 7-3 Receiver-operator characteristic curves of the DSC index against cardiovascular mortality at 1 and 2 years, and at the end of the follow-up period.....	216
Figure 7-4 Comparison of events in the present cohort and in the CARE-HF study	217

LIST OF TABLES

Table 1-1 The baseline entry parameters of patients entered into trials of CRT.....	7
Table 1-2 Comparison of the onset of left ventricular contraction in controls vs LBBB measured using signal average ECG (ms).....	13
Table 1-3 Table showing mean relative time intervals from Q wave to onset of wall motion measured using M mode echocardiography	16
Table 1-4 Clinical measures of dyssynchrony used in studies of CRT.	48
Table 1-5 Methods of Determining Strain – Echo and MRI studies	78
Table 3-1 Clinical, electrocardiographic and magnetic resonance characteristics for patients included in the study, grouped according to QRS duration.	115
Table 4-1 Baseline clinical and cardiovascular magnetic resonance imaging characteristics for patients undergoing cardiac resynchronisation therapy	134
Table 4-2 Clinical and echocardiographic outcome at baseline and last available follow up	136
Table 4-3 Uni variable and multi-variable Cox proportional hazards analyses of clinical endpoints in relation to cardiac magnetic resonance variables according to imaging modality	138
Table 5-1 Baseline clinical and cardiovascular magnetic resonance characteristics of the study group	160
Table 5-2 Baseline and last available clinical and echocardiographic parameters according to presence or absence of posterolateral scar.....	162

Table 5-3 Baseline and last available clinical and echocardiographic parameters according to presence or absence of PL scar.....	164
Table 5-4 Baseline and last available clinical and echocardiographic parameters according to either non-transmural or transmural posterolateral scar	165
Table 5-5 Univariate Cox proportional hazard analyses of clinical magnetic resonance variables in relation to clinical endpoints	166
Table 6-1 Baseline clinical and cardiovascular magnetic resonance imaging characteristics	185
Table 6-2 Clinical endpoints for patients undergoing CRT in relation to PL scar	187
Table 6-3 Uni-variable Cox proportional hazards analyses of clinical endpoints.....	188
Table 6-4 Clinical and echocardiographic variables during follow-up in patients undergoing cardiac resynchronisation therapy, grouped according to degree of dyssynchrony and presence of posterolateral scar at baseline.....	191
Table 7-1 Clinical characteristics of the study patients, grouped according to survival status at the end of the study period.....	210
Table 7-2 Univariate Cox proportional hazard analyses of predictors of mortality	212
Table 7-3 Final model from bootstrapped stepwise multivariate Cox proportional hazard analyses of predictors of mortality	213

LIST OF ABBREVIATIONS

2D	Two dimensional
3D	Three dimensional
6MWD	Six minute walk distance
ACC	American College of Cardiology
ACEI	Angiotensinogen converting enzyme inhibitor
AF	Atrial fibrillation
AHA	American Heart Association
AIB	Angiotensin II inhibitor
AV	Atrio-ventricular
AVC	Aortic valve closure
AVO	Aortic valve opening
BiV	Biventricular
BNP	B type natriuretic peptide
CABG	Coronary artery bypass graft

CARE-HF	Cardiac resynchronisation in heart failure trial
CI	Confidence interval
CMR	Cardiovascular magnetic resonance
CMR-LVEDV	Cardiovascular magnetic resonance left ventricular end diastolic volume
CMR-LVESV	Cardiovascular magnetic resonance left ventricular end systolic volume
CMR-TSI	Cardiovascular magnetic resonance tissue synchronisation index
CO	Cardiac output
CRT	Cardiac resynchronisation therapy
CRT-D	Cardiac resynchronisation defibrillator
CRT-P	Cardiac resynchronisation pacemaker
CSPAMM	Complimentary spatial modulation of magnetisation
CURE	Circumferential uniformity ratio estimate
D-PEP	Left ventricular post ejection period minus right ventricular post ejection time
DCM	Dilated cardiomyopathy
DICOM	Digital Imaging and communication in medicine standards

dP/dt	Ratio of change in pressure over time
DSC	Dyssynchrony Scar Creatinine
DVI	Diastolic ventricular interaction
ECG	Electrocardiogram
EF-CMR	Ejection fraction measured using CMR
FUP	Follow up
HF	Heart failure
HR	Hazard ratio
ICM	Ischaemic cardiomyopathy
IHD	Ischaemic heart disease
IVCT	Isovolumic contraction time
IVT	Isovolumic time
LBBB	Left bundle branch block
LV	Left ventricle
LVEDD	Left ventricular end diastolic volume
LVEF	Left ventricular ejection fraction
LVESV	Left ventricular end systolic volume
MCE	Major cardiovascular events

MIRACLE	Multicentre Insync Randomised Clinical Evaluation trial
ms	Milliseconds
MUSTIC	Multisite Stimulation in Cardiomyopathies trial
NICM	Non-ischaemic cardiomyopathy
NYHA	New York Heart Association class
PCWP	Pulmonary capillary wedge pressure
PET	Positron emission tomography
PL	Postero-lateral
PROSPECT	Prospective evaluation of echocardiographic measures of dyssynchrony study
PSI	Perfusion score index
QRS	QRS on ECG
RT3DE	Real time three dimensional echocardiography
RVVPS	Regional variance of vector strain
S0	No dyssynchrony
S1	Maximum dyssynchrony
SD	Standard deviation
SDI	Systolic dyssynchrony index

SLWMD	Septal to lateral wall motion delay
SPAMM	Spatial modulation of magnetisation
SR	Sinus rhythm
SSFP	Steady state in free precession
SV	Stroke volume
<i>T</i>	Time
TDI	Tissue Doppler Imaging
TSI	Tissue synchronisation index
TVI	Tissue Velocity Imaging

CHAPTER 1. INTRODUCTION

INTRODUCTION

Systolic heart failure was first described by the Egyptians, believed to be around 3000 BC. (Saba et al., 2006) The Edwin Smith Papyrus described “his heart (his spirit or his mind) is too weary to speak. His heart beats feebly.”

Worldwide systolic heart failure is an important cause of morbidity and mortality. Pharmacological treatment has been refined and implemented. However, despite excellent pharmacological treatment, many patients remain highly symptomatic and at risk of premature death. Over the last decade, cardiac resynchronisation therapy has emerged as a valuable treatment, substantially reducing morbidity and mortality in selected patients. (Cleland et al., 2005b)

Cardiac resynchronisation therapy is thought to exert its effect by several mechanisms, of which the main mechanism is improving the co-ordination of left ventricular contraction in patients who have dyssynchrony. Dyssynchrony was first recognised in patients with cardiomyopathy and bundle branch block, who were noted to have delay in the contraction of the posterior wall relative to the septum on m-mode echocardiography in 1994. (Xiao et al., 1994) The presence of bundle branch block identified electrical delay in conduction results in mechanical delay in contraction.

Electrical delay is significant as it identifies a population of patients with heart failure who are at high risk of mortality. The presence of left bundle branch block is associated with a higher mortality in patients with heart failure. (Baldasseroni et al., 2002)

Furthermore, prolongation of the QRS is associated with adverse left ventricular

haemodynamic performance. An inverse relationship between QRS duration and left ventricular end diastolic pressure has been found. (Burkhoff et al., 1986) Furthermore, prolonged QRS has been shown to have other adverse consequences, resulting in diastolic mitral regurgitation, and reduced cardiac output.

1.1.1 Cardiac resynchronisation pacing

The demonstration of the relationship between poor left ventricular systolic function with prolonged QRS duration resulting and adverse outcomes lead to attempts to pre-excite myocardial areas using pacing, which became known as “resynchronisation”. The aim of resynchronisation is to restore the normal conduction and hence the normal mechanical activation.

Potentially, resynchronisation pacing could result in improved left ventricular function by improving left ventricular co-ordination, thus improving dyssynchrony. The first testament to this was in patient who underwent temporary biventricular pacing having failed to respond to other therapies. The patient was found to have such a dramatic improvement in haemodynamics that a permanent system was implanted. (Cazeau et al., 1994) The patient’s breathing improved from NYHA class IV to II.

Since that time, CRT has been shown in large multi-centre randomised studies to improve quality of life and survival in selected patients with moderate to severe systolic heart failure. (Bristow et al., 2004, Cleland et al., 2005b) Overall, CRT is estimated to result in a 26% reduction in mortality and 22% reduction in hospitalisation for heart failure. (Cleland et al., 2005b) CRT has been shown to be cost effective in heart failure patients. (Caro et al., 2006)

The physiological benefits of cardiac resynchronisation in patients with heart failure can be dramatic. As a result of resynchronisation, cardiac output is increased. (Duncan et al., 2003) Systolic blood pressure and maximum rates of left ventricular pressure rise improve.

In patients with mitral regurgitation, CRT can improve the function of the papillary muscles, immediately reducing mitral regurgitation. (Kanzaki et al., 2004) Over time, the adverse geometric changes that occur in patients with heart failure are reversed achieving with reverse remodelling and improved ejection fraction. (Yu et al., 2005b) As a result of left ventricular remodelling, the loss of mitral valve coaptation can be reversed, resulting in reduction of mitral valve regurgitation.

Whilst CRT is a highly successful treatment for selected patients with heart failure some patients do not report improvements in symptoms. It is unclear how to determine which patients with heart failure will have symptomatic improvement following CRT, as not all do. Imaging techniques which can identify patients who will benefit from CRT could be used to exclude patients who do not gain a symptomatic or survival benefit. (Sanderson, 2009) Increasingly, clinicians and purchasers are looking towards advanced imaging to predict outcome from CRT.

Cardiac resynchronisation therapy often results in a noticeable improvement in symptoms, such that an absence of symptomatic improvement can be regarded as a failure of therapy, or “non-response”. In addition, CRT results in left ventricular remodelling and some authors propose that a response to CRT in terms of improvement in left ventricular function implies a survival advantage, and the therapy is not effective if a significant improvement in left ventricular function is not seen. (Yu et al., 2005b)

However, clinical trials have failed to identify a sub-group who do not benefit from CRT. (Cleland et al., 2008b)

Furthermore, there is discordance between the symptomatic response and survival benefit from CRT. (Foley et al., 2008) Indeed patients who demonstrate reverse remodelling may not demonstrate a survival benefit. (Yu et al., 2005b)

The aim of this thesis is to determine whether pre-implant cardiac magnetic resonance can predict response to CRT. Cardiac magnetic resonance (CMR) has many advantages over echocardiography for determination of both the aetiology of heart failure, left ventricular volume assessment and prognosis in patients not treated with CRT. Using CMR to assess response to cardiac resynchronisation is novel.

1.2 Clinical studies of CRT

1.2.1 Baseline characteristics in clinical trials

Large scale randomised clinical trials of CRT have used similar selection criteria. These include impaired ejection fraction, NYHA class II to IV and evidence of broad QRS duration (greater than 120 ms). Overall, all these studies have shown benefit in terms of symptomatic response (see Table 1-1).

Suspicion that the selection of patients could be improved to increase the benefit of CRT by excluding those deemed not likely to benefit has led to the application of novel imaging techniques. Sophisticated echocardiographic methods of dyssynchrony have been used to determine if these could improve selection of patients.

As yet no randomised studies have enrolled patients on the basis of echocardiographic criteria alone, although a study of echocardiographic predictors of response to CRT (PROSPECT study) has reported. (Chung et al., 2008) Additionally, a major randomised clinical trial of patients with narrow QRS (≤ 130 ms), a group excluded from current guidelines, has reported. In this study, patients were selected on the basis of the presence of sufficient mechanic dyssynchrony, measured using tissue Doppler (RETHINQ). (Beshai et al., 2007) The details of the studies are discussed below (see Table 1-1).

Table 1-1 The baseline entry parameters of patients entered into trials of CRT.

	MUSTIC Cazeau et al., 2001)	PATH -CHF Auricchio al., 2002)	MIRACLE Abraham al., 2002)	MIRACLE-ICD (Young et al., 2003)	CONTAK (Higgins et al., 2003)	COMPANION (Bristow et al., 2004)	CARE-HF Cleland al., 2005b)
No.	67	36	453	369	490	1520	813
Device	CRT-P	CRT-P	CRT-P	CRT-D	CRT-D	Both	CRT-P
Rhythm	SR	SR	SR	SR	SR	SR	SR
NYHA class	III	III, IV	III, IV	III, IV	II, III, IV	III, IV	III, IV
NYHA class distribution, %	100	86/14	91/9	89/9	33/59/8	85/15	94/6
IHD or DCM	Both	Both	Both	Both	Both	Both	Both
Distribution, %	37/63	29/71	54/46	70/30	69/31	55/45	38/62
QRS, ms	150	120	130	130	120	120	>120
Mean ± SD, ms	176 ± 19	175 ± 32	166 ± 20*	164 ± 22*	158 ± 26*		
LVEF	0.35	N/A	0.35	0.35	0.35	0.35	0.26
Mean ± SD	0.23 ± 7	0.21 ± 7	0.22 ± 6.3*	0.24 ± 0.06*	0.21 ± 7*	0.22	0.25
LVEDD, mm	60	N/A	55	55	N/A	N/A	NA

Mean ± SD, mm	73 ± 10	73 ± 11	69 ± 10*	76 ± 10*	71 ± 10*	67	72
6-Min walk, m	N/A	N/A	450	450	N/A	N/A	NA
Mean ± SD, m	320 ± 97	357 ± 20	298 ± 93*	243 ± 123*	318 ± 120*	262	NA

*SD is estimated from data provided in citation.

Median value is shown

CRT-P = cardiac resynchronisation pacemaker. CRT-D = cardiac resynchronisation pacemaker with defibrillator. QRS is QRS duration. NYHA class = New York health association Class. 6 minute walk test is the distance walked in 6 minutes. LVEF = left ventricular ejection fraction. LVEDD = left ventricular end diastolic diameter.

1.3 Response to CRT

The magnitude of any treatment effect will vary between patients depending on host factors including the severity of the underlying condition. Measuring effectiveness is difficult beyond binary measures such as mortality. However, the response to therapy is well recognised in other field of medicine, such as response of cancers to chemotherapy, (Dose Schwarz et al., 2005) and in the field of acute myocardial infarction after revascularisation in terms of ST segment change, cardiac biomarker release and left ventricular function. (Markis et al., 1981)

The use of the term response in patients treated with CRT is controversial. The identification of non-responders is often made difficult by the absence of control patients in clinical studies. (Cleland et al., 2009) Clinical studies suggest that there is no evidence that patients who do not gain a symptomatic response or evidence of reverse remodelling are worse off after CRT, and clinical trials suggest that all patients meeting current criteria gain a mortality advantage. (Cleland et al., 2008b) However, in the field of CRT, “response to therapy” is regularly measured in clinical studies, which may simply be a reflection of the dramatic effectiveness of CRT to improve some patients’ symptoms. Heart failure treatments can improve symptoms without necessarily having an effect on mortality.

Clinical response to diuretics is well characterised in terms of loss of oedema, but the long term change in condition after initiation of prognostic heart failure medication is not discussed in routine or research clinical practice. Hence, the term “response” used in the context of treatment with CRT is almost unique and is not discussed in relation to other

prognostic treatments of HF, such as angiotensinogen converting enzyme inhibitors (ACEI) or beta blockers.

Clinical response is commonly assessed by measuring exercise tolerance in terms of six minute hall walk distance and symptom score using both the NYHA class and the Minnesota living with heart failure questionnaire. (Rector, 2005) Clinical response is usually defined as an increase in 6 minute walk time by 25% or a reduction in NYHA class by one or more. (Chung et al., 2008) Additionally, a reduction in Minnesota living with heart failure score by 10 points has been used in some studies as an indicator of clinical response. (Gras et al., 1998)

Reverse left ventricular remodelling is well described after CRT. Echocardiographic response has been used in some studies as an endpoint, and has been defined as reflecting a reduction of the left ventricular end systolic volume by 15%. (Chung et al., 2008)

Dichotomising groups of patients as responders and non-responders is common in clinical studies. (Bleeker et al., 2006a) However, the so-called non-response is relative to other patients treated with CRT, rather than controls. Therefore, non-response does not exclude benefit from CRT.

Failure to demonstrate either clinical or echocardiographic response to CRT is multifactorial. Reverse left ventricular remodelling after CRT appears to be greater in patients with dilated cardiomyopathy (DCM) compared with patients with previous myocardial infarction (Duncan et al., 2003) and a history of ischaemic heart disease is associated with a worse outcome after CRT. (Zhang et al., 2009)

Response may be affected by the viability of the myocardium. Studies into response to revascularisation (Kim et al., 2000) and beta blockers (Bello et al., 2003) have shown that sufficient viable myocardium is required to obtain a response from these treatments. Two small studies into patients undergoing CRT have suggested that the position of the scar as well as the volume of viable myocardium may be implicated. (Bleeker et al., 2006c, White et al., 2006)

1.3.1 The surface electrocardiogram and CRT

Initial studies into CRT required a broad QRS duration as a criterion for inclusion. Prolonged QRS duration (greater than 120 ms) is a marker of delayed ventricular depolarisation and is a surrogate for mechanical dyssynchrony. Patients with left ventricular dilation and impairment have worse outcome than those with normal function. (Grines et al., 1989, Xiao et al., 1996) A study of 5517 heart failure outpatients found that the presence of left bundle branch block (n = 1391) was associated with increased 1 year mortality (hazard ratio (HR), 1.70) and sudden death (HR 1.58). (Baldasseroni et al., 2002)

Patients with left bundle branch block (LBBB) have delay in left ventricular activation, contraction and relaxation due to the reversal of the normal sequence of ventricular activation. (Grines et al., 1989) 18 subjects who were found to have incidental LBBB were examined. The subjects had normal size hearts on echocardiography, and no regional wall motion abnormalities. Ten controls were compared with those with LBBB. The onset of anterior and posterior wall contraction was timed from the onset of the QRS complex on M-mode ultrasound, and the septal position measured in relation to the

maximal left ventricular ejection period (see Table 1-2). The timing of the contraction of the left and right ventricles was assessed using radionuclide imaging.

Table 1-2 Comparison of the onset of left ventricular contraction in controls vs LBBB measured using signal average ECG (ms).¹

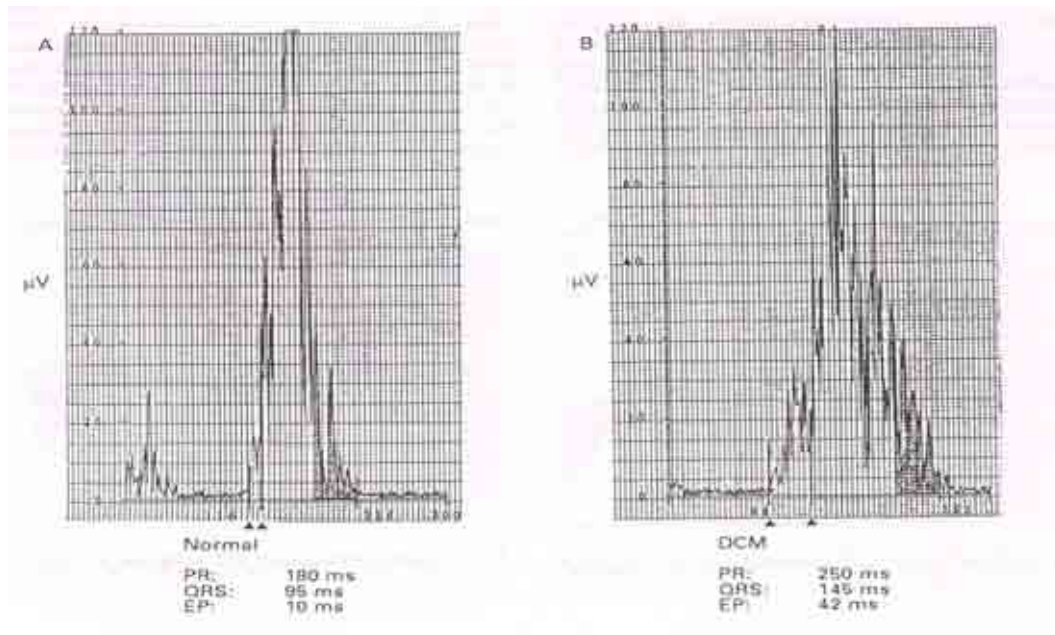
	Left bundle branch block (ms)	Controls (ms)	P
Q to apex	72 ± 20	35 ± 12	0.0005
Q to posterior wall contraction	165 ± 25	122 ± 22	0.0001
Delay between RV and LV contraction	85 ± 31	6 ± 9	0.0001

¹ Reproduced from Grines, C.L., Bashore, T.M., Boudoulas, H., et al. (1989) Functional abnormalities in isolated left bundle branch block. The effect of interventricular asynchrony. **Circulation**, 79: (4): 845-853.

The period of isovolumic contraction was similar in controls (62 ms) and patients with left bundle branch block (68 ms), although the later group had a wider range which implies delay in activation of the ventricle. 15 of the 18 patients had intra-ventricular asynchrony, with septal contraction occurring prior to posterior, and one patient had paradoxical septal motion. Right ventricular contraction was delayed in patients with LBBB in comparison to the controls. Radionuclide imaging showed that whilst the apical and lateral walls contracted normally, the inter-ventricular septum contribution to ejection fraction was reduced ($40\% \pm 16$ compared with $67 \pm 7\%$, $p < 0.001$).

Patients with dilated hearts and LBBB pattern have delay in activation of the lateral wall of the left ventricle on m-mode echocardiography compared with controls. (Xiao et al., 1994) This study was a landmark study which initiated the interest in both the assessing and treatment of dyssynchrony. 77 patients with dilated left ventricles, with diastolic left ventricular diameter greater than 6mm and fractional shortening less than 15% were included. The time to contraction was measured from the onset of the R wave. The QRS duration was longer in patients with dilated hearts ($127 \text{ ms} \pm 25$) vs. normal sized hearts ($90 \text{ ms} \pm 10$, $p < 0.05$). Patients with dilated hearts had delayed activation of the free wall whether there was intra-ventricular conduction delay (110 - 120 milliseconds, or > 120 ms with septal q wave) or LBBB (see Figure 1-1, Table 1-3).

Figure 1-1 Signal averaged ECG from normal patient and patient with dilated cardiomyopathy and left bundle branch block pattern



The arrows mark the early potential time. Y axis = micro volts, x axis = time.²

² Reproduced from Xiao, H.B., Roy, C. and Gibson, D.G. (1994) Nature of ventricular activation in patients with dilated cardiomyopathy: evidence for bilateral bundle branch block. **Br Heart J**, 72: (2): 167-174 with permission from BMJ Publishing Group Ltd.

Table 1-3 Table showing mean relative time intervals from Q wave to onset of wall motion measured using M mode echocardiography

	Normal	RBBB	Intra-ventricular conduction defect	Left bundle branch block
	(n = 15)	(n = 6)	(n = 29)	(n = 20)
Q to septal thickening SD (ms)	75 (15)	75 (15)	43 (14)*	43 (12)*
Corrected Q to septal thickening SD (ms)	82 (12)		75 (12)	78 (15)
Septum to LV posterior wall SD (ms)	30 (13)	35 (15)	85 (30)*	100 (25)*
Septum to left free wall SD (ms)	20 (12)	27 (25)	95 (30)*	100 (30)*
Septum to right free wall SD (ms)	20 (14)	75 (10)*	65 (25)*	65 (12)*

Corrected Q to septal thickening = signal averaged ECG Q wave to septal thickening. $P < 0.01$ vs. normal.³

³ Reproduced from Xiao, H.B., Roy, C. and Gibson, D.G. (1994) Nature of ventricular activation in patients with dilated cardiomyopathy: evidence for bilateral bundle branch block. *Br Heart J*, 72: (2): 167-174 with permission from BMJ Publishing Group Ltd.

This study suggests that the onset of QRS complex does not mark the onset of ventricular activation. The signal averaged ECG is able to detect small voltage potentials which are too small for the 12 lead ECG. These lasted up to 25 ms in controls, and up to 60 ms in patients with dilated left ventricles. Furthermore, all patients with dilated hearts had delay in the longitudinal motion of the right atrio-ventricular junction on M mode, similar to patients with right bundle branch block.

1.3.2 Role of 12 lead ECG in predicting response to CRT

The twelve lead ECG has shortcomings which may limit the ability to determine response to CRT. The correlation between QRS duration and acute response to CRT is modest ($r = 0.6$). (Bleeker et al., 2004) In addition, QRS duration does not predict outcome from CRT. (Molhoek et al., 2004) A 12 lead ECG does not accurately determine the onset of ventricular contraction when compared with signal averaged ECGs. (Xiao et al., 1994) In addition, neither the mass of myocardium affected by the dyssynchrony or the site of latest activation can be determined. Comparison of ECG and tissue Doppler imaging (TDI) has found disagreement in 20 to 50% of patients regarding the presence of dyssynchrony. (Achilli et al., 2003)

1.3.3 Relationship between QRS duration and mechanical dyssynchrony

The relationship between dyssynchrony and QRS does not appear consistent when examined with TDI. (Bleeker et al., 2004) The left ventricular volumes at baseline were related to the QRS duration. The greater the size of the left ventricle, the wider the QRS duration. The QRS duration did not correspond with difference in the time of peak velocity between the septal and the lateral wall delay on tissue Doppler. It was found that 30 - 40% of patients with a broad QRS duration did not have dyssynchrony; whilst 27% of those with QRS duration of less than 120ms had dyssynchrony when using tissue Doppler based criteria.

1.3.4 QRS and response to CRT

QRS duration does not appear to predict response to CRT. (Molhoek et al., 2004) In a study of 61 patients, the reduction in QRS duration in responders between baseline and 6 months was not significantly different from the non-responders (20 ± 29 ms vs. 3 ± 38 ms, $p = 0.08$). Using receiver operator characteristic analysis, the optimum cut-off value for predicting response was a QRS reduction of 30ms (sensitivity 56%, specificity 56%). In summary, a reduction in QRS duration is not suggestive of a response to CRT due to its modest sensitivity and specificity.

CRT may be effective in patients with narrow QRS. Achilli et al. compared the effect of CRT in patients with wide QRS duration, and 14 patients with normal (< 120 ms) duration. (Achilli et al., 2003) There was no significant difference in mortality between the groups 21.4% vs. 18.4% ($p = 1$). There were no significant differences in the change of echocardiographic parameters of dyssynchrony in both groups at follow up. This

study supports the concept that QRS duration alone does not predict response to CRT, and that heart failure patients with a normal QRS may respond to CRT.

In summary, the ECG does not determine the onset of ventricular activation, and a wide QRS duration may not ensure benefit from CRT. The ECG may be too blunt a tool to determine which patients with heart failure should receive CRT.

1.3.5 Response to CRT in patients with a narrow QRS

In large randomised clinical trials CRT has been restricted to patients with a QRS of greater than 120 milliseconds. The effect of CRT in patients with narrow QRS has not been well established. A demonstration of benefit from CRT in narrow QRS heart failure patients would suggest either that this group has dyssynchrony or an alternative mechanism lies behind the benefit. This was examined in an acute study of nine patients with NYHA class III or IV heart failure and narrow QRS (79 to 120ms) undergoing left ventricular pacing of the free wall showing clinical benefit in terms of reduced NYHA class immediately post procedure. (Turner et al., 2004) Biventricular pacing in patients with a narrow QRS resulted in decreased mitral regurgitation, increased filling time, and a trend towards increased synchrony both radially and longitudinally. The authors conclude that patients with heart failure and narrow QRS duration experience electromechanical uncoupling.

The only multi-centre randomised clinical study of CRT in patients with narrow QRS (\leq 130ms) selected patients on the additional basis of the presence of sufficient mechanical dyssynchrony, measured using tissue Doppler. (Beshai et al., 2007) At six months, there

was no benefit of CRT in terms of six minute walk distance or maximum oxygen uptake, although there was a benefit in terms of NYHA class.

1.4 Diastolic function and diastolic ventricular interaction

Systolic heart failure is associated with left ventricular dilation, and this has been shown to be associated with diastolic ventricular interaction. Left ventricular filling is impaired in approximately 50% of patients with heart failure with raised pulmonary capillary wedge pressure (PCWP) due to diastolic ventricular interaction (DVI). (Bleasdale et al., 2004) Right ventricular overload results in the inter-ventricular septum physically impeding the left ventricle, resulting in reduced left ventricular filling. The pericardium constrains both ventricles. (see Figure 1-2)

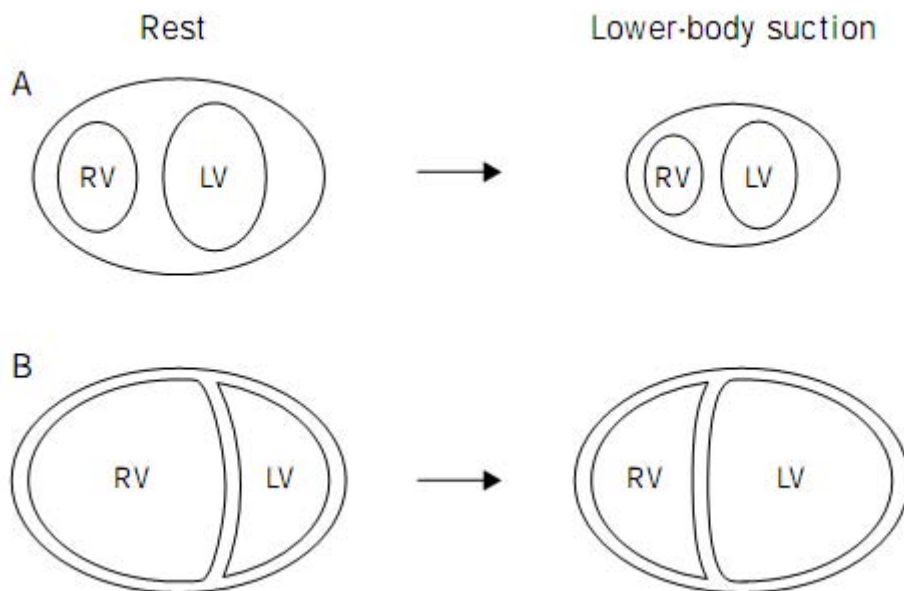
Reduction in right ventricular filing by use of lower body negative pressure increases the left ventricular volume and stroke volume by reducing right ventricular and pericardial constraint. DVI occurs when the PCWP is greater than 15 mmHg, when external constraint increases LV diastolic pressure reducing LV filling. Whilst the PCWP is an indirect measure of left atrial pressure, and therefore LVEDP, it will also be raised by external constraint, such as from the pericardium.

Patients with elevated PWCP (>15 mmHg) and heart failure (NYHA II – IV) have been demonstrated to show acute haemodynamic benefit from left ventricular pacing despite narrow QRS duration (Turner et al., 2004). A temporary wire paced the left ventricle resulting in a significant increase in cardiac output from 3.9 to 4.5 l/min, with a fall in PCWP from 24.7 mmHg to 21.0 mmHg. In the 10 patients with normal PCWP and good baseline cardiac output (CO) (5.4 ± 1.1 l/min) there was no change in PCWP, or CO.

Figure 1-2 Effect of lower body negative pressure on diastolic ventricular interaction⁴

A – normal

B – heart failure with pericardial constraint



⁴ Reproduced from Atherton, J.J., Moore, T.D., Lele, S.S., et al. (1997) Diastolic ventricular interaction in chronic heart failure. **The Lancet**, 349: (9067): 1720-1724 with the permission of Elsevier

Overdrive left ventricular pacing has been shown to reduce diastolic ventricular interaction. 18 patients with congestive heart failure underwent temporary left ventricular pacing. (Morris-Thurgood et al., 2000) In 9 of these patients the QRS duration was less than 120ms. The patients were dichotomized into two groups on the basis of the PCWP, normal pressure (< 15mm Hg) and raised PCWP indicative of likely DVI. The PCWP significantly decreased during left ventricular pacing (25.3 vs. 19.5 mmHg) and cardiac output significantly increased (3.9 vs. 4.4 L/min) in patients with baseline high PCWP values and likely DVI. In patients with normal PCWP, where the diastolic ventricular interaction would be small, there was no significant effect of LV pacing in terms of PCWP (10.5 vs. 10.5 mmHg) or CO (5.5 vs. 5.3 L/min).

1.4.1 Reduction of DVI with left ventricular pacing is independent of QRS

The relationship between DVI and QRS was explored. There was no relationship between QRS duration and haemodynamic response to left ventricular pacing in terms of stroke volume or pulmonary capillary wedge pressure. The haemodynamic benefit of LV pacing was seen in the patients with raised PCWP and normal QRS duration. It is postulated that LV pacing reduces diastolic ventricular interaction, increases LV filling and improves cardiac output. One of the mechanisms by which CRT may benefit patients is may be the reduction of DVI, although reduction of DVI has only been demonstrated with LV pacing alone.

1.5 Echocardiographic assessment of dyssynchrony

Dyssynchrony is associated with systolic heart failure, and its presence is believed to be a sine non qua for CRT, and its absence results in failure of response to CRT. (Bax et al., 2003a) On this basis, in the absence of other factors affecting response, the greater the dyssynchrony, the greater then benefit.

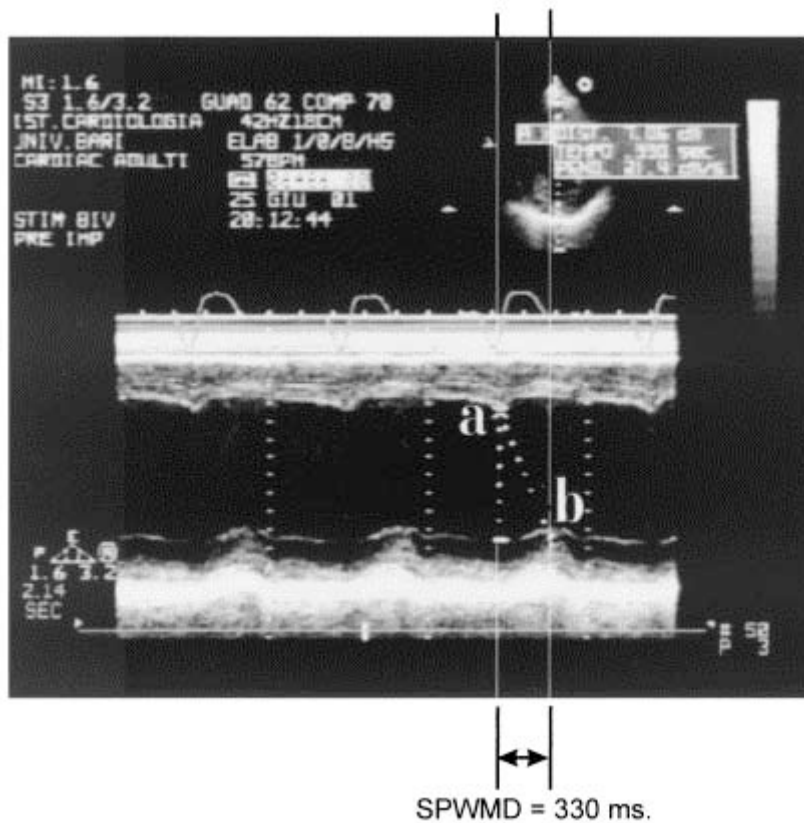
In an attempt to quantify dyssynchrony with the aim of improving selection of patients for CRT, a number of different echocardiographic measures have been devised. Since visual assessment of 2D echocardiography by the human eye cannot detect differences of less than 70 milliseconds, more reliable methods of assessment are required. (Kvitting et al., 1999) Single centre studies of echocardiographic measures of dyssynchrony have been shown to correspond to short term clinical response, and a few studies have followed up patients for outcome at up to 14 months. It should be noted that no study has excluded patients from CRT on the basis of absent dyssynchrony.

1.5.1 M-Mode echocardiography

Calculation of intra-ventricular conduction delay can be determined using M-mode to determine and compare septal to lateral wall delay. (Xiao et al., 1994) Pitzalis et al found the extent of posterior - lateral delay corresponded with response to CRT in 20 patients (see Figure 1-3). (Pitzalis et al., 2002) Pitzalis et al. found a delay of greater than one hundred and thirty milliseconds between the septum and posterior wall had a specificity of 63% and positive predictive value of 80% for reverse LV remodelling in a study of 20 patients undergoing CRT. However, this measurement can be difficult to obtain, with one study obtaining the measurement in only 45% of patients. (Marcus et al., 2005) The main

problem with this measurement arises where one of the walls is akinetic; hence this measurement is more suited to patients with DCM than to those with ICM.

Figure 1-3 Measuring septal to posterior wall motion delay



Short axis M-mode at the level of the papillary muscles.

a marks the onset of septal contraction and b marks the onset of posterior contraction. The difference is termed the septal to posterior wall motion delay.⁵

⁵ Reproduced from Pitzalis, M.V., Iacoviello, M., Romito, R., et al. (2002) Cardiac resynchronization therapy tailored by echocardiographic evaluation of ventricular asynchrony. *J Am Coll Cardiol*, 40: (9): 1615-1622 with permission of Elsevier.

The critical amount of dyssynchrony required to predict a response is unknown. (M. V. Pitzalis et al., 2005) A SPWMD ≥ 130 ms was associated with benefit from CRT (see Figure 1-4) Kaplan-Meier survival curves for patients with septal to posterior wall motion delay). The SPWMD correlated with heart failure progression on univariate analysis (HR 0.9) and on multivariate analysis was the only factor to be associated with heart failure progression (HR 0.91). Interestingly, QRS duration did not predict response.

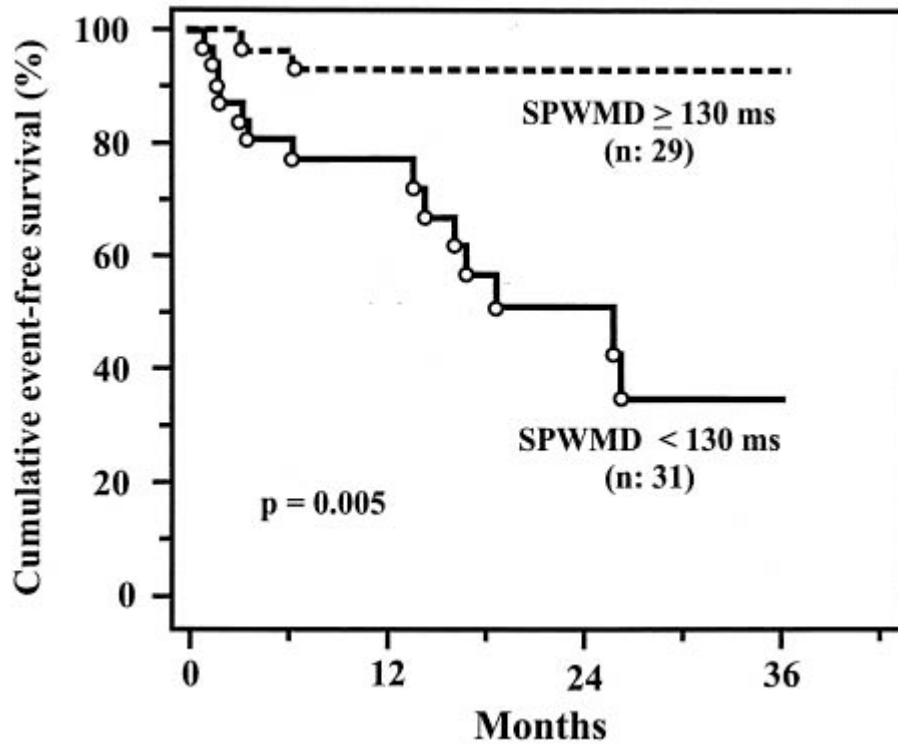


Figure 1-4 Kaplan-Meier survival curves for patients with septal to posterior wall motion delay

Dichotomised by septal to posterior wall motion delay of 130ms.⁶

⁶ Reproduced from Pitzalis, M.V., Iacoviello, M., Romito, R., et al. (2005) Ventricular asynchrony predicts a better outcome in patients with chronic heart failure receiving cardiac resynchronization therapy. *J Am Coll Cardiol*, 45: (1): 65-69. with permission of Elsevier.

The role of SPWMD and prediction of response from CRT remains unclear. Marcus et al. analysed data from two multi-centre studies and found that septal to posterior wall motion delay did not correlate with response. (Marcus et al., 2005) This may be due to the inter-observer precision of this measurement, which was found to be poor.

1.5.2 Doppler blood pool echocardiography

Blood pool spectral Doppler can be used to determine mechanical delay. The aortic pre-ejection delay is the delay between the onset of the QRS to the start of the aortic ejection envelope on Doppler. It allows assessment of the left intra-ventricular delay (with a value of greater than >140 ms taken as abnormal), and prolongation of this reduces the left ventricular filling time.

Pulse Doppler in the outflow tracts of the pulmonary and aortic valves allows differentiation between the ejection times of the right and left ventricle (inter-ventricular delay). A delay in the time to aortic valve (left ventricular pre-ejection delay) opening greater than 140ms was a criterion for entry in the CARE-HF trial. (J. G. Cleland et al., 2001) Delay in contraction of the right ventricle is measured from the start of the ventricular QRS complex to the onset of pulmonary contraction (right ventricular pre-ejection delay). Blood pool Doppler is one of the most reproducible measures of dyssynchrony. (Chung et al., 2008)

Two out of the following three criteria had to be satisfied to enter CARE-HF if the QRS duration was between 120 and 149 ms: a delay of greater than 40 ms between the left and right pre-ejection times, a pre-aortic ejection delay of greater than 140 ms or intra-

ventricular mechanical delay. (Cleland et al., 2001) The number of patients enrolled with QRS between 120 and 149ms was relatively small. Sub-group analysis of the CARE-HF trial found the HR of the composite end points were reduced in patients with a QRS <160ms treated with CRT rather than medical treatment (hazard ratio (HR) 0.74, 95% CI 0.54 – 1.02), and where the intra-ventricular delay (all QRS duration) was less than 49.2 ms (HR 0.77, 95% CI 0.58-1.02).

1.5.3 Use of an echocardiographic global measure of dyssynchrony and CRT

A global measure of dyssynchrony is the total isovolumic time (IVT), which is the period when the heart is resting, neither emptying nor filling. (Duncan et al., 2006) Peak oxygen consumption is accurately predicted by the total isovolumic time in patients with DCM. The ejection time per minute = ET per cycle * heart rate/1000. The total isovolumic time = 60 – (total ejection time + filling time). The difference between the onset of pulmonary and aortic ejection was calculated as left ventricular pre-ejection period – right ventricular pre-ejection period (D-PEP).

The IVT can predict response from CRT. In a retrospective analysis reduction in IVT predicted short term response. Responders at six months (29/39) had a significant reduction in isovolumic relaxation time due to shorter isovolumic contraction time (IVCT) and longer filling time as D-PEP decreased by 38 ms. In non-responders IVCT increased and filling time shortened. The only variables to independently predict response to CRT were IVT and D-PEP on univariate analysis. Patients with IVT and D-PEP in the normal ranges did not benefit from CRT, and actually became more dyssynchronous on echocardiographic parameters.

1.5.4 Tissue Doppler imaging

Tissue Doppler imaging (TDI) measures the velocity of the myocardium. TDI is restricted to measuring longitudinal myocardial velocities in systole and diastole. The apex of the heart is relatively fixed, so the velocity of movement of the mitral annulus will give a measure of longitudinal function. Some torsional movement will be included in the measurement of longitudinal function. Measurement of radial and circumferential movement is limited as Doppler relies on detecting motion in parallel to the ultrasound beam. Due to the effect of tethering, myocardial movement can result from attachment to actively contracting tissue rather than contracting itself. A limitation in interpreting the results is that scar tissue may have a velocity resulting entirely from passive movement. There are two different methods of TDI: Pulsed spectral TDI relies on specifying a sector of interest; whereas colour coded TDI can acquire information about a sector of interest.

Early studies used TDI imaging to determine the SPWD with greater precision than m-mode imaging, and now multiple indexes have been derived. Differences between the peak myocardial motion of the basal regions of greater than 65ms or standard deviation of greater than 33 milliseconds are taken as indicative of dyssynchrony. Over 19 different methods of determining dyssynchrony had been published, yet only 4 had clinical outcome data with the longest follow up period being 14 months and the maximum number of patients in the study was 85. (Bax et al., 2005) The end points in many studies were not sufficient to make a useful assessment of the studies applicability.

Tissue Doppler imaging has good temporal resolution, yet limitations arise due to poor signal to noise ratio. It has not found widespread use due to unfamiliarity. Spatial resolution is low due to dependency on 2D colour Doppler imaging of the heart, and if

the alignment of the probe is off axis, both longitudinal and radial velocities are included. The measurement of longitudinal motion has a smaller range and wider variability than circumferential motion when measured with tagged MRI. (Helm et al., 2005) Colour coding indicates the velocity of myocardium, not myocardial contraction, allowing myocardial velocity curves to be constructed. Scarred areas will therefore be pulled by non scarred contracting areas, resulting in velocity without contraction.

A high prevalence of dyssynchrony has been detected using TDI in HF patients. In a prospective study of 200 subjects, 112 with heart failure (67 patients QRS < 120, 45 > 120) and 88 healthy controls (C. M. Yu et al., 2003b) the standard deviation of the time to peak in the 12 segments model was calculated. Dyssynchrony measured with TDI in patients with narrow and wide QRS HF and controls. Figure 1-5 shows the scatter plot, which demonstrates an overlap between all groups, suggesting that it would be difficult to select patients for CRT on the basis of this model alone. If a maximum difference in Ts of greater than 100 ms was used to define systolic dyssynchrony the prevalence was 0% in controls, 51% of the narrow QRS patients and 73% of the wide QRS.

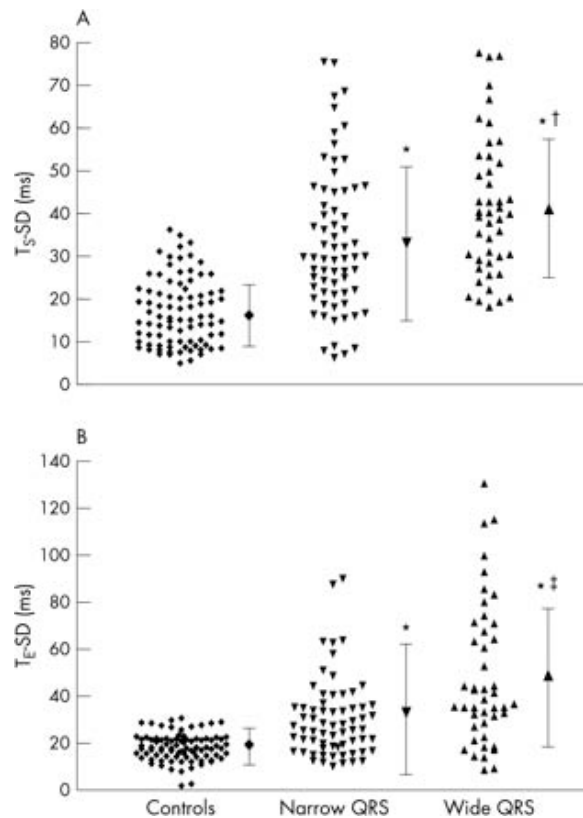


Figure 1-5 Dyssynchrony measured with TDI in patients with narrow and wide QRS HF and controls

The standard deviation of the time to peak myocardial sustained systolic velocity (Ts-SD) and early diastolic velocity (Te-SD) of all 12 left ventricular segments in controls, narrow QRS complexes (≤ 120 ms) and wide QRS complexes (> 120 ms).⁷

⁷ Reproduced from Yu, C.M., Lin, H., Zhang, Q., et al. (2003) High prevalence of left ventricular systolic and diastolic asynchrony in patients with congestive heart failure and normal QRS duration. **Heart**, 89: (1): 54-60 with the permission of BMJ Publishing Group Ltd.

Studies of TDI in heart failure patients with narrow QRS

Although TDI can identify dyssynchrony, it is not necessarily clinically applicable in patients with normal QRS and heart failure. (Cho et al., 2005) ROC curves analysis demonstrated that the optimal cut off value for the SD of the time to peak systolic velocity was 37ms (sensitivity 68%, specificity 71%) and the SD of the maximal temporal difference was 91 milliseconds (sensitivity 70%, specificity 68%) for detecting clinical events. The presence of dyssynchrony in 316 patients with left ventricular impairment was determined using pulsed spectral Doppler. (Perez de Isla et al., 2005) The sensitivity and specificity of this method of determining dyssynchrony in patients with left bundle branch block was 69.4% and 75.3%, respectively.

1.5.5 Reproducibility of measures of dyssynchrony

Curiously, the reproducibility of TDI measurements is poor. 40 subjects were studied to determine the reproducibility of myocardial and blood pool Doppler measures of dyssynchrony. (Gabriel et al., 2007) Each patient underwent two echocardiograms within an hour of each other by two experienced echo cardiographers. Blood pool Doppler was more reproducible (inter-study $r = 0.8 - 0.86$) than TDI (inter-study $r = 0.28 - 0.59$) and m-mode septal to posterior wall motion delay (inter-study $r = 0.31$). The peak velocity measures were more reproducible than the onset to wall motion using TSI. The poor reproducibility appears to reflect the limits of echocardiographic imaging techniques. The use of peak velocities, although more reproducible, may be problematic due to the variation in the timing of peak motion which may be affected by tethering, pre and after-

load and sympathetic drive. These findings were mirrored in the PROSPECT study. (Chung et al., 2008)

1.5.6 Predicting response to CRT using TDI

Early small studies suggested that TDI could reliably predict response to CRT. (Bax et al., 2003a) In a study of 25 patients, analysis of the baseline data showed no correlation between aetiology of cardiomyopathy, QRS duration at baseline, LV ejection fraction and left ventricular volume and response. The septal to lateral peak systolic velocity delay was the only variable that differed between responders and non-responders.

1.5.7 Studies of CRT in patients with echocardiographic evidence of dyssynchrony regardless of QRS duration

Preliminary studies suggest that TDI could predict response, and further studies suggested that it might have a role in selection independent of QRS duration. (Bleeker et al., 2006b) In a study of 66 patients, half who had QRS duration of less than 120ms. These patients were implanted with CRT if there was tissue Doppler evidence of dyssynchrony. No correlation between QRS duration and dyssynchrony was found.

1.5.8 Prediction of reverse remodelling using TDI

In small studies, TDI was shown to predict reverse remodelling. (Yu et al., 2005b) The systolic synchronicity index was the only parameter on multiple regression analysis in

this study to predict response to CRT in terms of improved end systolic volumes at 3 months.

Although the presence of dyssynchrony on TDI predicts response, excess dyssynchrony prevents reverse remodelling. (Bax et al., 2004a) ROC curve analysis found 65ms was the optimal cut off for predicting symptomatic response with a sensitivity and specificity of 80%, predicting a reduction of left ventricular end systolic volumes of 15% with a sensitivity and specificity of 92%. Interestingly, whilst reverse remodelling occurred in a linear fashion, once the heart was extremely dyssynchronous ($\geq 100\text{ms}$) reverse remodelling remained did not occur ((see Figure 1-6) relationship between dyssynchrony and change in LVESV.). This observation suggests there is a limit of dyssynchrony beyond which the LV cannot be resynchronised.

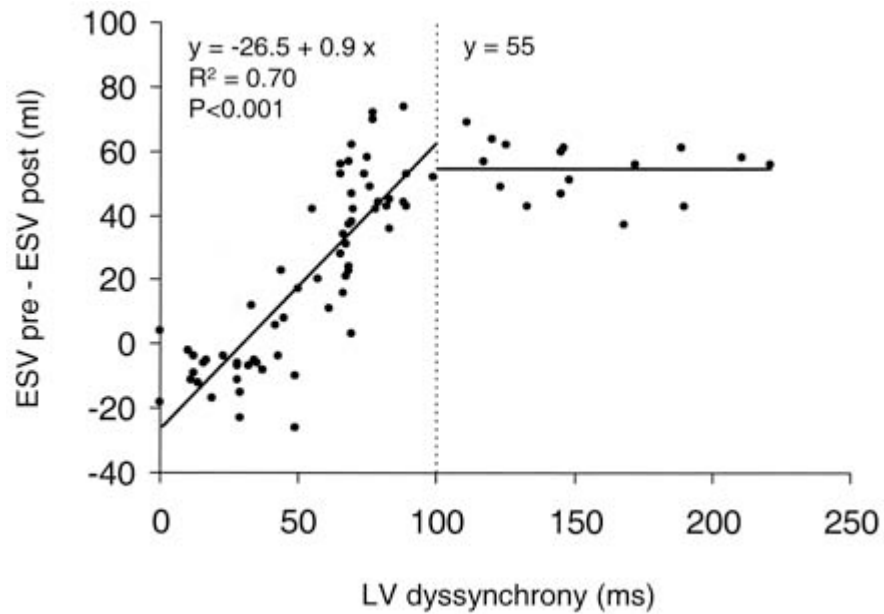


Figure 1-6 Relationship between dyssynchrony and change in LVESV

A linear relation existed between the extent of left ventricular (LV) dyssynchrony and the change in LV end-systolic volume (ESV) after cardiac resynchronization therapy. However, LV dyssynchrony over 100 ms did not result in further reduction in LV end-systolic volume.⁸

⁸ Bax, J.J., Bleeker, G.B., Marwick, T.H., et al. (2004) Left ventricular dyssynchrony predicts response and prognosis after cardiac resynchronization therapy. **J Am Coll Cardiol**, 44: (9): 1834 - 1840. with permission from Elsevier.

1.6 Tissue Doppler strain imaging

One of the limitations of TDI is the inability to distinguish between active and passive movement, such that akinetic myocardium will move passively due to tethering. As a result, TDI imaging will facilitate time to peak motion analysis, which could be misleading. Strain imaging attempts to fill this void by determining whether the myocardium is changing length or just being pulled due to tethering. The timing and amount of myocardial movement can be determined using strain imaging, and is measured in terms of percentage change from original length.

Acquisition of strain can be acquired using TDI or speckle tracking. TDI based strain analysis is derived from comparison of adjacent tissue velocities, so called “velocity-regression”. More recently, two dimensional speckle tracking strain analysis from gray-scale imaging acquired on standard echocardiography has been developed (see next section).

There are limitations to strain rate imaging. TDI based strain analysis is limited by small windows, as a high frame rate is required. Thus only 2 walls may be visualised at any one time, and spatial resolution is low as one point in each wall is compared. Lagrangian strain analysis relies on measuring the change in length between two points, and strain rate requires the first derivative of each measurement. Strain echocardiographic imaging was found to correlate with sonomicrometry when studied in a dog model. (Dohi et al.,

2006) One study of 18 patients with left bundle branch block has suggested that abnormal strain relationships may be reversed by CRT. (Helm et al., 2005)

Strain analysis is complex and it can be difficult to acquire reliable data. (Marwick, 2006) Myocardial strain imaging should allow assessment of systolic and diastolic function. Strain rate appears to give similar results to dP/dt , where as strain is better related to left ventricular ejection fraction. To obtain optimal results, the tissue Doppler signal must be optimal. The opening and closure of the aortic valve, and mitral valve opening must be defined, as post-systolic signals may be misinterpreted as systolic contraction. (Marwick, 2006) Reverberation artefact and adequate pulse-repetition are important to avoid aliasing. The Doppler frequency must be adequate to avoid including blood pool velocity in the signals. The angle of the transducer must be correct to avoid error. As the heart torts, the sample volume may move outside the myocardium, giving rise to further errors (see Figure 1-7).

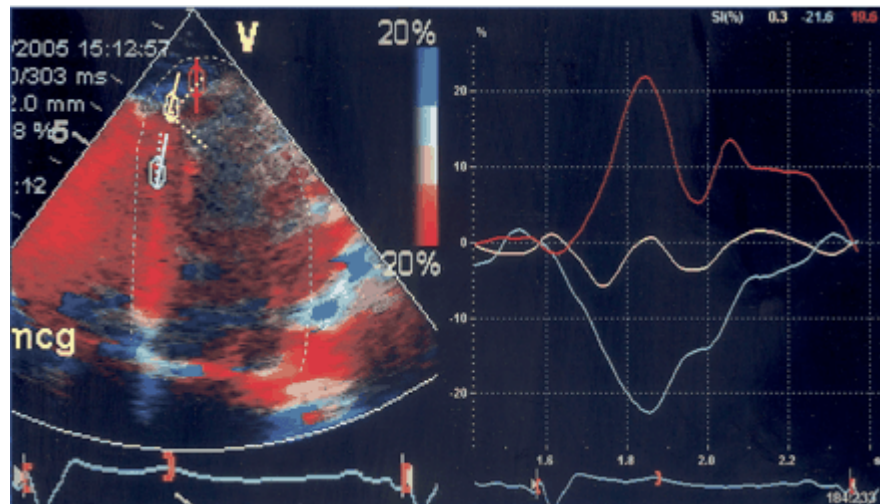


Figure 1-7 Example of possible error in strain imaging – the impact of angulation on strain rate imaging.

Interrogation parallel with the wall (mid-septum, shown in blue) identifies long-axis shortening, and at right angles to the wall (apex, shown in red) identifies short-axis thickening. However, an intermediate angle (apical septum, shown in yellow) causes underestimation—a mixture of vectors at 45° produces a net absence of recordable strain. Scan planes are shown as continuous lines, longitudinal and radial contraction vectors as broken lines.⁹

⁹ Reproduced from Marwick, T.H. (2006) Measurement of Strain and Strain Rate by Echocardiography: Ready for Prime Time? *J Am Coll Cardiol*, 47: (7): 1313-1327 with permission of Elsevier.

Animal models suggest that strain analysis can detect changes after CRT. (Dohi et al., 2006) In this study the dP/dt was measured with an electrode conductance catheter and left ventricular micro-manometer. This study demonstrated that angle corrected strain measurements are possible and correlate well with changes in dP/dt . Radial strain appears has a greater range than longitudinal strain, so the accuracy of radial strain is likely to be greater.

1.7 Speckle tracking

Tracking the myocardial speckles seen on two-dimensional echocardiography allows strain determination. Two advantages of speckle imaging are that it is not beam angle dependent as it does not rely on Doppler, and stored echocardiograms can be processed by the software. Speckle tracking has been validated with sonomicrometry, and correlated with cardiac magnetic resonance tagging ($r = 0.87$, $p < 0.001$). (Amundsen et al., 2006) Speckle tracking can measure Lagrangian strain from pre-systolic myocardial length, unlike tissue velocity based velocity-regression strain. However, speckle tracking requires high frame rates which can increase noise.

1.8 Studies of strain analysis in CRT patients

Small cohort studies suggest that strain analysis may be able to determine which patients will improve EF after CRT. (Suffoletto et al., 2006) The site of latest activation of left ventricle was determined and compared with the LV lead position. Using a cut off of radial speckle strain dyssynchrony of >130 ms predicted a response with 89% sensitivity and 83% specificity.

1.8.1 Strain analysis to determine optimal lead position

A further use of strain analysis is to target the area to site the LV lead. (Becker et al., 2007) The site of latest strain activation was targeted. Half the patients had sub-optimal positions, defined as not within immediate neighbourhood of the segment with latest contraction. The intra-observer and inter-observer agreement for whether the lead was optimal or sub-optimal were 0.95 and 0.91. Patients with optimal positions had statistically significant increases in ejection fraction (9% vs. 5%) at 3 months compared with sub-optimally positioned leads. However, there was no difference in NYHA class and peak VO₂ max, between those with optimal and sub-optimal positions.

1.8.2 Strain imaging and outcome of CRT

Conflicting results have been reported in the use of strain analysis to predict response. Using $\geq 15\%$ increase in acute EF, a cut off of 130ms predicted response with 95% sensitivity and 88% specificity. (Dohi et al., 2005a) However, speckle tracking dyssynchrony analysis did not appear to predict CRT response at six months. (Knebel et al., 2007) A small study found it had sensitivity of 0.64 and specificity of 0.8 to predict volumetric response. However, the study has limitations in that clinical response was not measured and the number of patients was small.

1.8.3 Tissue Doppler strain rate compared with tissue velocity imaging

Strain imaging would be expected to be more effective than TDI as the effects of passive motion due to tethering would be detected. To determine whether strain detected with

TDI could predict outcome it was compared with TDI alone in 54 patients undergoing CRT. (Yu et al., 2005c) They found that TDI was more predictive of reverse remodelling after CRT than strain rate imaging. The time to peak strain did not predict reverse remodelling. Previous work processing 120 segments had found an intra-observer and inter-observer variability for TDI of 3% and 5% and for strain rate imaging 16% and 19%. The presence of post systolic shortening and strain rate imaging parameters did not predict response to CRT. On multi-variable analysis only the SD of the time to peak systolic velocity predicted significant reverse remodelling.

Targeting the LV lead position appears to improve myocardial function. (Breithardt et al., 2003). At baseline, shortening is low in terms of systolic strain values. CRT had no significant effect on the maximum rate of strain or the peak shortening. During the isovolumic contraction time and in the ejection period there were significant differences in the longitudinal shortening (see table below). At baseline systolic septal shortening occurred during isovolumic contraction time (IVCT), and lateral wall shortening occurred during the ejection period. During CRT, the septum shortened during the ejection period, and lateral wall shortening occurred earlier. Prior to CRT the lateral wall shortened more than the septal wall, this was reversed during CRT (see Figure 1-8, Figure 1-9). The time to peak systolic contraction occurred earlier than the maximal negative strain, hence motion occurs before shortening. Breithardt et al conclude that targeting the left ventricular lead to areas of late activation improve cardiac output by relieving over stretched myocytes.

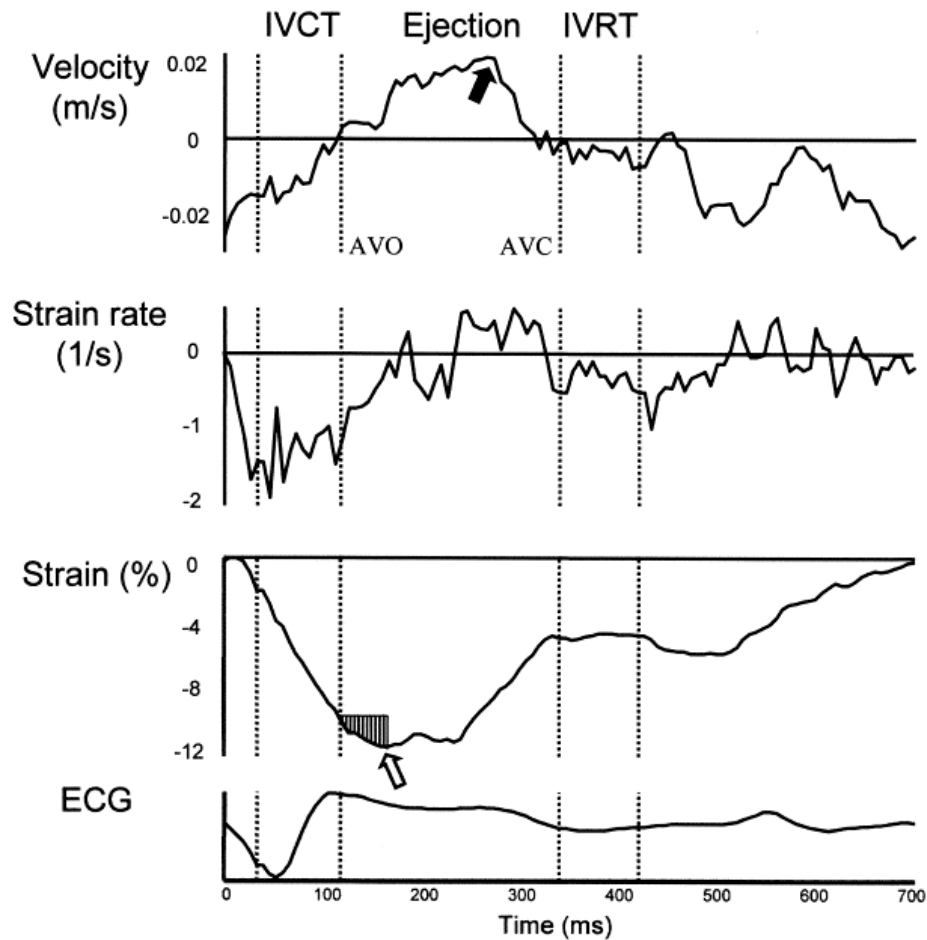


Figure 1-8 Typical velocity, strain rate and strain curve from the mid septum in LBBB

AVO = aortic valve opening, AVC = aortic valve closure. Peak shortening is during systole (open arrow) and peak shortening velocity is during late systole (closed arrow).

IVCT = isovolumic contraction time. IVRT = isovolumic relaxation time.¹⁰

¹⁰ Reproduced from: Breithardt, O.A., Stellbrink, C., Herbots, L., et al. (2003) Cardiac resynchronization therapy can reverse abnormal myocardial strain distribution in patients with heart failure and left bundle branch block. *J Am Coll Cardiol*, 42: (3): 486-494 with permission from Elsevier.

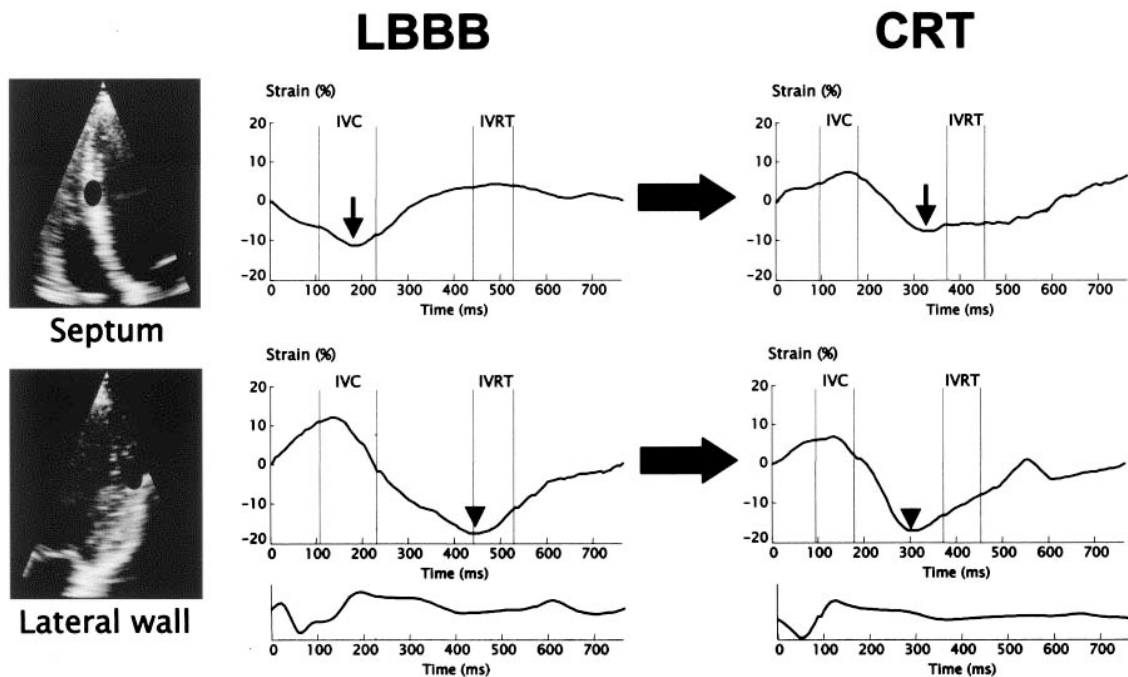


Figure 1-9 Velocity and strain curves before and after CRT

Taken from the septal and lateral wall mid-segments in a 73-year-old patient.

The derived strain curves from the mid-segments portray the regional asynchrony in deformation. Maximal septal contraction occurs before aortic valve opening (top left panel, arrow) and is accompanied by lateral wall lengthening. The septum lengthens after aortic valve opening and does not contribute to ejection. Peak lateral wall contraction is observed very late in systole and persists into the post-systolic period (bottom left panel, arrowhead). During CRT, systolic contraction occurs simultaneously in both walls, contributing equally to ejection (right panels). Note also the shorter isovolumic contraction (IVC) time with CRT. IVRT = isovolumic relaxation time.¹¹

¹¹ Reproduced from: Breithardt, O.A., Stellbrink, C., Herbots, L., et al. (2003) Cardiac resynchronization therapy can reverse abnormal myocardial strain distribution in patients with heart failure and left bundle branch block. *J Am Coll Cardiol*, 42: (3): 486-494 with permission from Elsevier.

1.8.4 Echocardiographic Tissue Synchronisation Index

Semi-automated construction of myocardial velocity curves, termed tissue synchronisation imaging (TSI) (GE Vingmed), uses colour to code time-to-peak tissue Doppler velocities. Using this technique, acute response to CRT may be detected.

(Gorcsan et al., 2004) A ≥ 65 ms delay in contraction measured from the anterior septum to the posterior wall (typical for LBBB patients) using had 87% sensitivity and 100% specificity for predicting an acute response. Placing the left ventricular lead in the area with the greatest regional delay was associated with acute response.

Comparison between automated TSI and TDI shows good correlation. (Van de Veire et al., 2007) TSI ≥ 65 ms was found to predict clinical response and reverse LV remodelling after 6 months of CRT with a sensitivity of 81% and specificity of 89%. The correlation between the automated and manual methods was $r=0.95$. Interestingly, those patients with the most extreme dyssynchrony responded worst.

1.8.5 Real time three dimensional echocardiography (RT3DE)

Three dimensional echocardiography provides reliable left ventricular volume analysis and generates parametric polar maps of the timing of LV contraction. Three thousand points can be examined instead of limited segments. The site of latest activation may be colour coded, allowing this site to be targeted for placement of the left ventricular lead.

This has been compared to tissue velocity imaging for assessment of dyssynchrony.

Proponents claim that this technique allows simultaneous evaluation of dyssynchrony in

all segments, including those that cannot be imaged by tissue velocity imaging, and also allows longitudinal, circumferential and radial timings to be measured. One great advantage is the rapid acquisition of the whole ventricular volume dataset in 4 cardiac cycles. Potential limitations include poor temporal resolution and the need for good image quality.

A direct comparison between TDI and RT3DE suggests two different parameters are measured. (Burgess et al., 2007) Dyssynchrony measured by TDI reflects peak systolic ventricular pressure which is reached early in systole, where as RT3DE measures minimal systolic volume which is reached late in systole. There is little evidence for selecting patients on the basis of velocity should be preferred over volumetric change. In this study, 23% were excluded from analysis of RT3DE due to poor imaging, whilst in 51% TDI could not be assessed in all twelve segments. Inter-observer and intra-observer reproducibility were 24% and 13% for TDI and 18% and 14% respectively for RT3DE. There was no statistical correlation between TDI and RT3DE in this study ($r=0.11$). There was no correlation between the imaging techniques in determining the site of maximum delay. This study found significant limitations with TDI.

The Systolic Dyssynchrony Index (SDI) is a measure of dispersion in the time taken to reach the minimal regional volume for each segment during the cardiac cycle. In a small study, at follow up after CRT implantation those who felt symptomatically better were classed as responders and were found to have a significant decrease in SDI, where as non responders had an increase in SDI. (Kapetanakis et al., 2005)

1.8.6 Echocardiographic studies of dyssynchrony

The table below lists published studies into CRT where echocardiographic measures of dyssynchrony were evaluated to determine response. Clinical outcome was evaluated in 4 of the 21 studies (see Table 1-4 Clinical measures of dyssynchrony used in studies of CRT.). In total, nineteen different measures of dyssynchrony were used.

Table 1-4 Clinical measures of dyssynchrony used in studies of CRT.

Study	Patients	Follow Up (months)	Measure	Outcome measured	Outcome
(Pitzalis et al., 2002)	20	1	SPWMD ≥ 130	Reverse LV remodelling	+
(Pitzalis et al., 2005)	60	14	SPWMD ≥ 130	Event-free survival	+
(Marcus et al., 2005)	79	6	SPWMD ≥ 130	Reverse LV remodelling	-
(Breithardt et al., 2002)	34		Acute Lateral WM	Delayed Acute haemodynamics	+
(Kawaguchi et al., 2002)	10	9	Δ sept-lat fractional area 40% LV dyss		
(Penicka et al., 2004)	49	6	Ts basal LV, basal RV Inter + intra LV delay	Left ventricular ejection fraction	+
(Ansalone et al., 2001)	21	1	Systolic dyss 5 basal seg LV dyssynchrony	Symptoms and LVEF	+
(Garrigue et al., 2001)	12	12	Ts onset, set v lateral	Improvement in Dyssynchrony, Symptoms	+
(Yu et al., 2002)	25	3	Ts 12 segments SD of Ts	Improvement in dyssynchrony	+
(Bax et al., 2003a)	25		Acute Sept-lat delay in Ts Delay ≥ 60 ms	LVEF	+
(Makaryus et al., 2003)	30	3	Ts-SD 12 LV segments TsSD > 33 ms	Reverse LV remodelling	+
(Bax et al., 2003b)	85	12	Sept-lat delay in Ts Ts ≥ 65	Reverse LV remodelling and events	+

			<i>ms</i>		
(Notabartolo et al., 2004)	49	3	Diff Ts 6 basal segments Diff Ts ≥ 65 ms	Reverse LV remodelling	+
(Yu et al., 2004b)	54	3	Ts-SD 12 LV segments Ts-SD >31 ms	Reverse LV remodelling	+
(Søgaard et al., 2002a)	20	12	Longitudinal contraction	Delayed LVEF	+
(Søgaard et al., 2002b)	20		Acute Tissue tracking Optimise V-V delay	LVEF	+
(Breithardt et al., 2003)	18		Acute SRI septal+lateral Higher lateral SR	Strain rate reversal, lat to sept	+
(Dohi et al., 2005a)	38		Acute Radial strain sept./post ≥ 130 ms	Stroke volume	+
(Gorcsan et al., 2004)	29		Acute TSI Sept/post delay >34 ms	Reverse LV remodelling	+
(Yu et al., 2005b)	56	3	TSI 12 LV segments Ts-SD >34 ms	Reverse LV remodelling	+
(Zhang et al., 2005)	13	3	3D echo Tmsv	Improvement Tmsv Correlation	+
(Penicka et al., 2007)	48	32	Ts basal LV, basal RV Inter + intra LV delay	Clinical response, Events (9 deaths, 15 hospitalisations; these patients defined as non-responders, all others as responders).	+

1.8.7 Prospective evaluation of echocardiographic measures of dyssynchrony

The largest study of echocardiographic techniques to predict outcome from CRT did not support its use in selection of patients for CRT. A prospective evaluation of echocardiographic predictors of outcome of CRT (PROSPECT study) in 300 patients with NYHA class III and IV attempted to assess the ability of echocardiographic factors in predicting outcome. (Chung et al., 2008) Tissue Doppler, strain rate imaging and conventional echocardiography were assessed. (Yu et al., 2005a) Clinical and reverse remodelling outcomes were reported at six months follow up. The primary outcome was a clinical composite score. Patients were classified as unchanged, worsened (hospitalised with heart failure, worsening NYHA class, or improved, or improvement in left ventricular end systolic volume by at least 15%.

The study found that no single echocardiographic measure predicted outcome from CRT. The inter-observer variability was high for many measurements, 72% for septal to posterior wall motion delay, 33.7% for the Yu index, and 31.9% for the maximum difference for the time to peak systolic contraction in 6 basal segments. The sensitivity and specificity of the 12 measures studied were modest, and the authors concluded that on this basis the echocardiographic measures should not be used in clinical decision making.

The PROSPECT study has cast into doubt the use of TDI and echocardiographic measures in deciding whether patients undergo CRT. One reason for the result seen in the study is the possibility that dyssynchrony does not predict outcome. However, the designers of the study have recently published a criticism of the study conduct, casting

into doubt the methods used to acquire the tissue Doppler indices. (Yu et al., 2009) The authors comment that lack of rigor in the acquisition of the TDI is responsible for the high inter-observer variability seen in the study. However, as a result of this study, current guidelines from the American Society of Echocardiography state that dyssynchrony analysis should not be used to select patients for CRT. (Gorcsan et al., 2008)

1.8.8 Myocardial Contrast Perfusion Echocardiography

Patients with ischaemic heart disease have a poorer clinical response to CRT when compared with patients with dilated cardiomyopathy. (Reuter et al., 2002, Zhang et al., 2009) This may be due to the inability of scarred areas to contribute to myocardial function.

Myocardial perfusion echocardiography could aid patient selection. (Hummel et al., 2005) All patients underwent myocardial contrast imaging to assess perfusion and had previously documented coronary artery disease. The myocardial perfusion was graded for each segment, using a 15 segment model as follows 0 to 2, 2 = normal, 1 = reduced and 0 = absent. Patients were re-assessed clinically and with echocardiographic follow up at 6 months. A perfusion score index was calculated (total segment score/ number of interpretable segments). The perfusion score index (PSI) correlated with improvement in stroke volume ($R = 0.46$, $p = 0.08$), change in ejection fraction ($R=0.49$, $p=0.06$) and change in Tei index ($R=-0.78$, $p=0.002$). The improvement in 6 minute walk test correlated well with the perfusion score index tertile (low = 5 ± 54 , medium 211 ± 145 , high 358 ± 123 , $p = 0.01$). The peak septal to lateral delay measured with tissue Doppler improved in some patients with poor viability, despite a lack of response to CRT, which

may be due to synchronization of passive movements. There was no reverse remodelling in patients with a $PSI < 1$.

Contrast echocardiography may have a role in measuring dyssynchrony. (Kawaguchi et al., 2002) Within the ventricle, the contrast is high, and within the myocardial wall it is lower. The regional fractional area change time plots showed early septal shortening followed by early lateral stretch then lateral shortening (see Figure 1-10 Contrast echocardiography in the detection of dyssynchrony). When biventricular pacing was switched on, the regional fractional area change showed all plots contracting during systole. In this study, ventricular pacing prevented paradoxical septal motion rather than improving the function of the lateral wall, although this may have resulted from mixed left ventricular and biventricular pacing. This study demonstrates the feasibility of this technique to measure dyssynchrony, but does not have any measure of outcome.

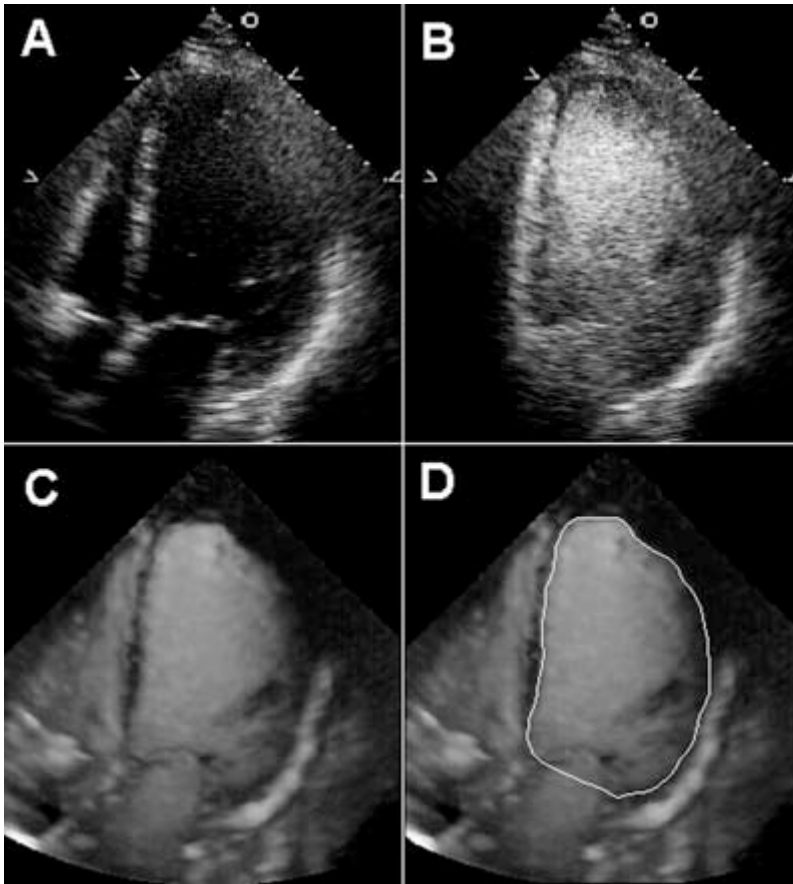


Figure 1-10 Contrast echocardiography in the detection of dyssynchrony

A shows the apical 4 chamber view without contrast, B shows an unprocessed image after the injection of contrast, C shows the enhanced view of the endocardial border, and D shows a super-imposed manual trace of the endocardial border.¹²

¹² Reproduced from: Kawaguchi, M., Murabayashi, T., Fetcs, B.J., et al. (2002) Quantitation of basal dyssynchrony and acute resynchronization from left or biventricular pacing by novel echo-contrast variability imaging. *J Am Col Cardiol*, 39: (12): 2052-2058 with permission of Elsevier.

1.9 Nuclear Imaging – Myocardial Scintigraphy

Equilibrium radio nucleotide angiography can detect dyssynchrony (Fauchier et al., 2002). The SD of the difference between the mean phases of each ventricle was taken as the measure of inter-ventricular dyssynchrony. In a study of DCM patients, the SD of the mean phase of right and left ventricles, and QRS duration were predictive of long term cardiac events ($p < 0.001$), but the inter-ventricular dyssynchrony calculated with his method was not predictive. Univariate analysis of 13 factors, found that the SD of the left ventricle mean phase and pulmonary capillary wedge pressure were predictive of major cardiac events.

1.9.1 Nuclear Cardiology – Positron Emission Tomography

Evidence from cardiac magnetic resonance studies on scar burden and morphology identified the presence of scar as important in predicting response to CRT. Initial evidence from PET scanning suggests that the presence of significant scar adversely effects response to resynchronisation. (Sciagra et al., 2004) Patients with significant perfusion defects had significantly worse quality of life and walk distance compared to those without defects. Whilst symptomatic benefit was seen in both groups, patient with significant perfusion defects did not exhibit reverse remodelling, unlike those without perfusion defects.

Viability measured with PET correlates with response to CRT. (Ypenburg et al., 2007b)

The total number of scarred segments correlated with response. Receiver operating characteristic curve analysis suggested that viability in 11 segments yielded a sensitivity

of 74% and specificity of 87%. Non response was predicted by a scar score of 14 with a sensitivity of 83% and specificity of 74% (AUC 0.86).

Mapping the position of the left ventricular lead with areas of scar predicts response to CRT. (Adelstein and Saba, 2007) The total amount of scar, the presence of scar adjacent to the LV lead and the number of segments with no uptake of tracer correlated with failure of left ventricular re-modelling after CRT.

1.10 Endocardial mapping in CRT

Intuitively, the site of latest intrinsic activation would be the ideal pacing site to achieve the greatest re-synchronisation response. Epicardial mapping has shown that the site of latest activation is the postero-basal or postero-lateral segments in normal hearts, and this is exaggerated in the presence of LBBB.

Endocardial mapping identifies areas of slow conduction. (Lambiase et al., 2004) Pacing the area of normal activation compared with slow conduction resulted in 22% rise in dP/dt_{max} and increased cardiac output by 15%. Without mapping, the coronary sinus lead may be placed in areas of slow conduction caused by fibrosis and scarring. Avoiding pacing areas of slow conduction had the greatest haemodynamic benefit due to reduction in septal dyskinesia and early papillary muscle contraction. This has been shown to reduce mitral regurgitation and increases left ventricular filling times. (Fried et al., 1999) The response of patients with heart failure and prolonged activation times to CRT is dependent on the reduction in activation times.

1.11 Cardiovascular magnetic resonance

Cardiovascular magnetic resonance (CMR) has a higher spatial resolution, better left ventricular border definition and lack of geometric assumptions in comparison with echocardiography, resulting in greater accuracy of left ventricular volume measurements. (Grothues et al., 2002) However, using present technology, this is at a cost of reduced temporal resolution.

1.11.1 Myocardial tagging

Tagging is a process where non physical markers are placed on the ventricle using magnetising pulses with a gradient. Tags are regions of tissue whose longitudinal magnetization has been altered before imaging so that they appear dark in subsequent magnetic resonance images. The pattern of deformation of the tags can be analysed during systole. The magnetisation pattern is called spatial modulation of magnetisation (SPAMM). This was later improved, termed complimentary spatial modulation of magnetisation (CSPAMM). Tagging allows motion to be determined in 3 dimensions, circumferentially, radially and longitudinally which enables determination of strain. Tags have approximately a one second lifetime, and are usually generated on the R wave. The initial use of tagging was to measure blood velocity.

The development of SPAMM uses non selective excitation to produce parallel bands, which fade due to T1 relaxation. CSPAMM acquires two tagged images which are 180 degrees out of phase with one another and then subtracts them, at the cost of increasing

acquisition time. The advantage of CSPAMM is the tags last longer, and thus both systole and diastole may be tagged. Each pulse sequence balances speed against signal to noise ratio.

Analysis of tagging is now semi-automated. Tags are usually subjected to two dimensional Fourier transformations, which results in several spectral peaks. Fourier analysis gives both amplitude and phase of the frequencies, allowing the signal to be expressed as a vector (see Figure 1-11 Analysis of a CMR tagged image). Isolating an off-origin spectral peak from each image, and inverting the Fourier transformation of this peak results in a harmonic image (see Figure 1-12, Figure 1-13, Figure 1-14, Figure 1-15, Figure 1-16, Figure 1-17). Harmonic images are advantageous in that they involve a sinusoidal pattern with a sine and cosine image. A harmonic image has both real and imaginary images, and two components: magnitude and phase. The frequency of the harmonic image reflects strain. Compression (systole) results in the peaks moving closer together, and relaxation results in the crests moving apart.

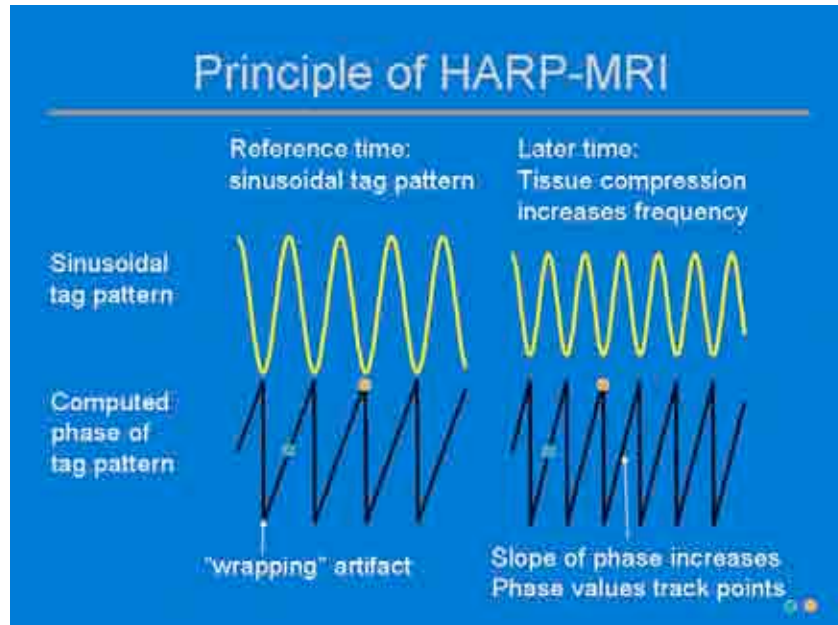


Figure 1-11 Analysis of a CMR tagged image

The signal has a sinusoidal pattern, which is converted into a phased image, where the slope changes with compression and expansion of the signal.

time = 0



time = 320 ms

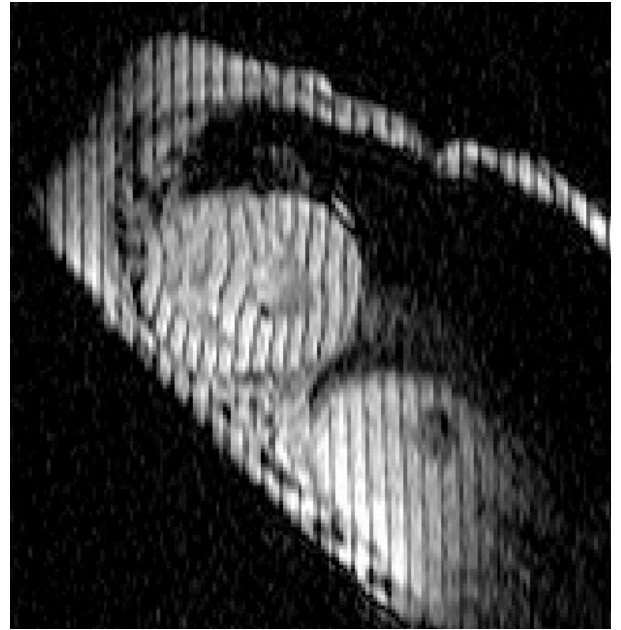


Figure 1-12 Vertical tags at two time points during the cardiac cycle

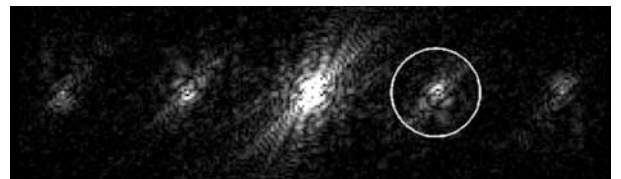
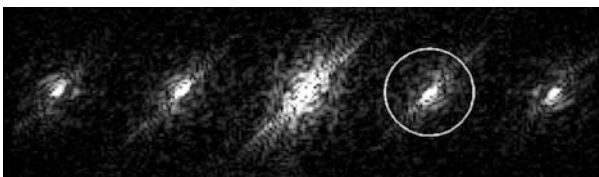


Figure 1-13 Central slab of the Fourier transform magnitudes taken from Figure 1-12

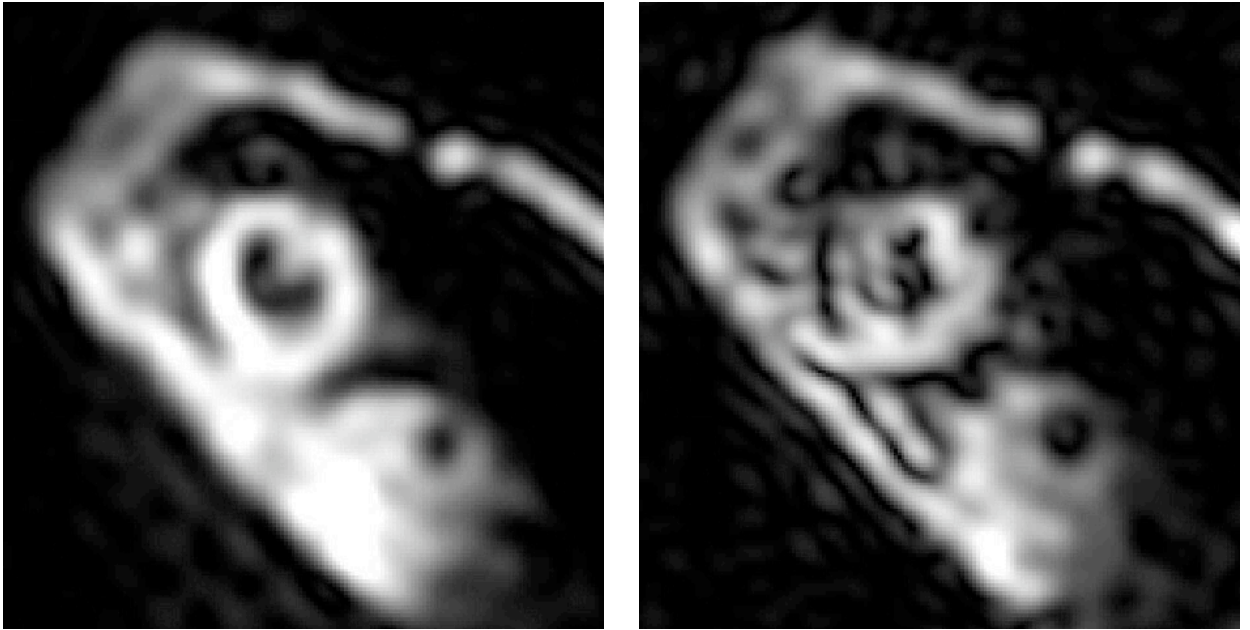


Figure 1-14 Harmonic magnitude images taken from figure 1-13



Figure 1-15 Mask derived from the harmonic magnitude images from figure 1-14

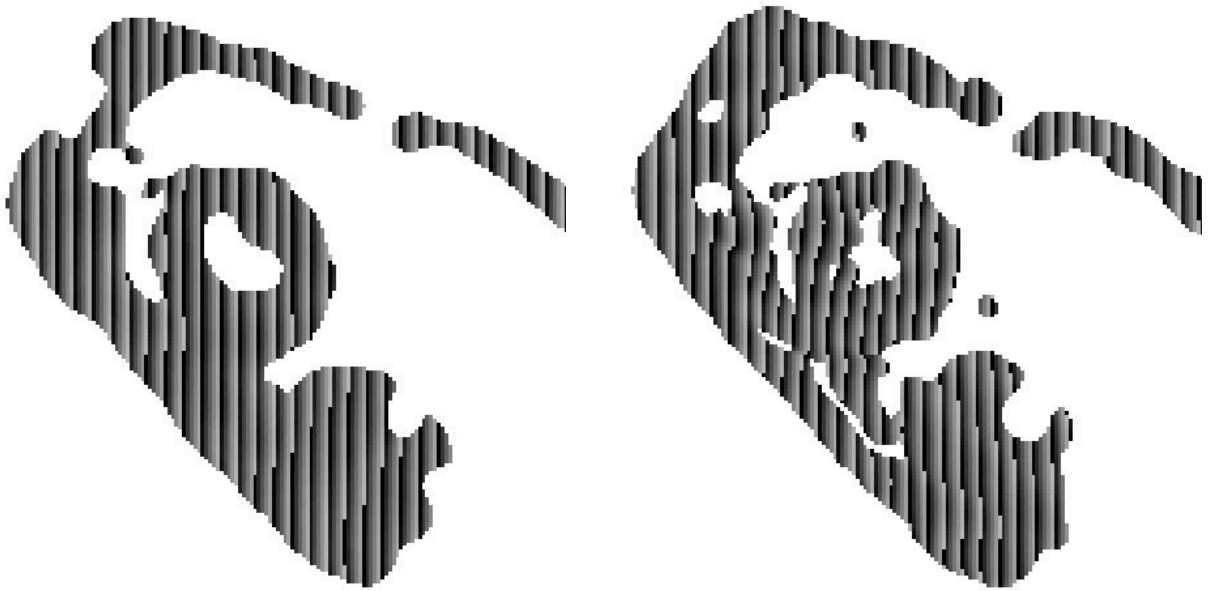


Figure 1-16 Harmonic phase images (masked).

The figures demonstrate the transformation from a vertical tagged image to harmonic phase images. Isolating an off-origin spectral peak from each image, and inverting the Fourier transformation of this peak results in a harmonic image

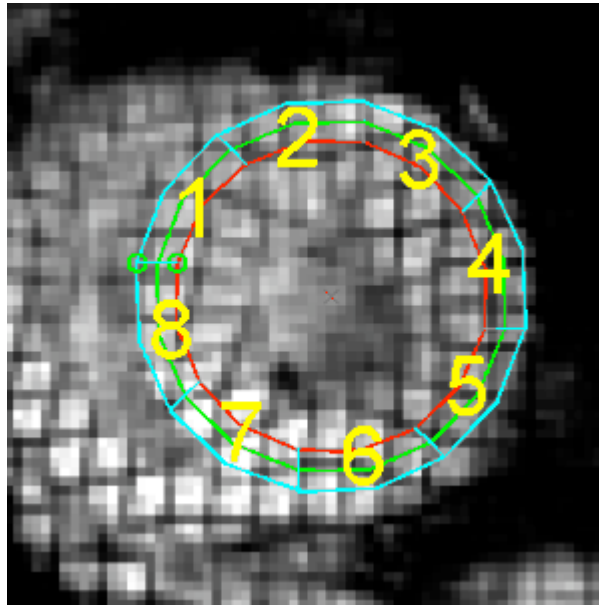


Figure 1-17 Annular mesh style tagged image

Endocardial (red) and epicardial borders (turquoise), midwall (green) of the left ventricle, segmented into octants.¹³

¹³ From www.iacI.ece.jhu.edu/projects/harp (accessed 1st September 2007)

Circumferential and radial strains are measured by determining the change in distance as the heart moves through the cardiac cycle. Eulerian strain can be determined from the harmonic phase magnetic resonance using two images at 2 different parts of the cardiac cycle. This can be calculated at all points in the cardiac cycle and this will result in a strain map. In addition circumferential, radial strains, minimal and maximal strains and the contraction angle can be measured. The spacing between the crests of the harmonic MRI is related to the slope of the harmonic phase, thus the strain can be calculated from the slope of the harmonic phase. Lagrangian strain is a measure of deformation and required 2 points to be identified (see Figure 1-18).

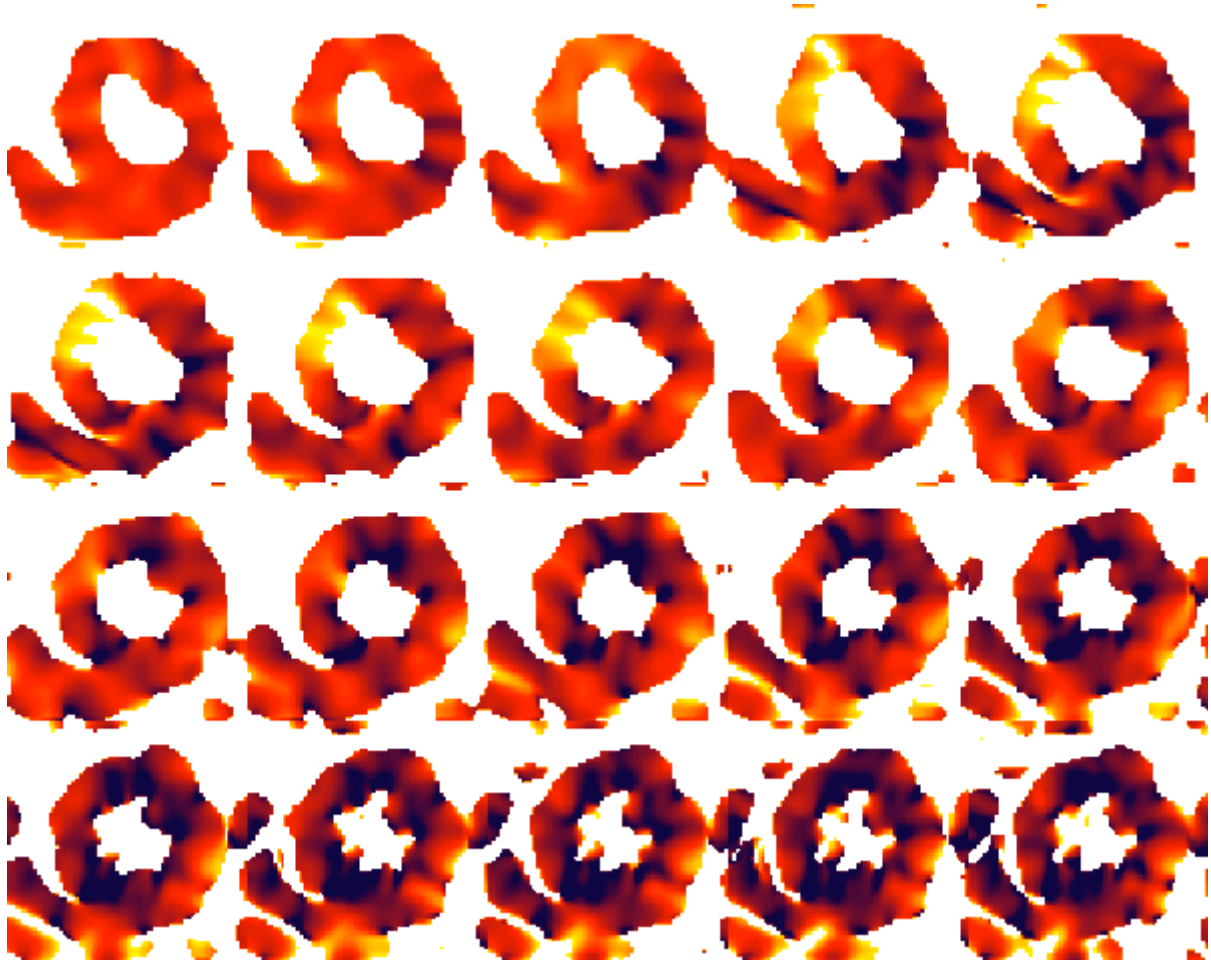


Figure 1-18 A sequence of Eulerian strain maps from a Canine heart

Red indicates circumferential shortening, yellow indicates stretch. A pacing lead is positioned at 5 o'clock, and stretching is seen at 10 o'clock.¹⁴

¹⁴ Reproduced from www.iacl.ece.jhu.edu/projects/harp. (Accessed 1st September 2007)

The time to onset of shortening (T_{onset} , in ms from the ECG R wave) is defined as the beginning of the circumferential strain curve, and may be determined semi-automatically.

The time to peak onset of shortening may also be determined, and as some patients will have multiple waves, the time to first peak and maximum peak may be determined.

(Zwanenburg et al., 2005) In normal hearts, left ventricular strain is highest at the base and decreases progressively towards the apex. (Moore et al., 2000) Strain and torsion were maximal in the endocardium and decrease from mid-wall to epicardium.

Tagged CMR can be used to measure dyssynchrony. Interestingly, tagged CMR suggests that TDI may have significant limitations in the analysis of dyssynchrony due to limitation inherent in analysis of longitudinal motion. (Helm et al., 2005) In a canine model, mechanical dyssynchrony was measured using three measures. These were the temporal uniformity of strain, regional variance of strain and regional variance vector (RVVPS) which combining strain magnitude and location. At each of 28 segments a time-plot of strain was made, and each plot subjected to Fourier analysis. A straight line indicates no dyssynchrony, whilst first order indicates perfect dyssynchrony (S1) (see Figure 1-19).

The effect of pacing on strain analysis was investigated. Longitudinal based motion only improved with BiV and not LV pacing. Circumferential analysis of strain showed improved synchrony during the whole cardiac cycle. Whereas, longitudinal based strain analysis during systole showed no improvement with LV pacing, and of borderline significance during diastole ($P = 0.04$). The RVVPS dyssynchrony score of circumferential motion improved with LV and BiV pacing. All 3 methods of dyssynchrony assessment based on longitudinal function found little resynchronisation

effect until diastole, whereas circumferential analysis demonstrated improvement in synchrony during systole and diastole with LV and BiV pacing.

The authors found that longitudinal strain had less than half the dynamic range of circumferential strain and had twice the intra-subject variability, making assessment difficult. Based on longitudinal assessment of strain, LV pacing did not appear to resynchronise the heart, whereas circumferential measures showed evidence of LV pacing induced resynchronisation. These findings suggest that TDI may have limited ability to discriminate between synchrony and dyssynchrony because of the limitations of longitudinal motion.

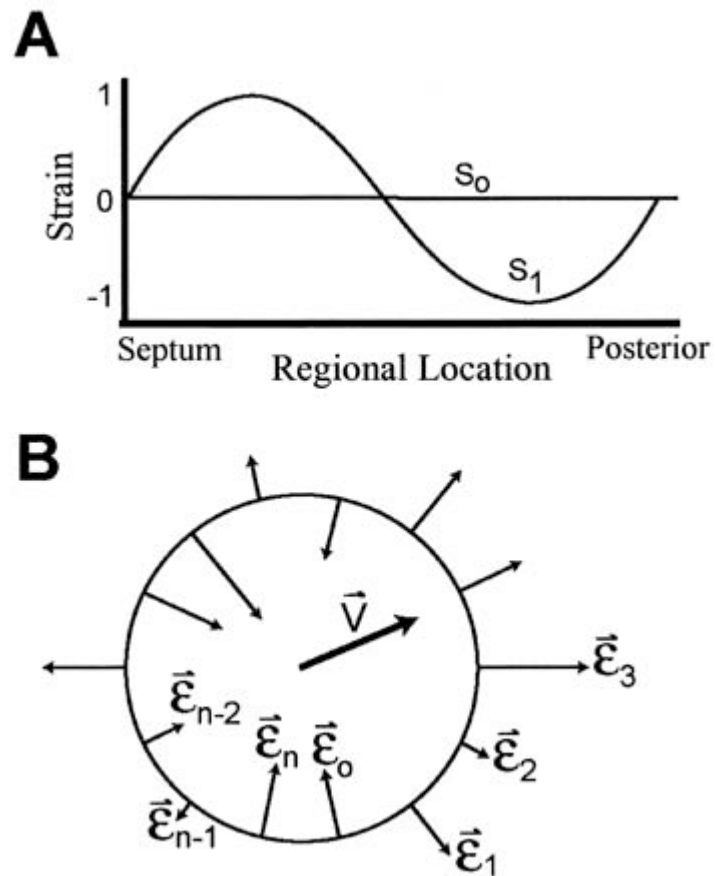


Figure 1-19 Mechanical dyssynchrony measured using temporal uniformity of strain, regional variance of strain and regional variance vector (combining strain magnitude and location)¹⁵

¹⁵ Reproduced from Helm, R.H., Lecquerq, C., Faris, Q., et al. (2005) Cardiac dyssynchrony analysis using circumferential versus longitudinal strain: Implications for assessing cardiac resynchronization. *Circulation*, 111: (21): 2760-2767. Reproduced with permission from Wolters Kluwer Health

Tagged analysis suggests that mechanical synchrony is more important than electrical synchrony. (Leclercq et al., 2002) Mechanical dyssynchrony was delineated using “circumferential uniformity ratio estimate” (CURE). Using this analysis, synchronous contraction gave a CURE value of 1, and dyssynchronous contraction gave a value of 0. Analysis of the electrical activation showed that atrio-LBBB pacing resulted in activation spreading from right to left, atrio-left ventricular pacing produced the reverse, and atrio-biventricular pacing caused electrical synchrony (see Figure 1-20). Left ventricular pacing resulted in the longest activation time. Electrical synchrony was impaired by left ventricular pacing as compared with biventricular pacing (see Figure 1-20, Figure 1-21.). Left ventricular and BiV pacing generated less early and late systolic stretch in the opposing wall compared with left bundle pacing.

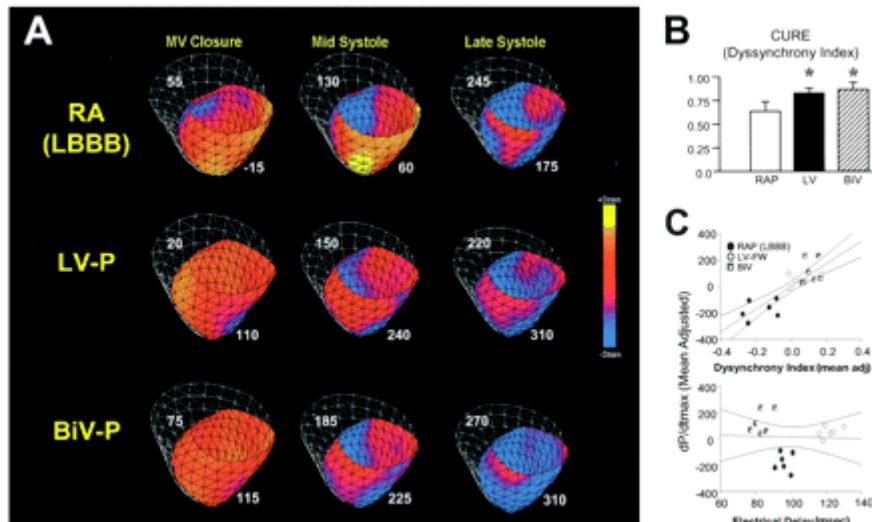


Figure 1-20 Mechanical activation maps for atrio-LBBB, atrio-biventricular and atrio-left ventricular pacing.

The colour bar indicates movement, with blue indicating shortening and yellow stretching. Biventricular and left ventricular pacing modes produced a significantly lower dyssynchrony index ($p < 0.001$). The CURE index correlated with dP/dt_{max} but not with electrical delay (inter-electrode maximal electrical dispersion).¹⁶

¹⁶ Reproduced from: Leclercq, C., Faris, O., Tunin, R., et al. (2002) Systolic Improvement and Mechanical Resynchronization Does Not Require Electrical Synchrony in the Dilated Failing Heart With Left Bundle-Branch Block. *Circulation*, 106: (14): 1760-1763. Reproduced with permission from Wolters Kluwer Health.

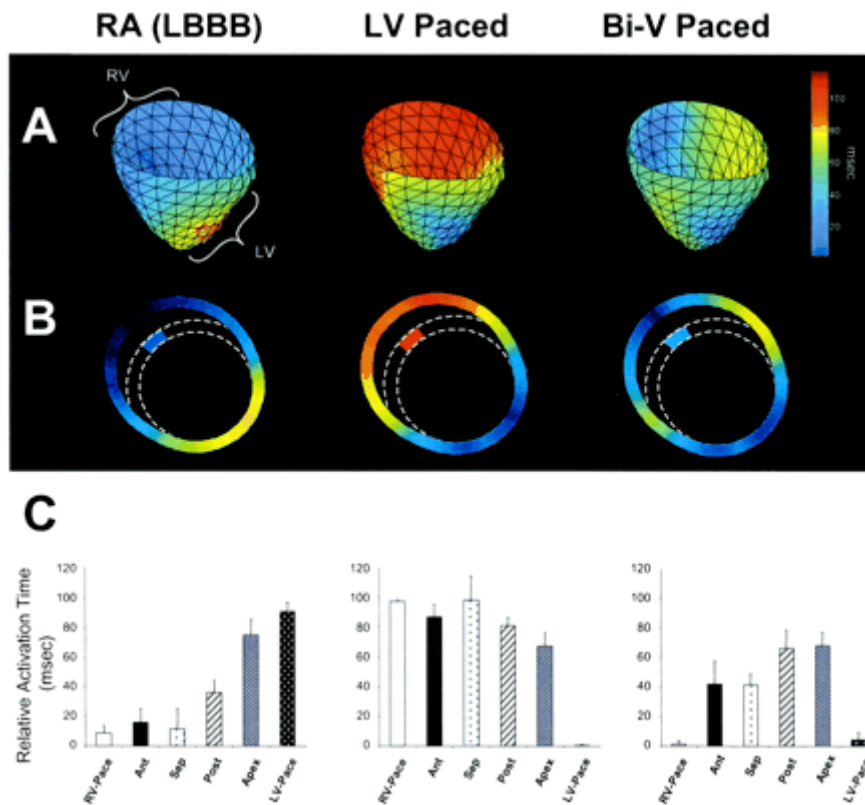


Figure 1-21 Electrical activation map derived from nylon mesh electrode array

The colour indicates the timing of activation, blue indicates early and red late activation. RA-LBBB shows right to left activation, with atrio-LV pacing showing the opposite pattern, and biventricular pacing showing more uniform activation. The relative activation time for each mode is shown for each mode.¹⁷

¹⁷ Reproduced from: Leclercq, C., Faris, O., Tunin, R., et al. (2002) Systolic Improvement and Mechanical Resynchronization Does Not Require Electrical Synchrony in the Dilated Failing Heart With Left Bundle-Branch Block. *Circulation*, 106: (14): 1760-1763. Reproduced with permission from Wolters Kluwer Health

Three dimensional strain analyses do not appear to offer advantages over 2D. (Tecelao et al., 2007) Three dimensional images were acquired by using an additional long axis scan, and then analysed by using HARP software (Diagnosoft, North Carolina). Strain, timing of circumferential shortening (time to onset, time to maximum first peak) were determined for each segment. The maximum peak shortening and the first peak of circumferential shortening were computed. The time to onset of circumferential strain was similar in normal subjects and LBBB on both 2D and 3D analysis. The coefficient of variance of circumferential shortening was used to determine dyssynchrony. The authors found no significant differences between 2D and 3D analysis, and thus 2D analysis will suffice.

1.11.2 Tagging and Ventricular Interaction

Right ventricular volume overload results in impairment of LV filling. (Vonk-Noordegraaf et al., 2005) It was hypothesised that long right ventricular contraction time is related to bowing of the inter-ventricular septum to the left, and thus impaired cardiac output. Pulmonary artery flow was measured to determine stroke volume and calculate the cardiac output. Right and left ventricular volumes were determined on cine imaging. The LV filling rate was inversely related to a decreased peak filling rate of the LV and stroke volume. This study demonstrates that LV filling is impaired resulting in a decrease in stroke volume, showing that pulmonary hypertension impairs diastolic ventricular interaction.

Ischaemic patients do not exhibit uniform patterns of strain onset. (Zwanenburg et al., 2005) The onset of shortening can be manipulated by pacing, whereas the time to maximal strain peak is the most common measurement of dyssynchrony. The first peak correlated best with time to onset of strain measured from the start of the R wave. In non-ischaemic patients the time to onset of strain propagated from septum to lateral wall, but there was no consistent pattern in ischaemic patients. The authors comment that the lack of a consistent pattern may account for the less reliable response to CRT as compared with patients without ischaemia.

Tagging has been used to determine the best site for LV lead implantation in an animal model, and this site may be the site of maximum dyssynchrony. (Helm et al., 2007) In this study, the optimum pacing area (> 70% peak response) covered 40% of left ventricular area in both controls and heart failure dogs. The optimal pacing site was situated on the lateral wall directed towards the apex, and was similar for failing and non-failing hearts. The circumferential uniformity estimate (CURE) index was 0.57 ± 0.08 at baseline, and when 90% of the maximum dP/dt was achieved, it increased to 0.87 ± 0.01 . The optimal CURE region was $32.2 \pm 6.6\%$ of the left ventricle, resulting in a CURE index of 0.81 ± 0.01 . Stroke work correlated with increasing CURE index ($r = 0.56$, $p < 0.0001$), and the lateral wall produced the greatest response in both measures. Apical pacing in all regions was more effective in terms of stroke work than basal regions ($p < 0.001$). The optimal pacing site in all hearts is situated at the mid to lateral apex. The site of maximal dyssynchrony is the area which if paced will result in the greatest haemodynamic improvement.

The apex appears to be the best site for LV leads. (Vanagt et al., 2005, Vanagt et al., 2004) which may be due to the onset of torsion at the apex prior to spreading through the heart up to the base.

One small acute haemodynamic study suggests that targeting the LV lead to the most dyssynchronous area results in the greatest acute improvement. (Nelson et al., 2000) The optimal pacing site depended on bundle branch block; patients with LBBB were best paced in the mid-lateral or antero-lateral coronary veins, and those with RBBB at the mid-right ventricular septum. Tagging analysis found a marked phase delay between early septal and late lateral shortening. On lateral wall contraction the antero-septum stretched, and akinetic transition zones were seen in the posterior wall. The greater the dyssynchrony, the greater the response seen in terms of maximum dP/dt measured.

Circumferential strain appears more reliable than longitudinal strain (see Figure 1-22). The amount of circumferential strain was three times greater than the longitudinal strain. (Waldman and Covell, 1987, Waldman et al., 1988) Radial strain cannot be assessed reliably due to insufficient myocardial tags. (Helm et al., 2005) A limitation of TDI measurements is the inclusion of not only longitudinal motion, but also torsion and translational movement. Contrasting Helm et al.'s study with Yu et al. experience, echocardiographic measures of longitudinal strain were poor at predicting response to CRT. The methods of determining strain and the relationship with outcome is shown in Figure 1-23.

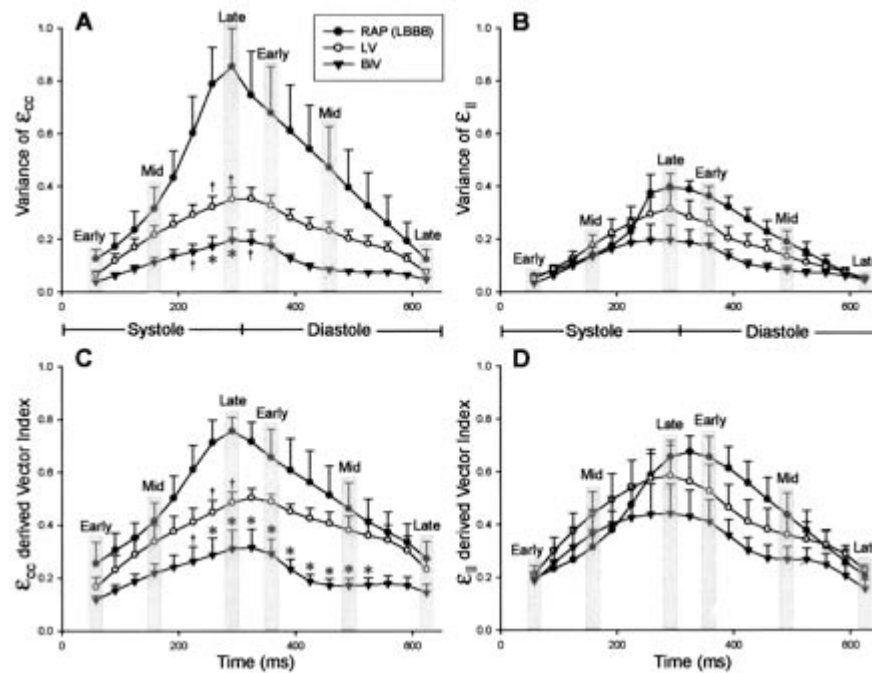


Figure 1-22 Time-dependent plots of cardiac dyssynchrony and resolution of dyssynchrony

Based on analysis of Eulerian circumferential strain (ϵ_{cc}) and Eulerian longitudinal strain variance (ϵ_{ll}) (A, B) and spatially weighted strain disparities (C, D). The strain variance rises (more dyssynchrony) and peaks at late systole and early diastole. For each pacing mode, LV and BiV are compared with RA (dyssynchronous) pacing at early, mid, and late time points in both systole and diastole (gray highlight). The time-dependent spatially weighed vector index (RVVPS) is also displayed for Eulerian circumferential strain and Eulerian longitudinal strain (C, D). * $P < 0.009$, † $P < 0.05$ vs dyssynchronous (RA pacing, LBBB) baseline.¹⁸

¹⁸ Reproduced from: Helm, R.H., Lecquerq, C., Faris, Q., et al. (2005) Cardiac dyssynchrony analysis using circumferential versus longitudinal strain: Implications for assessing cardiac resynchronization. **Circulation**, 111: (21): 2760-2767 Reproduced with permission of Wolters Kluwer Health

1.12 Left ventricular torsion analysis

The myocardium contracts in three ways during systole: longitudinally, circumferentially and as well as rotating. Tagged magnetic resonance imaging can demonstrate reduction of torsion in diseases of diastole such as aortic stenosis. Torsion analysis with CMR based tagging and TDI correlate well (see Figure 1-23, Figure 1-24). (Notomi et al., 2005) Rotation of the LV can be calculated on the basis of the average motion of the midwall points.

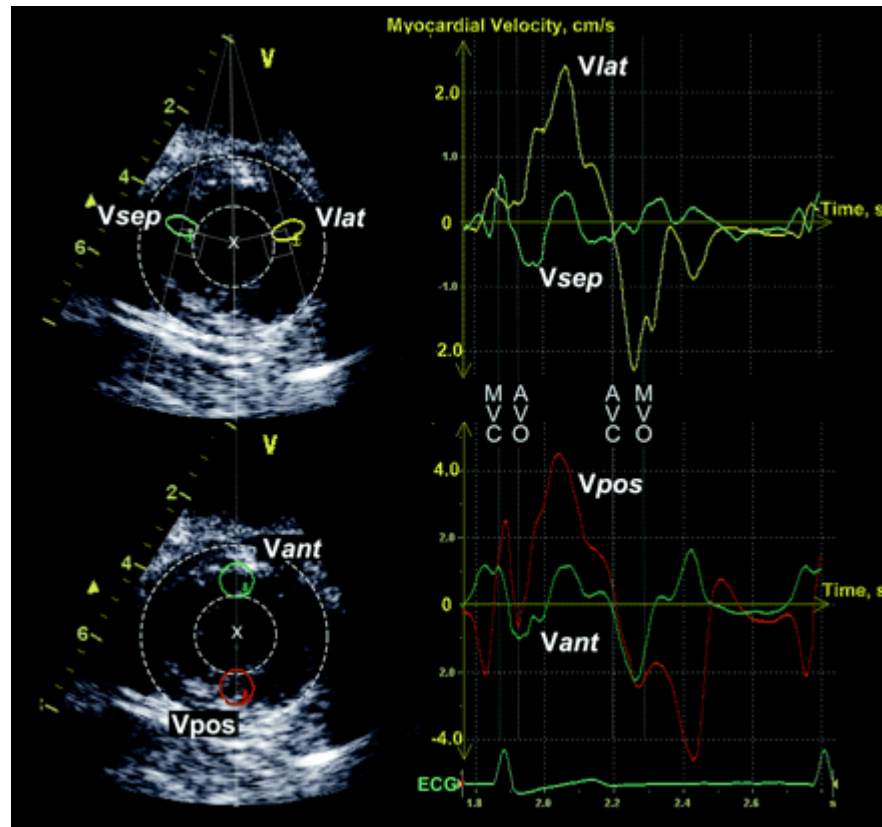


Figure 1-23 Myocardial velocity sampling regions and velocity profiles for LV rotation measurements (apical level).

Top panels: septal (V_{sep}) and lateral (V_{lat}) regions, difference of which yields rotational velocity (without radial component). Bottom panels: anterior (ant) and posterior (pos) regions, integral of which allows LV radius to be tracked (without any component of tangential motion). MVC and MVO indicate mitral valve closing and opening, whereas AVO and AVC indicate aortic valve opening and closing, which were determined by LV inflow and outflow Doppler profiles.¹⁹

¹⁹ Reproduced from Notomi, Y., Setser, R.M., Shiota, T., et al. (2005) Assessment of Left Ventricular Torsional Deformation by Doppler Tissue Imaging: Validation Study With Tagged Magnetic Resonance Imaging. *Circulation*, 111: (9): 1141-1147. Reproduced with permission of Wolters Kluwer Health.

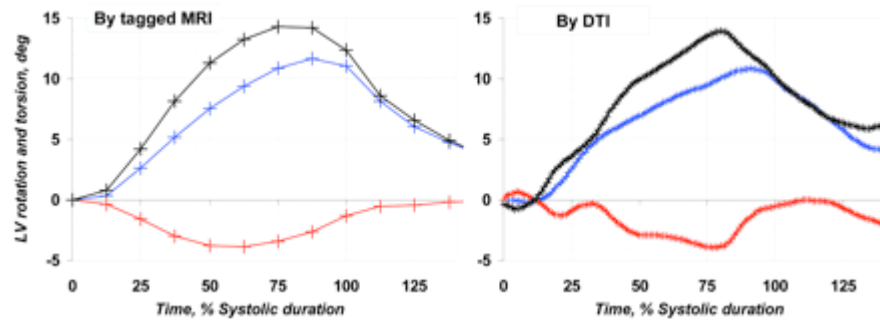


Figure 1-24 LV rotation profile by CMR and TDI in representative case.

Blue, red, and black lines indicate apical rotation, basal rotation, and LV torsion, respectively.²⁰

²⁰ Reproduced from Notomi, Y., Setser, R.M., Shiota, T., et al. (2005) Assessment of Left Ventricular Torsional Deformation by Doppler Tissue Imaging: Validation Study With Tagged Magnetic Resonance Imaging. **Circulation**, 111: (9): 1141-1147. Reproduced with permission of Wolters Kluwer Health.

Table 1-5 Methods of Determining Strain – Echo and MRI studies

Study	Patients	Follow Up	Strain Measure	Outcome
		(months)		
(Suffoletto et al., 2006)	50	8 ± 5	Difference in peak radial strain between anterior and posterior > 130ms	Increase in EF by 15% (89 sensitivity, 83 specificity)
(Breithardt et al., 2003)	18		Strain, strain rate	
(Becker et al., 2007)	47	3	Earliest and last peak systolic circumferential strain	Optimal lead position
(Dohi et al., 2005b)	38	Acute	Radial: Difference in peak strain anterior vs. posterior	Increase in EF by 15%. Cut off of 130ms – sensitivity 95% and 88% specificity
(Yu et al., 2004b)	54	3	Time to peak strain, SD of strain rate, Absolute and Maximal differences in strain	15% reduction in end systolic volume
(Dohi et al., 2006)	8 dogs	Acute	Radial strain, peak segmental strain, work	
(Kayano et al., 2006)	7	Acute	Strain (septal vs. posterior), regional strain	
(Helm et al., 2005)	7 dogs	Acute	Tagged circumferential and	Temporal uniformity of strain, temporal variance of

			longitudinal	strain, regional variance vector. Circumferential positive, longitudinal negative
(Leclercq et al., 2002)	7 dogs	Acute	Tagged circumferential	Circumferential Uniformity Ratio Estimate
(Tecelao et al., 2007)	5	Diagnostic	Tagged strain, circumferential shortening (time to onset, time to maximum first peak), Coefficient of variance	
(Zwanenburg et al., 2005)	29	Diagnostic	Tagging: Circumferential strain	Onset of strain, time to peak strain
(Prinzen et al., 1999)	7 dogs	Acute	Tagging	Circumferential strain, external work and total work
(Helm et al., 2005)	5 dogs RV paced, 5 dogs CCF	Acute	Tagging	Circumferential Uniformity Ratio Estimate, Time to peak circumferential strain
(Azevedo et al., 2004)	14 dogs	Diagnostic	Tagging Lagrangian circumferential strain, strain rate, peak strain, torsion, peak untwisting rate	
(Paetsch et	31	Diagnostic – stress	Tagging – circumferential	

al., 2005)		tagging for CAD	shortening, maximal lengthening velocity, mean rotation, untwist time	
(Nelson et al., 2000)	22	Acute	Tagging – midwall strain, Lagrangian strain, Circumferential strain, Coefficient of variance	Mean strain and strain variance useful
(Kramer et al., 1996)	28	5 ± 2 days post anterior MI	Tagging – percent circumferential shortening in endocardial, midwall and epicardial	Reduced shortening in basal lateral and trend to decreased shortening in mid-inferior wall

1.13 Predictors of response

Reverse remodelling has been postulated as a marker of response to CRT, and has become widely used in clinical studies. Reverse remodelling in heart failure trials of angiotensin converting enzyme inhibitors have shown that left ventricular end systolic volume is the strongest predictor of survival. (Konstam et al., 1992)

The use of left ventricular volume reduction as a surrogate for mortality in patients treated with CRT has not been conclusively proven. Heart failure studies in the era prior to CRT have demonstrated a decrease in LVESV correlates with improvement in survival. Beta blockers have been shown in echocardiographic studies (Doughty et al., 1997) and CMR imaging (Bellenger et al., 2004) studies to cause reverse remodelling in patients with heart failure. Reverse left ventricular remodelling is associated with increased survival. (H. D. White et al., 1987) However, an intervention which results in an improvement in ejection fraction does not necessarily translate into an improvement in mortality. (Packer et al., 1991) Furthermore, when heart failure is advanced, therapies may reduce neurohormonal activation but have little effect due to ongoing myocyte changes which become independent of neuro-hormones (Mann and Bristow, 2005). The use of reverse remodelling in the CRT population as a surrogate for mortality requires clarification.

A further issue regarding the use of left ventricular volumes in studies is the accuracy of the measurements. Left ventricular ejection fraction and volume measurements can be difficult to perform with accuracy. In a comparison of echocardiography with CMR analysis all patients in the study underwent two CMR and two echocardiograms, which were completed on the same day and within 60 minutes. (Grothues et al., 2002) The

results were analysed by two observers for each technique. To detect a 3% absolute change in ejection fraction by echocardiography in patients with heart failure would require 115 patients, and 14 by CMR, and to detect a 10ml reduction in end systolic volume would require 82 and 12 patients respectively. The coefficient of variability was 7.4% by CMR and 19.4% by echocardiography. This suggests that small studies which use left ventricular volumes determined using Simpson's rule as an end point, could be inaccurate.

Cardiac resynchronisation therapy results in reverse remodelling. (Yu et al., 2005b) The largest study of 141 patients found that baseline variables including QRS duration, NYHA class, 6 minute walk distance, quality of life score and left ventricular volumes were not significantly different between survivors and non-survivors. TDI dyssynchrony was significantly higher in survivors compared with those who died, 62.9 ± 47.3 ms vs. 28.3 ± 23.5 ms. At follow up, there was no statistical difference between those who survived and those who died in terms of change in NYHA class, 6 minute walk distance and quality of life scores. In this study, patients with the greatest dyssynchrony score had the best survival, (≥ 60 ms mortality 6.6% vs. < 60 ms 21.8%). ROC curve analysis found that a LVESV reduction of 9.5% was identified as the optimum cut off for predicting long term survival. 61.7% of the patients had a greater than 10% reduction in LVESV and were termed responders. 93% of the responders survived during follow up compared with 70.4% of non responders. Clinical response in terms of NYHA class, 6 minute walk distance and quality of life scores did not predict survival. It was concluded that this study demonstrates that reverse remodelling predicts survival benefit from CRT, consistent with previous studies of medical therapy. In view of the inaccuracies inherent

in measurement of EF, large scale studies are required to validate the cut off value of a 10% reduction in LVESV. Reverse remodelling is straight forward to measure, and is now widely reported in clinical trials of CRT.

1.13.1 Role of dyssynchrony in predicting response

Although difficulties remain in defining what is a response to CRT and what represents a failure of therapy, (Cleland et al., 2009) both in clinical practice and studies a definition of outcome is required. Clinical evidence supports the effectiveness of CRT to be related to the presence of dyssynchrony, the amount of scarring and viability, optimisation of atrio-ventricular pacing delay and diastolic ventricular interaction. There is no gold standard for measuring dyssynchrony, and early work by Xiou et al demonstrates that all patients with dilated hearts have evidence of dyssynchrony measured using signal averaged ECG when compared with normal QRS on the standard surface 12 lead ECG.

In this thesis, I intend to examine whether CMR based methods of determining dyssynchrony offer accurate determination of response. Cardiac magnetic resonance imaging offers the possibility of determining the aetiology of heart failure and prognosis after CRT in one examination.

It is likely that all patients studied in currently published clinical trials have dyssynchrony. Yet, at present, 70% of patients with heart failure are excluded from CRT on the basis of QRS duration of less than 120ms. However, Xiou et al have demonstrated that in patients with cardiomegaly, the surface QRS duration underestimates the true QRS. (Xiao et al., 1996) On the basis of experimental series, pacing patients with narrow

QRS heart failure, (Turner et al., 2004) and preliminary cohort studies, patients with narrow QRS heart failure may respond to CRT. (Bleeker et al., 2006b, Yu et al., 2006)

Recruitment of patients with severe dyssynchrony may reduce the detectable benefits of CRT. At extremes of dyssynchrony, there is a point beyond which reverse remodelling does not occur. (Bax et al., 2004b) The absence of viable myocardium is associated with a lack of reverse remodelling. (Bleeker et al., 2006c, White et al., 2006)

1.13.2 Scar Burden on CMR

The presence of myocardial scar detected on MRI has an adverse impact on prognosis in both ischaemic (Kwong et al., 2006) and dilated cardiomyopathy. (Assomull et al., 2006) Myocardial scar is delineated by scanning after injection of intravenous gadolinium. Gadolinium accumulates in oedematous area, resulting from loss of cell membranes and hence at sites of myocardial infarction. (Saeed et al., 1990) Increasing myocardial scar correlates with a poorer response in terms of NYHA class, 6 minute walk time and quality of life questionnaires. (White et al., 2006) In multi-variable analysis, only percentage of total scar by delayed enhanced CMR was predictive of clinical response to CRT. Using a percentage scar of 15% resulted in a sensitivity and specificity of 85% and 90% for clinical using ROC analysis, whilst septal scar less than 40% provided 100% sensitivity and specificity for response. (See Figure 1-25)

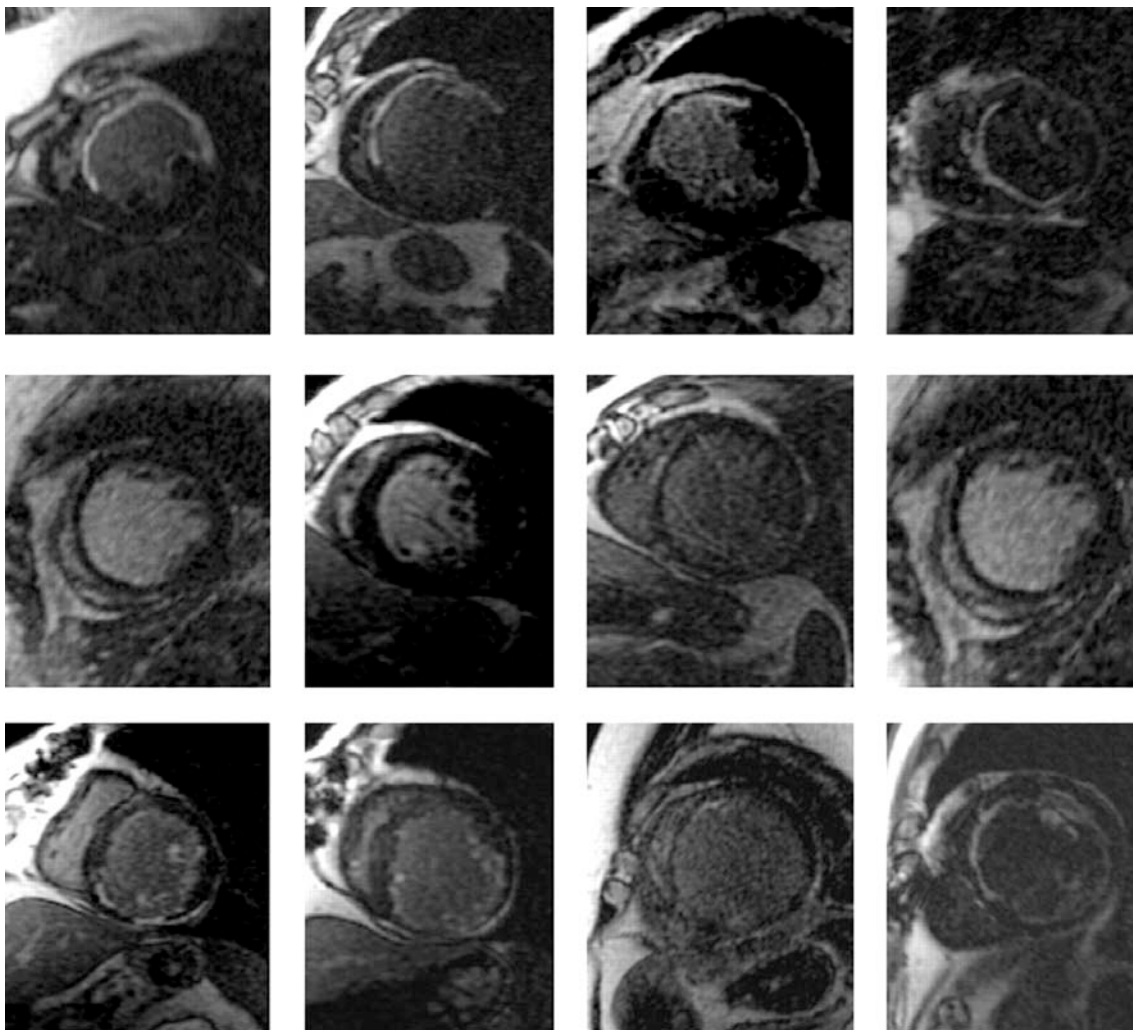


Figure 1-25 Scar imaging and response to CRT

Examples of scar distribution (bright signal) on delayed gadolinium enhancement magnetic resonance imaging from clinical non-responders (top row), responders without scar (middle row), and responders with scar (bottom row).²¹

²¹ Reproduced from: White, J.A., Yee, R., Yuan, X., et al. (2006) Delayed enhancement magnetic resonance imaging predicts response to cardiac resynchronization therapy in patients with intraventricular dyssynchrony. *J Am Coll Cardiol*, 48: (10): 1953-1960. with permission of Elsevier.

The location of scar is a key determinant of response. (Bleeker et al., 2006c) Patients with postero-lateral scar did not respond clinically or experience beneficial re-modelling in terms of improved left ventricular ejection fraction. TDI imaging found that the site of latest activation was the postero-lateral region in all patients. In this study, there was no optimisation of the left and right ventricular pacing parameters. In this study, a septal to lateral delay of greater than 65ms was taken as the criterion for dyssynchrony, with inter-observer and intra-observer agreement of 90% and 96%, respectively.

1.13.3 B-type natriuretic peptide and response

Heart failure results in activation of neuro-hormonal pathways. A sensitive marker of this activation is the serum B type natriuretic peptide (BNP). Mortality in heart failure is predicted by the level of BNP. In comparison with heart failure patients treated with best medical therapy alone, patients treated with CRT have reduced levels of BNP. (Fruhwald et al., 2007)

Baseline levels of BNP predict hospitalisation after CRT implantation. (Pitzalis et al., 2006) On multivariate analysis BNP at baseline (HR 2.09) and one month predicted those patients who would be hospitalised (HR 2.23). Higher baseline BNP levels were associated with adverse outcome.

Baseline BNP also appears to predict CRT response. (Lellouche et al., 2007) Indeed, BNP was the only significant predictor of response on multivariate analysis. The optimum cut off for predicting response was 447 pg/ml, which had a specificity of 79% and sensitivity of 62% in predicting response to CRT. The pre-implantation BNP was

significantly higher in patients with intra-ventricular dyssynchrony (845 ± 779 pg/ml vs. 248 ± 290 pg/ml). Thus, BNP was correlated with intra-ventricular dyssynchrony. Follow up BNP measurements appear to detect response to CRT. (Yu et al., 2005c) NT-proBNP reduction correlated with reduction in LVESV.

The available evidence suggests that BNP can be a sensitive marker of benefit from CRT, suggesting that CRT has a beneficial effect on decreasing neuro-hormonal activation.

1.14 Summary

The effect of CRT appears to be mediated by correction of dyssynchrony. Other factors are important, including correction of diastolic mitral regurgitation and DVI. Numerous echocardiographic methods of detecting dyssynchrony are discussed, but determination of outcome using these techniques appears problematic. CMR, using myocardial tagging appears to be promising, but little human data is available to validate the animal findings. Patients with myocardial scar do not appear to fare as well in the short term, but long term data are not available.

CHAPTER 2. CARDIOVASCULAR MAGNETIC RESONANCE
TISSUE SYNCHRONISATION INDEX (CMR-TSI)

2.1 Introduction

Dyssynchrony has been demonstrated in patients with systolic HF. However, the proportion of patients with dyssynchrony varies depending on the technique used to measure it. Early studies using M-mode echocardiography in patients with HF and LBBB demonstrated delay in the contraction of the posterior wall in relation to the septum. Thus, the link between electrical and mechanical delay was clearly established. The aim of cardiac resynchronisation therapy is to correct this electro-mechanical delay.

Although the exact mechanism by which CRT achieves its effect required further clarification, correction of dyssynchrony has been extensively studied. Identification of dyssynchrony could allow precise targeting of device therapy to achieve the greatest benefit. Clinical trials have shown that patients with symptomatic heart failure and poor left ventricular function may benefit from CRT, providing there is evidence of prolonged QRS duration. (Bristow et al., 2004, Cleland et al., 2005b)

It was shown using M-mode echocardiography that patients with dilated left ventricles and left bundle branch block pattern on the surface electrocardiogram had delayed activation of the posterior wall. (Xiao, 1994) TDI is now widely used to measure delay in activation of the left ventricle, and several authors have measured delay in activation of the left ventricle in an attempt to predict response to CRT. More recently, cohort studies of patients with mechanical dyssynchrony measured using TDI but without prolonged QRS (greater than 120 ms) have been found to respond to CRT. (Achilli et al., 2003, Bleeker et al., 2006b, Yu et al., 2006)

Identification of mechanical dyssynchrony in patients without evidence of conduction delay may result in benefit from CRT. However, the only randomised controlled trial of CRT in patients with cardiomyopathy undergoing ICD implantation, did not find a benefit from CRT in patients with a QRS < 120 ms at six months follow up. (Beshai et al., 2007)

Cardiac magnetic resonance (CMR) imaging is the gold standard for measuring left ventricular volumes and ejection fraction as measurements are made without geometric assumptions. (Jenkins et al., 2008) In contrast, echocardiographic images of patients with heart failure are often poor due to left ventricular dilatation which makes accurate assessment difficult, coupled with the problems of poor acoustic windows. The most accurate two-dimensional echocardiographic measure of ejection fraction, Simpson's methodology makes geometric assumptions.

Sophisticated echocardiographic techniques, such as tissue velocity imaging are angle dependent and inter-observer reproducibility is variable. Yu et al. compared heart failure patients with controls and found considerable overlap between patients and controls. (Yu et al., 2003b) CMR offers high quality images with good temporal and spatial resolution. We sought to measure left ventricular radial wall motion synchrony in normal subjects, to allow comparison with patients with cardiac failure. Short axis stacks of the left ventricle have been used to quantify segmental wall motion and thickening.

The assessment of cardiac dyssynchrony is becoming increasingly important in clinical practice. In patients with HF, echocardiographic studies using TDI have shown that intraventricular dyssynchrony is an independent predictor of clinical decompensation. (Bader et al., 2004) In the field of CRT, numerous studies have shown that cardiac

dysfunction results from mechanical dyssynchrony. (Burkhoff et al., 1986, Pak et al., 1998, Park et al., 1985) Accordingly, echocardiographic markers of cardiac dyssynchrony are being used to predict the response to CRT. (Auricchio and Yu, 2004, Kass, 2003, Nelson et al., 2000, Pitzalis et al., 2005, Søggaard et al., 2001, Yu et al., 2003a)

Echocardiographic studies, however, have shown a considerable overlap in measures of left ventricular dyssynchrony between healthy controls and patients with HF, (Yu et al., 2003b) suggesting that not all patients with HF have LV dyssynchrony. In the assessment of cardiac dyssynchrony, echocardiography provides excellent temporal resolution, but it is limited to imaging only a portion of the left ventricle. CMR may be more sensitive at detecting cardiac dyssynchrony as it can image the whole heart. We have used short axis stacks of the LV to quantify segmental wall motion. Time-to peak wall motion (T_{wm}) has been employed in the derivation of dyssynchrony scores, in a manner similar to echocardiographic methods. (Yu et al., 2003a) We have assessed these CMR-derived dyssynchrony scores, expressed in terms of the standard deviation (SD) of T_{wm} for all segments (CMR-TSI).

2.2 Methods

The methods used in this technique were first described by Chalil who described the technique, comparing heart failure patients and controls. In the same paper, the technique was validated against symptoms and clinical events in 77 patients with heart failure undergoing CRT. (Chalil et al., 2007d)

2.2.1 Cardiovascular magnetic resonance

All subjects underwent a CMR study. Images were acquired on a 1.5 Tesla General Electric Signa scanner using a phased array cardiac coil during repeated 8-second breath holds. A short axis stack of LV images was acquired using a steady state free precession (SSFP) sequence (repetition time 3.0 to 3.8 ms; excitation time 1.0 ms; image matrix 224 x 224; temporal resolution 27 to 34 ms; field of view 36 to 42 cm; flip angle 45°) in sequential 8 mm slices (2 mm inter slice gap) from the atrioventricular ring to apex. Left ventricular volumes, ejection fraction and mass (myocardial density=1.05 g/cm³) were quantified using manual planimetry of all short-axis SSFP cine images with MASS analysis software (Medis, The Netherlands). Each slice in the short axis stack was divided into 6 equal segments in a clockwise fashion (see Figure 2-1), with the first segment commencing at the junction between the inferior right ventricular free wall and the interventricular septum. This yielded up to 60 segments per patient (see Figure 2-2)

Each short axis slice in the short axis stack was divided into 100 cords in a clockwise manner, from the junction between the inferior right ventricular free wall and the interventricular septum (See figure 1). Radial wall motion was quantified for all cords at all phases in each R-R interval. The radial wall motion data (y) were fitted to an empirical sine wave function $y = a + b * \sin (t/RR + c)$. The mean segmental radial wall motion (a), the segmental radial wall motion amplitude (b) and the segmental phase shift of the maximum radial wall motion (c) were extracted from the fit. The CMR-TSI, a global measure of dyssynchrony, was expressed as the SD of all segmental phase shifts of the radial wall motion extracted from the fit.

Effectively, the CMR-TSI is based on the temporal dispersion of the time-to-peak inward endocardial motion. To assess the degree to which the fitted sinus curve agreed with the observed curve, the CMR data was fitted to increasingly complex harmonic models, starting with a zero order (naïve) model and then adding first, second and third order harmonic components in a stepwise manner. Higher than third order harmonic models were not explored, so as to avoid over fitting. For each modelling step, the full model was compared to the naïve model, to decide if the more complex model improved the model significantly and if this caused a substantial change in the first order phase shift. In all cases, the first order model was statistically superior to the naïve model ($p < 0.05$). Second order harmonic models did increase the goodness of fit in most cases, while third order models did only improve the fit in some cases. As expected, the first order phase was not altered by adding higher order components to the fit, while the overall shape of the motion curve was better described with higher order harmonic fits.

The wall motion in the six segments was plotted against time. (see Figure 2-3). Two examples are shown, comparing the heterogenous motion of the patient with HF and LBBB with the control participant. The data were exported to MatLab to create polar maps and four dimensional models (see Figure 2-4, Figure 2-5). The data were exported from Mass (Medis, The Netherlands) as an advanced report to R language to a bespoke program written by Berthold Stegemann, Principle Scientist at the Bakken Research Centre, Maastricht, The Netherlands.

The patients studied were undergoing CMR and some underwent CRT implantation for HF. The studies were analysed at different time points during the research program, hence the number of patients in each study varied.

2.3 Figure legends

Figure 2-1 shows the left ventricle sliced from base to apex, and then divided into 6 segments.

Figure 2-2 shows the intersection between the right ventricular free wall and the infero-posterior aspect of the left ventricle is used to denote the first segment, which then spread in a clockwise fashion around the left ventricle.

Figure 2-3 shows a plot of left ventricular wall motion against time in a control and a patient with heart failure and left bundle branch block. This illustrates the homogenous appearance of the wall motion in controls when compared with the heterogenous appearance seen in patients with heart failure and left bundle branch block, and illustrates the benefit of the spatial resolution afforded by CMR.

A three dimensional plot of the left ventricle with the time of peak wall motion superimposed, allowing comparison between the control (Figure 2-4) and a patient with heart failure and left bundle branch block (Figure 2-5). This image is produced in Matlab, and derived from the advanced reports produced in Mass. A four dimensional image illustrates the spread of wall motion over time.

Figure 2-1 Division of the left ventricular myocardium into slices

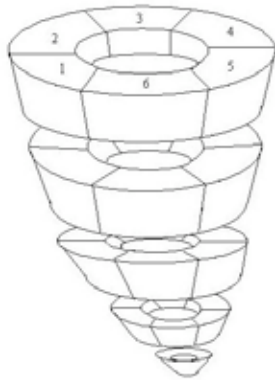


Figure 2-2 Division of the left ventricular myocardium slices into segments

This shows the junction between the interventricular septum and the right ventricular free wall delimits the beginning of segment 1 and the end of segment 6, counting clockwise. Wall motion in each segment is plotted over time in control patient, patient with heart failure and left bundle branch block.²²

Figure 2-3 Wall motion over time

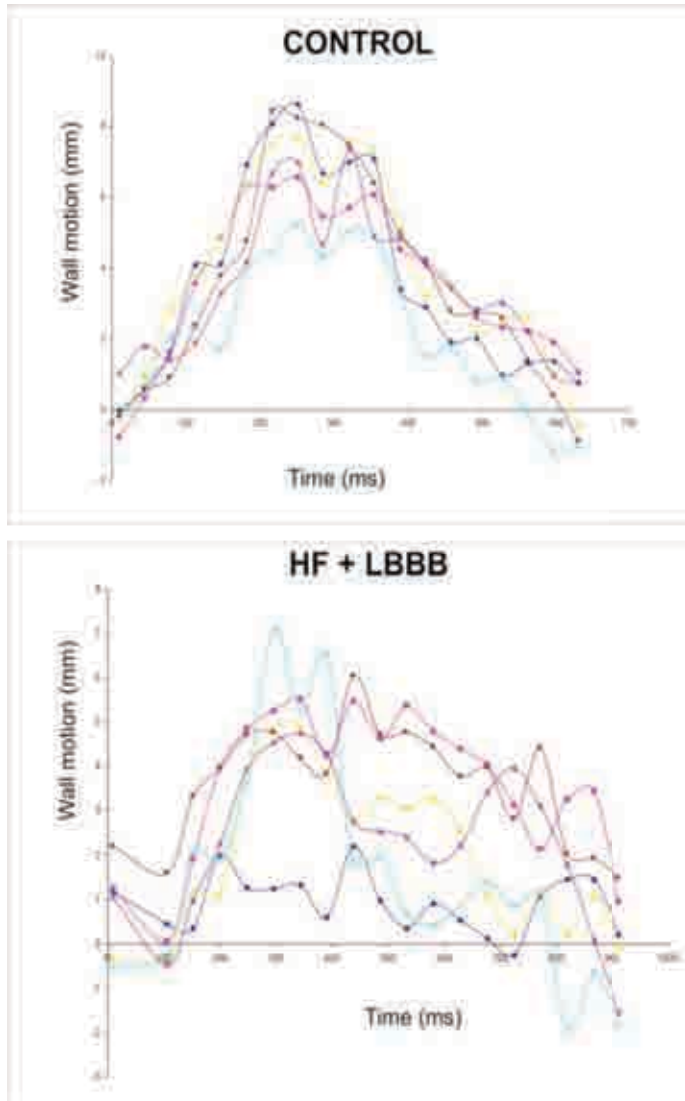


Figure 2-4 Three dimensional representation of the mechanical activation of the left ventricle in control

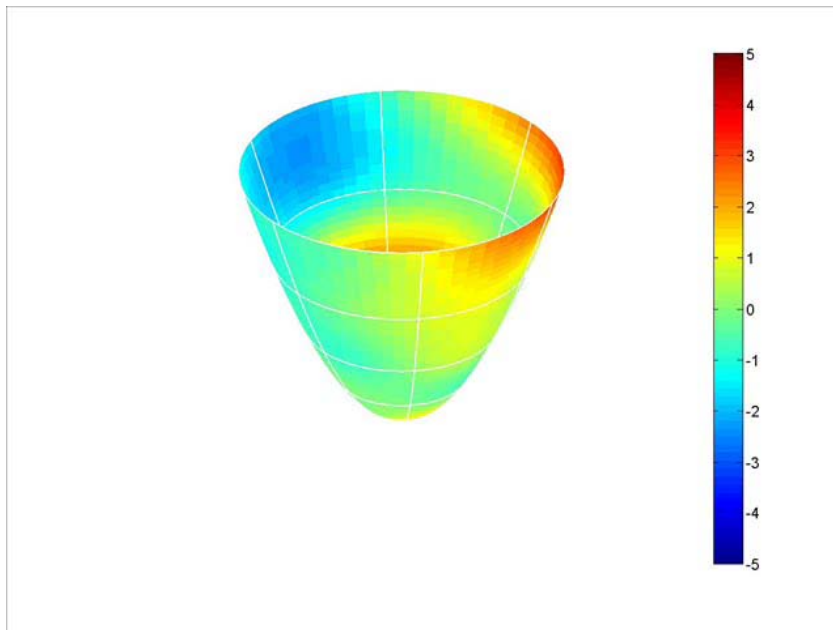
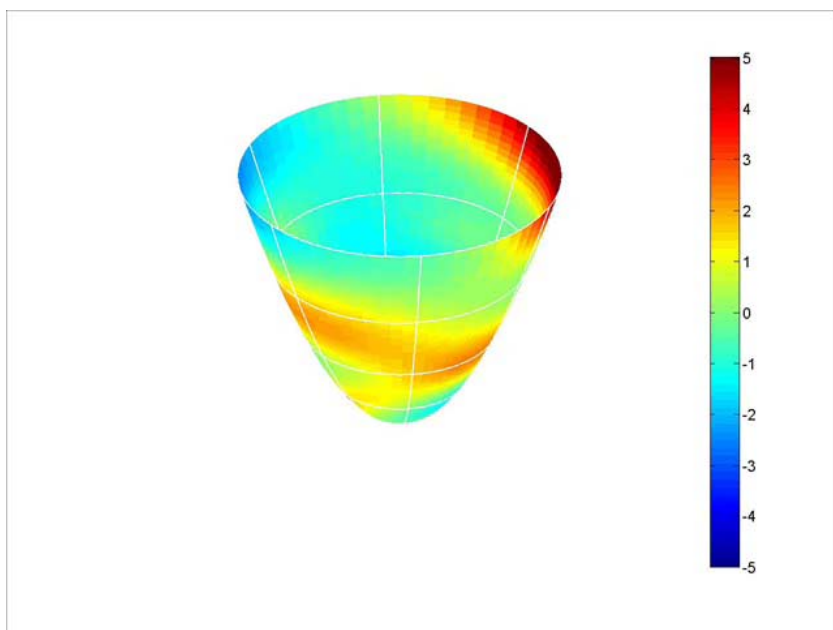


Figure 2-5 Three dimensional representation of the mechanical activation of the left ventricle in patient with HF and LBBB



**CHAPTER 3. LEFT VENTRICULAR FUNCTION AND
RELATION TO RADIAL DYSSYNCHRONY AND QRS
DURATION – A CARDIOVASCULAR MAGNETIC RESONANCE
STUDY**

3.1 Introduction

Dyssynchrony has been demonstrated to be present in many patients with systolic HF.

The relationship between HF and dyssynchrony is unclear, with some echocardiographic studies suggesting patients with HF and LBBB may not have any dyssynchrony. (Yu et al., 2003b) Furthermore, these studies suggest that mechanical dyssynchrony is present in only certain populations of patients with heart failure, with little relationship to QRS duration. (Yu et al., 2003b) Thus some patients with heart failure do not have dyssynchrony. The uncertainty about how to measure dyssynchrony and the conflicting results of studies using different methodologies has led to an epidemic of dyssynchrony has been declared. (Kass, 2008)

The importance of the role of dyssynchrony extends beyond the interest in the imaging modality used to determine its presence, into the role of cardiac resynchronisation therapy (CRT) as a therapy for patients with heart failure. Currently, QRS duration alone is used to determine selection for CRT, with conduction delay used as a surrogate for mechanical dyssynchrony, with selection criteria pivoting on a QRS duration of 120 ms. However, concern has arisen that CRT may not benefit to all patients who meet the current criteria, and screening for mechanical dyssynchrony would avoid implantation in patients who do not gain a symptomatic benefit or reverse remodelling with CRT, the so called “non-responders”. Others argue that clinical trials show that all patients undergoing CRT benefit in terms of survival, with no subgroup shown to be at a disadvantage from CRT, and that lack of change in symptomatology may simply reflect underlying disease. (Cleland et al., 2008b)

The current paradigm of CRT is that mechanical dyssynchrony is required to gain benefit from CRT, and the greater the dyssynchrony, the greater the benefit from CRT. Avoiding pacing patients without sufficient mechanical dyssynchrony has been proposed in an attempt to improve the symptomatic response to CRT. (Auricchio and Yu, 2004, Van de Veire et al., 2007) However, there have not been any randomised clinical trial to examine this hypothesis, and the only prospective blinded multi-centre observational clinical study was unable to identify a single echocardiographic factor that predicted a change in the clinical composite score or left ventricular reverse remodelling. (Chung et al., 2008) The question as to whether this is a limitation of the tissue Doppler technology, (Marwick, 2008) or one of trial design and methodology remains unresolved. (Yu et al., 2005a, Yu et al., 2009) Alternatively, the failure of the study could reflect a more fundamental issue, that detecting mechanical dyssynchrony is not helpful in selecting patients for CRT.

Cardiac resynchronisation therapy has been studied in patients with evidence of electrical conduction delay determined from the twelve lead ECG. The advantage of identifying patients with mechanical dyssynchrony despite a narrow QRS (QRS < 120 ms.) would be to support clinical studies of CRT in patients with heart failure and narrow QRS. Small scale, non-controlled and single centre studies have suggested that the benefits of extending CRT to patients with narrow QRS and evidence of mechanical dyssynchrony on echocardiography is similar to those with a broad QRS in terms of symptomatic and echocardiographic change. (Bleeker et al., 2006b, Yu et al., 2006) However, the only randomised controlled study of CRT in patients with narrow QRS did not find a benefit from CRT at six months follow up. (Beshai et al., 2007)

We sought to explore the relationship between electrical synchrony, measured using the QRS duration, left ventricular volumes and ejection fraction and compare these to mechanical synchrony measured using CMR-TSI.

3.2 Methods

3.2.1 Subjects.

The study group consisted of 225 patients with HF. Patients were referred for a CMR study in a single centre (Good Hope Hospital). The diagnosis of HF was made if symptoms of HF were associated with objective evidence of LV dysfunction on echocardiography, or if pulmonary oedema had been documented on chest radiography in the absence of valvular disease. The diagnosis of ICM was made if systolic dysfunction was associated with a history of myocardial infarction (Alpert et al., 2000) or if there was angiographically documented coronary heart disease (>50% stenosis in ≥ 1 coronary arteries). Late gadolinium enhancement CMR was also used to distinguish between ICM from NICM. (Assomull et al., 2006) Patients with LV dysfunction in combination with the finding of transmural or subendocardial late gadolinium uptake were classified as having ICM whereas patients with LV dysfunction and no gadolinium uptake, patchy uptake or midwall hyperenhancement were classified as having NICM. Control subjects consisted of 50 asymptomatic individuals (age 47.8 ± 15.4 yrs) who had no history of cardiac disease and a normal ECG, including a QRS duration <120 ms (78.4 ± 21.5 ms). The study was approved by the local Ethics Committee. 77 patients had been included in an earlier study which described the technique. (Chalil et al., 2007d)

3.2.2 Cardiovascular magnetic resonance

This was undertaken as described in chapter 2.

3.2.3 Septal to lateral wall motion delay

The septal-to-lateral wall motion delay (SLWMD) was defined as the time difference (in ms) between the time-to-peak inward wall motion of the septal and lateral segments, from base to apex. The observer was blinded to all other clinical details of the patients, including the outcome measures.

3.2.4 Spatial Distribution of Dyssynchrony

The CMR techniques described above permits visualization of radial wall motion throughout the entire LV. The radial wall motion data derived from each short axis CMR slices were colour-coded to construct radial wall motion polar colour maps. Values for radial wall motion were colour-coded from blue to red, with red denoting extreme delay in radial wall motion.

3.2.5 Scar Imaging

For scar imaging, gadolinium-diethylenetriamine pentaacetic acid (0.1 mmol/kg) was administered intravenously and images were acquired after 10 minutes using a segmented inversion-recovery technique in identical short-axis slices. Inversion times were adjusted to null normal myocardium (260 to 400 ms). Quantification of myocardial scarring was carried out by planimetry of hyper enhanced tissue on late-enhancement short-axis images. Infarct volume was calculated in cm^3 by multiplying the planimetry area in each segment by the slice thickness. Scar volume was expressed as a % of left ventricular myocardial volume in the diastolic phase. Satisfactory images were obtained in 220/225 patients with HF (125/130 patients with ICM). The observer was blinded to other CMR, echocardiographic and clinical data.

3.2.6 Statistical Analysis

Continuous variables are expressed as mean \pm standard deviation (SD). Normality was tested using the Shapiro-Wilk test. Comparisons between continuous variables were made using the unpaired Student's *t* test. Categorical data were presented as frequencies and were compared using the Chi-squared test and Fisher's exact post-hoc test. Linear regression and Pearson's correlation analyses were used to explore the relationship between continuous variables. Statistical analyses were performed using Statview (Cary, NC). A two-tailed *p* value of <0.05 was considered statistically significant.

3.3 Results

Ischaemic cardiomyopathy was associated with higher levels of mechanical dyssynchrony measured using CMR-TSI compared to patients with dilated cardiomyopathy, despite similar QRS duration and left ventricular ejection fraction. Only one patient had an ejection fraction of less than 35% and no dyssynchrony, defined as a CMR-TSI less than 30 (mean + two standard deviations). Echocardiographic left ventricular ejection fraction did not relate to CMR-TSI. There appeared to be an exponential relationship between CMR-EF and CMR-TSI, such that the worse the ejection fraction, the worse the dyssynchrony.

Compared to patients with a QRS <120 ms, patients in the QRS 120-149 ms and the QRS ≥ 150 ms groups were older, had a higher NYHA class and had higher LV volumes and a worse LVEF (Table 3-1). A greater proportion of patients in these groups had undergone CABG. Likewise, a greater proportion of patients in these groups were on

treatment with loop diuretics and spironolactone. In controls, there was no correlation between CMR-TSI and age ($r=-0.16$, NS).

3.3.1 Dyssynchrony and QRS duration

The distribution of CMR-TSI in healthy controls was narrow, at 21.8 ± 6.3 ms.

Compared to healthy controls, CMR-TSI was 3.4 times higher in the QRS <120 ms group (74.8 ± 34.6 ms), 4.2 times higher in the QRS 120-149 ms group (92.4 ± 39.4 ms) and 4.8 times higher in the QRS ≥ 150 ms group (104.6 ± 45.6 ms) (all $p < 0.0001$) (see Figure 3-1). Adopting a cut-off of 34 ms for the definition of dyssynchrony (21.8 plus 2 x SD for healthy controls is 34.4 ms), it was present in 68/75 (91%) patients with a QRS <120 ms, 71/75 (95%) patients with a QRS 120-149 ms and in 74/75 (99%) patients with a QRS ≥ 150 ms. On this basis, a total of 213/225 (95%) of patients with heart failure had dyssynchrony. If only patients in NYHA class III or IV were considered, dyssynchrony was present in 36/38 (95%) patients with a QRS <120 ms, 58/61 (95%) patients with a QRS 120-149 ms and 63/64 (97%) patients with a QRS ≥ 150 ms.

In contrast to CMR-TSI, the distribution of SLWMD in healthy controls was wider (50.8 ± 28.6 ms). Compared to healthy controls, SLWMD was 2.1 higher in the QRS <120 ms group (109.0 ± 82.6 ms $p=0.0022$), 2.9 times higher in the QRS 120-149 ms group (148.0 ± 104.8 ms, $p < 0.0001$) and 3.3 times higher in the QRS ≥ 150 ms group (168.5 ± 113.0 ms, $p=0.0004$).

As shown in Figure 3-1, however, there was a considerable overlap between the SLWMD in healthy controls and patients with heart failure. Adopting a cut-off of 99.4

ms for the definition of dyssynchrony (48.7 plus 2 x SD [2 x 25.4 ms] for healthy controls is 99.4 ms), dyssynchrony was present in 46% in the QRS <120 ms group, 62% in the QRS 120-149 ms group and 62% in the QRS \geq 150 ms group (168.5 \pm 113.0 ms). A total of 56% patients with heart failure had dyssynchrony on the basis of a SLWMD \geq 99.4 ms.

As shown in Figure 3-2, CMR-TSI correlated positively with QRS duration in patients with HF ($r = 0.35$, $p < 0.0001$). The correlation between SPWMD and QRS duration was also significant, although weaker ($r = 0.27$, $p = 0.0003$). As expected, there was a correlation between CMR-TSI and SLWMD ($r = 0.37$, $p < 0.0001$). The patients classified as dyssynchronous by CMR-TSI were not necessarily the same as patients classified as dyssynchrony on SLWMD (discordance rate: 45%).

3.3.2 Dyssynchrony and left ventricular function

Dyssynchrony was demonstrated in 170/174 (97%) patients with LVEF<35%. As shown in Figure 3-3, CMR-TSI was related to LVEF across the whole study population, governed by the exponential function $\text{CMR-TSI} = 178.3 \cdot e^{(-0.033 \cdot \text{LVEF})}$ ($p < 0.0001$).

Similar exponential relationships were observed in relation to LVEDV and LVESV ($p < 0.0001$). When all patients with HF were classified according to quartiles of scar size, the most extreme dyssynchrony was observed in patients with scars>75%. (Figure 3-4).

For patients such as those included in the CARE-HF study, namely patients in NYHA class III or IV with an LVEF<35% and a QRS \geq 120 ms, dyssynchrony was present in 132/133 (99%) patients.

3.3.3 Spatial distribution of dyssynchrony and QRS duration

As shown in Figure 3-5, patients with heart failure had a relatively heterogenous distribution of radial wall motion, with polar colour maps showing numerous 'patches' of radial wall motion throughout the LV. In patients with heart failure, the number of patches of late radial wall motion correlated positively with QRS duration ($r = 0.21$, $p = 0.0060$).

3.4 Discussion

The most salient finding from this study is that almost all heart failure patients with an ejection fraction of less than 35%, who currently meet criteria for cardiac resynchronisation therapy, exhibit dyssynchrony. This is in contrast to findings from echocardiographic techniques, which suggest that only certain patients exhibit sufficient dyssynchrony to benefit from CRT. (Bax et al., 2003a, Yu et al., 2003a) The relationship between increasing mechanical dyssynchrony and increasing ventricular conduction delay assessed using QRS duration appears intuitive, and is clearly seen with CMR-TSI, but not always with echocardiographic measures of dyssynchrony. (Yu et al., 2003b) Bleeker et al. noted dyssynchrony, defined as a septal to lateral wall delay in peak systolic velocity of 60 ms, in 20% of heart failure patients with a QRS less than 120 ms, 60% in those with a QRS of 120 to 150 ms, and 70% in those with a QRS greater than 150 ms. (Bleeker et al., 2004)

3.4.1 Left ventricular volumes

The greatest dyssynchrony was seen in patients with the lowest left ventricular ejection fractions and highest volumes. An exponential relationship between left ventricular volumes, ejection fraction and CMR-TSI existed. The equation $\text{CMR-TSI} = 178.3 e^{(-0.033 \cdot \text{LVEF})}$ explained the relationship between LVEF and CMR-TSI. Extreme dyssynchrony was therefore seen in those patients with the worst myocardial function.

A criticism of CMR-TSI is the relationship between CMR-TSI and LVEF, suggesting that CMR-TSI is simply a reflection of function. However, the CMR-TSI technique involves the timing of peak wall motion, rather than simply being a reflection of left ventricular volume. Furthermore, we have previously shown that CMR-TSI is independent of left ventricular volumes using multivariate Cox proportional hazard analysis. (Chalil et al., 2007d) However, in contrast echocardiographic studies using tissue velocity imaging found no relationship between left ventricular function, volumes and septal to lateral wall motion delay. (Bleeker et al., 2004)

3.4.2 Myocardial Scar

Left ventricular dyssynchrony was significantly higher in patients with myocardial scar. Furthermore, expressed as a percentage myocardium scarred, the CMR-TSI was significantly greater as the scar burden increased, suggesting that the disruption to myocyte function and electrical conduction after myocardial infarction results in mechanical delay. Again in contrast, Bleeker et al. found patients with ischaemic heart disease had less dyssynchrony than patients with dilated cardiomyopathy when assessed using septal to lateral wall motion delay on tissue velocity imaging. (Bleeker et al., 2004)

Clinical outcome studies of CRT have used an echocardiographic EF $\leq 35\%$ as an entry criterion. (Bristow et al., 2004, Cleland et al., 2005b) In this study we have demonstrated that patients who meet the current clinical guidelines for CRT have dyssynchrony.

Furthermore, we found that left ventricular volumes were also subject to an exponential function, such that extreme dyssynchrony relates to extreme left ventricular dilation.

These findings suggest that the most extreme dyssynchrony is found in those with the worse cardiac function.

Reviewing the current literature surrounding CRT, of which the majority is based on echocardiography, suggests that the greater the dyssynchrony, the greater the benefit from CRT. (Bax et al., 2003a, Yu et al., 2004a) However, on the basis of this study, the paradigm that “dyssynchrony is good” (at least for patients treated with CRT) is counter-intuitive, when the most extreme dyssynchrony is associated with extreme left ventricular dysfunction and myocardial scarring. We and others have previously found that myocardial scar predicts a worse outcome after CRT. (Ypenburg et al., 2007b) Possibly those patients with the greatest dyssynchrony fare the worst in terms of morbidity and mortality. Consistent with these observations, Bax et al. demonstrated using tissue velocity imaging that beyond a posterior to lateral delay of 100 ms, there is no benefit from CRT in terms of reverse left ventricular remodelling. (Bax et al., 2004b) Similarly, findings in patients with heart failure untreated with CRT have found that extreme intra-ventricular dyssynchrony measured with tissue velocity imaging had the greatest risk of heart failure decompensation. (Cho et al., 2005) An alternative paradigm for CRT is suggested, that all patients with moderate to severe systolic heart failure have intra-

ventricular radial dyssynchrony, and that those with little response to CRT are those with the worst left ventricular function and the greatest volume of myocardial scar.

3.4.3 Relationship between QRS duration and dyssynchrony

The lack of symptomatic improvement to CRT in some patients with heart failure despite a QRS > 120ms has raised concern that the electrocardiogram is not sufficiently robust to measure dyssynchrony. (Perry et al., 2006) Perry et al. found that dyssynchrony was present in 65% of patients with systolic heart failure and a QRS < 120 ms, and 58% of patients with a QRS >120msec using a definition of time to peak systolic contraction, measured with TVI, greater than 105 milliseconds in opposing ventricular walls. Yu et al (Yu et al., 2003b) found that 3% of healthy controls had dyssynchrony, measured using the 12 segment TVI model, but as many as 36% of patients with a QRS \geq 120 ms and 57% of patients with a QRS<120 ms did not.

The relative importance of mechanical and electrical dyssynchrony and electro-mechanical coupling have not been resolved. It is possible that mechanical dyssynchrony may be more important than electrical dyssynchrony. Using tissue Doppler imaging, Yu et al. examined a 12 segment model of the left ventricle, and found that dyssynchrony was present in only 73% of patients with heart failure and a QRS > 120 ms. (C. M. Yu et al., 2003b) Our findings that 99% of patients with HF and an EF of less than 35% had dyssynchrony is in contrast to these and others findings using TVI. In relation to patients with HF and a QRS < 120 msec, TDI studies have suggested a prevalence of dyssynchrony of between 36 to 65% of patients, depending on the methodology. (Bleeker et al., 2004, Perry et al., 2006, Uchiyama et al., 2005, Yu et al., 2003b) When CMR-TSI

is used to measure intra-ventricular dyssynchrony, the prevalence in this study was much higher at 91% in patients with HF and a QRS < 120ms.

The discrepancy between echocardiography and CMR based studies of dyssynchrony may be explained by a number of factors. The CMR-TSI technique takes into account wall motion affecting the whole ventricle, whereas echocardiographic techniques are limited to parts of the left ventricle. CMR-TSI is based upon radial wall displacement, rather than longitudinal velocities. Studies of TDI have found greater inter-observer variability (interobserver coefficient of variation of 33.7% for 12 segment model) (Chung et al., 2008), where-as it is much lower (9%) for CMR-TSI. (Chalil et al., 2007d) The PROSPECT study found large variations in the different echocardiographic techniques used to detect dyssynchrony. (Chung et al., 2008)

The correlation between prolonged QRS and mechanical dyssynchrony is not consistent. QRS prolongation results in delayed left ventricular activation, and CMR tagging studies suggest that this is usually in the postero-lateral region. (Auricchio et al., 2004) Radio-nucleotide phase analysis has reported a correlation between QRS duration and intra-ventricular dyssynchrony, (Fauchier et al., 2002, Fauchier et al., 2003), although others have reported only a weak linear correlation. (Marcassa et al., 2007) In comparison, whilst one TDI study described a mild correlation (Haghjoo et al., 2007), many have not. (Bleeker et al., 2004, Perry et al., 2006, Yu et al., 2003b) Recently, Donal et al. reported a correlation between QRS duration and radial dyssynchrony using both two dimensional speckle tracking and tissue velocity imaging in heart failure patients with dilated cardiomyopathy, but not in patients with ischaemic cardiomyopathy. (Donal et al., 2008)

In this study QRS duration correlated ($r= 0.35$, $p<0.0001$) with CMR-TSI in patients with heart failure.

3.4.4 Implications for CRT in narrow QRS

The striking finding that the majority of patients with heart failure and narrow QRS (<120 milliseconds) exhibit dyssynchrony when measured with CMR-TSI suggest that CRT may have a role in treatment of patients with heart failure and a QRS < 120 milliseconds.

However, studies of CRT in patients with narrow QRS heart failure have reported mixed outcomes. The RETHINQ study comparing CRT-D to ICD therapy in patients with NYHA class III or IV heart failure and QRS < 130 milliseconds reported no improvement in peak metabolic activity, six minute walk test or quality of life at six months follow up, although there was a trend to improvement in NYHA class, which did not meet statistical significance. (Beshai et al., 2007) Yu et al. noted an improvement in NYHA class, six minute walk distance, quality of life and significant reverse remodelling in patients with heart failure and a QRS < 120 milliseconds. Switching off the therapy for four weeks resulted in reversal of the echocardiographic changes. (Yu et al., 2006) Single centre cohort studies have reported similar benefits, but have lacked a control group. (Bleeker et al., 2006b) In this study, we found the majority (91%) of patients and QRS < 120 milliseconds had radial dyssynchrony, which provides a basis for further studies of CRT in this population.

An acute haemodynamic study suggests that CRT in narrow QRS heart failure improves cardiac function. (Williams et al., 2009) However, the mechanism is not yet fully elucidated and may result from reduction of external constraint. It is likely that correction of dyssynchrony is not the only mechanism by which CRT exerts an effect.

3.5 FIGURE LEGENDS

Figure 3-1 Scattergrams of cardiovascular magnetic resonance tissue synchronisation index (CMR-TSI) in 50 healthy controls with a QRS <120 ms and in 225 patients with heart failure, grouped according to QRS duration;

Figure 3-2 Regression and correlation analyses of a) cardiovascular magnetic resonance tissue synchronisation index (CMR-TSI) and b) septal-to-lateral wall motion delay (SLWMD) in 225 patients with heart failure.

Figure 3-3 Regression analyses of CMR-TSI against parameters of left ventricular function

Figure 3-4 CMR-TSI in relation to scar size

Patients have been categorized according to strata of scar size.

Figure 3-5 Bull's eye maps of radial wall motion (colour bar indicates time in milliseconds)

Table 3-1 Clinical, electrocardiographic and magnetic resonance characteristics for patients included in the study, grouped according to QRS duration.

	QRS duration			<i>p</i>		
	A	B	C	B vs A	C vs A	C vs B
	<120 ms	120-149 ms	≥150 ms			
<i>N</i>	75	75	75			
Age, yrs	59.8 ± 11.6	66.5 ± 11.8	65.0 ± 11.9	0.0006	0.0078	NS
Gender, male (%)	57 (76)	55 (73)	56 (75)	NS	NS	NS
NYHA class, n (%)						
I	27 (36)	5 (7)	7 (9)			
II	10 (13)	9 (12)	4 (5)			
III	28 (37)	46 (61)	48 (64)			
IV	10 (13)	15 (20)	16 (21)			
As continuous variable						
*	2.28 ± 1.09	2.95 ± 0.77	2.97 ± 0.81	<0.0001	<0.0001	NS
Aetiology, n (%)						
ICM	41 (55)	43 (57)	46 (61)	NS	NS	NS
NICM	34 (45)	32 (43)	29 (39)	NS	NS	NS
Co-morbidity, n (%)						
Diabetes mellitus	7 (9)	15 (20)	8 (11)	0.0648	NS	NS
Hypertension	21 (28)	20 (27)	17 (23)	NS	NS	NS
CABG	5 (7)	18 (24)	13 (17)	0.0032	0.0444	NS
Medication, n (%)						
Loop diuretics	43 (57)	59 (79)	62 (83)	0.0051	0.0007	NS
ACE-I or ARB	64 (85)	66 (88)	62 (83)	NS	NS	NS
Spironolactone	11 (15)	31 (41)	31 (41)	<0.0001	<0.0001	NS

ECG variables

SR, n (%)	64 (85)	61 (81)	56 (75)	NSNS	NS
AF, n (%)	11 (15)	14 (19)	19 (25)	NSNS	NS
QRS duration, ms	94.2 ± 12.4	129.1 ± 10.6	169.6 ± 17.7	<0.0001	<0.0001 <0.0001

CMR variables

LVEDV, cm ³	184.5 ± 64.9	230.1 ± 88.9	266.6 ± 102.8	0.0016	<0.0001	0.0112
LVESV, cm ³	134.9 ± 63.0	181.2 ± 87.8	218.1 ± 100.4	0.0011	<0.0001	0.0087
LVEF, %	30.7 ± 13.2	24.6 ± 11.8	21.3 ± 9.2	0.0013	<0.0001	NS
% scar volume	21.5 ± 23.6	17.4 ± 21.3	18.3 ± 20.1	NS	NS	NS

p values refer to differences between the QRS<120 ms and the QRS≥120 ms groups. Continuous variables are expressed as mean ± SD. *, For functional class, statistical analyses were applied to NYHA class, expressed as a continuous variable. NYHA=New York Heart Association class. ICM = ischaemic cardiomyopathy; NICM = non-ischaemic cardiomyopathy; CABG = coronary artery bypass grafting; ACE-I=angiotensin converting enzyme inhibitors; ARB=angiotensin II receptor blockers; LVEF = left ventricular ejection fraction; LVEDV = left ventricular end-diastolic volume; LVESV = left ventricular end-systolic volume

Figure 3-1 CMR-TSI and QRS duration

CMR-TSI is on the y axis.

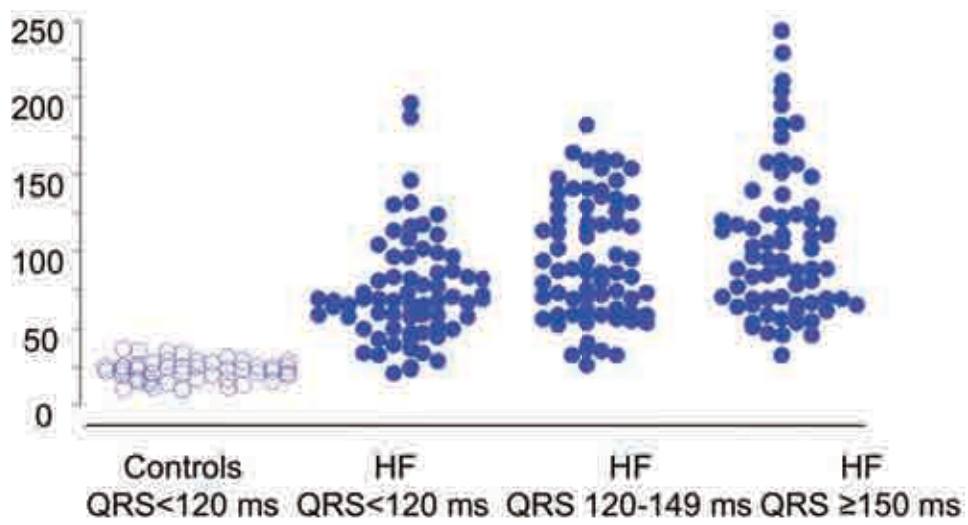


Figure 3-2 Correlation between CMR-TSI and QRS duration

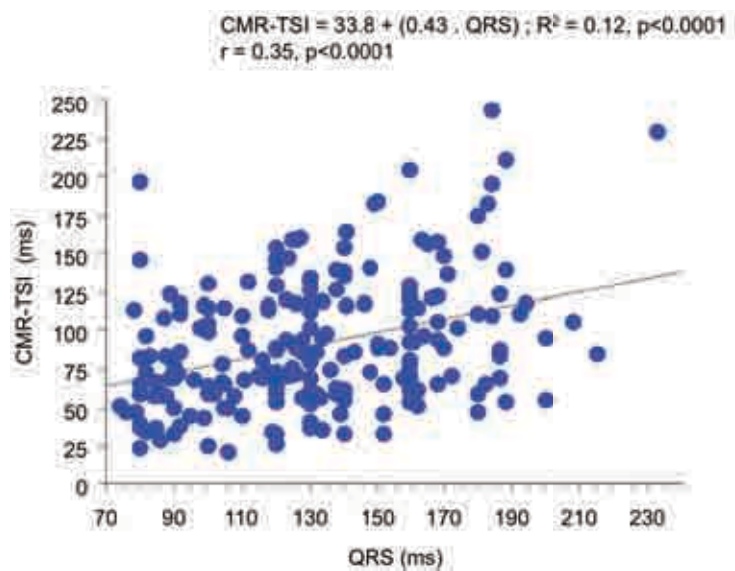
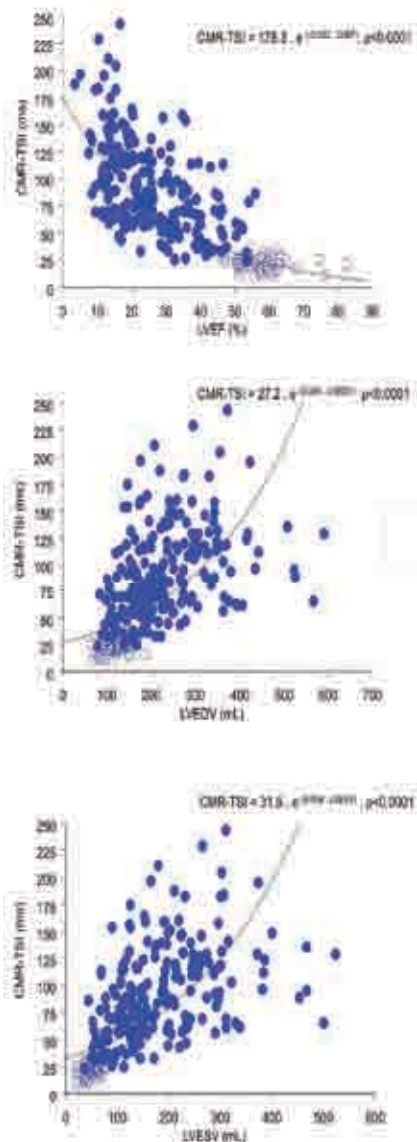


Figure 3-3 Regression analyses of CMR-TSI against parameters of left ventricular function²³



²³ CMR-TSI = cardiovascular magnetic resonance tissue synchronisation index; LVEF = left ventricular ejection fraction; LVEDV = left ventricular end-diastolic volume; LVSEV = left ventricular end-systolic volume in patients with heart failure (closed circles) and in healthy control subjects (open circles).

Figure 3-4 CMR-TSI in relation to scar size

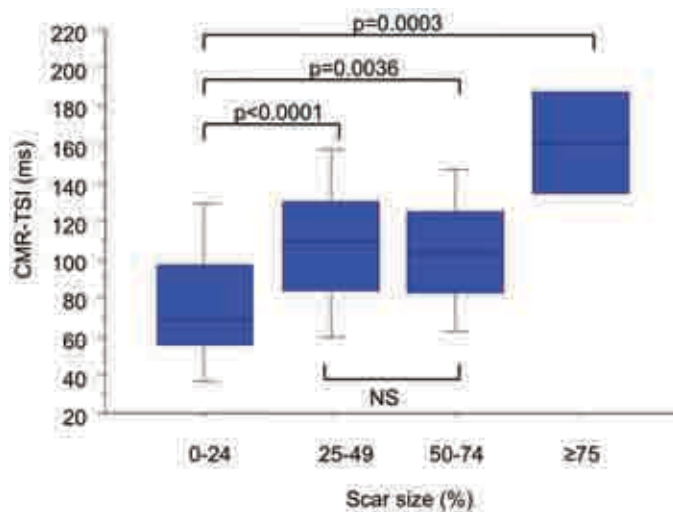
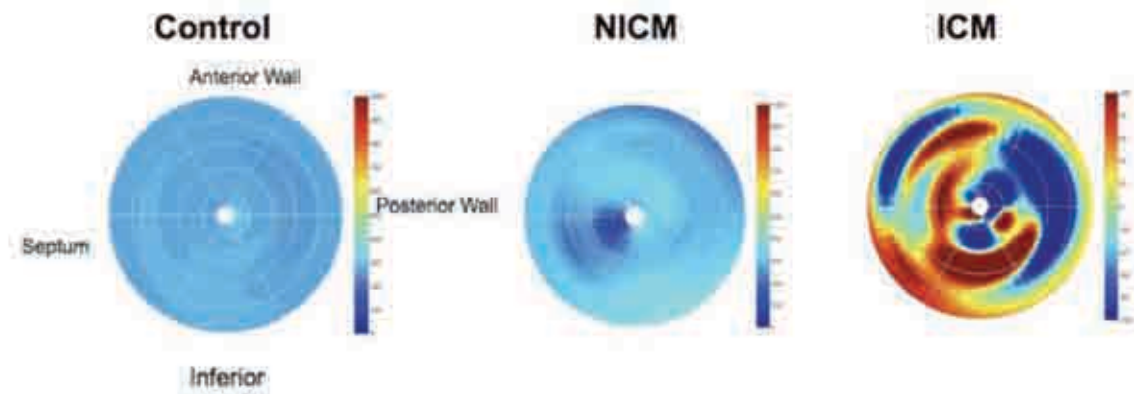


Figure 3-5 Bull's eye maps of radial wall motion²⁴



²⁴ Radial wall motion is colour-coded from blue to red, denoting early and late inward radial wall motion. The centre of the bull's eye relates to the left ventricular apex, whereas the outer perimeter relates to the base. Note the pattern of distribution in a healthy control, in patients with NICM and ICM.

CHAPTER 4. CMR-TSI PREDICTION OF OUTCOMES AND EVENTS

4.1 Introduction

Cardiac resynchronisation pacing improves survival and quality of life in patients with moderate to severe heart failure, ventricular conduction delay and impaired left ventricular function. (Bristow et al., 2004, Cleland et al., 2005b) One of the mechanisms by which CRT acts is to reduce left intra-ventricular dyssynchrony. However, some patients do not gain the expected symptomatic benefit of CRT or reverse remodelling despite ventricular conduction delay.

Echocardiographic studies have reported that a high proportion of these patients, those who do not experience negative remodelling, termed “non-responders”, do not have sufficient dyssynchrony, measured using advanced echocardiographic techniques such as TDI (Bleeker et al., 2006a, Yu et al., 2003a) and speckle tracking. (Ypenburg et al., 2008) Furthermore, some patients with normal left ventricular function have dyssynchrony when measured with TDI using the Yu twelve segment model, whilst a proportion of patients with left bundle branch block and impaired left ventricular function are not dyssynchronous. (Yu et al., 2003b) In contrast, we have found that dyssynchrony is present in almost all cases of heart failure when assessed with CMR. We therefore sought to determine the value of dyssynchrony in determined by CMR in predicting the response to CRT.

The aim of this study was to validate CMR-TSI against long term clinical-outcome in patients undergoing CRT. The clinical end-points used in this study were those used in the CARE-HF study. This study is a long term follow up study of CRT patients undergoing CRT.

4.2 Methods

4.2.1 Subjects

Participants were included if they met the criteria for implantation of cardiac resynchronisation pacing due to moderate to severe heart failure whilst treated with optimal tolerated medical therapy (QRS \geq 120 ms, ejection fraction \leq 35%, NYHA class III or IV). Patients in atrial fibrillation were included in the study. 153 participants underwent a pre-implant six minute walk test, Minnesota living with heart failure questionnaire and their NYHA class was documented. Written informed consent was taken prior to enrolment in the study. Ethics permission had been obtained from North Birmingham Research Ethics Committee, and the study was approved by the Research and Innovation Governance department. This was a long term follow up study, and included 77 patients who had originally been included in Chalil et al.'s paper which was the first description of this method of analysis of dyssynchrony. (Chalil et al., 2007d) Additional patients, clinical and echocardiographic follow up and clinical events were collected, extending the follow up by two further years.

4.2.2 Echocardiography

Standard two dimensional echocardiograms were acquired with Vivid 5, and 7 equipment and digital loops were recorded for offline analysis by observers blinded to the clinical outcome. Left ventricular ejection fraction was calculated as left ventricular end-diastolic

volume (LVEDV) – left ventricular end systolic volume /LVEDV *100 and expressed as a percentage.

4.2.3 Cardiovascular Magnetic Resonance

Images were acquired as described previously, and the CMR-TSI calculated.

4.2.4 Device Therapy

All patients underwent transvenous biventricular pacemaker implantation using standard techniques under local anaesthesia. Patients were entered into the study only after a successful implantation and were followed-up in a dedicated CRT clinic. None of the patients in atrial fibrillation underwent atrioventricular node ablation. Patients in sinus rhythm (n =122) underwent transmitral Doppler-directed optimisation of atrioventricular delay ((Ritter et al., 1999)) at every scheduled visit. Backup atrial pacing was set at 60 beats per minute, and the pacing mode was set to DDDR with no intraventricular delay. For patients in chronic atrial fibrillation (n=31), right ventricular and LV leads were implanted, and a Medtronic InSync III generator (model 8042, Medtronic, Minneapolis, Minnesota) was used, plugging the atrial port and programming the generator to a ventricular triggered mode. Generators used included the Medtronic InSync III, model 8040 8042, St. Jude Frontier (St. Jude Medical, St. Paul, Minnesota), Vitatron CRT 8000 (Vitatron B.V., Arnhem, the Netherlands), Biotronik Stratos (Biotronik GmbH, Berlin, Germany), and Guidant Contak Renewal TR2 (Guidant Corp., St. Paul, Minnesota).

4.2.5 Definition of events

After pacemaker implantation, patients were followed up in a dedicated cardiac resynchronisation clinic. At 6 weeks, 6 months and then 6 monthly thereafter patients underwent a 6 minute walk test, Minnesota Living with Heart Failure Questionnaire and echocardiogram. At each visit the NYHA class was documented.

As in the CARE-HF study, the clinical end points which considered were the composite of death from any cause or an un-planned hospitalisation for a major coronary event, which included cardiac transplantation. Hospitalisations for worsening heart failure, myocardial infarction, unstable angina, arrhythmia, stroke, pulmonary embolism, or upgrading to an implantable cardioverter-defibrillator were included in this endpoint. The first event was included in the analysis. The second end point considered was the composite of death from any cause and unplanned hospitalisation with worsening heart failure. The third endpoint considered was mortality from any cause. The additional endpoint of cardiovascular mortality was also considered. Sudden cardiac death was defined as “a natural, unexpected death due to cardiac causes, heralded by an abrupt loss of consciousness within one hour of the onset of acute symptoms”. (Myerburg and Castellanos, 1997) Mortality data were collected through medical records, death certificates and post-mortem data and, where appropriate, from interviews with patients’ care providers.

4.2.6 Statistics

Receiver-operating characteristic (ROC) curves were used to derive optimal cut off points of CMR-TSI for predicting cardiovascular events in patients undergoing cardiac

resynchronisation pacing in a group of 77 patients undergoing CRT-P. (Chalil et al., 2007d) The value of CMR-TSI with the optimum sensitivity and specificity was 110ms for all end-points.

The ability of CMR-TSI to discriminate between patients in the various risk categories at this cut off value was assessed using Cox proportional hazards analyses and Kaplan-Meier survival curves. Differences in survival curves between the groups were assessed using the log-rank (Mantel-Cox) test. Statistical analyses were performed using Statview (Cary, North Carolina) and SPSS 13.0 (Chicago, Illinois). A 2-tailed p value of 0.05 was considered as significant.

4.3 Results

4.3.1 Baseline Characteristics

The baseline clinical and CMR characteristics are shown in table 5.1. The patients were dichotomised according to the baseline CMR-TSI. There was no statistically significant difference in the age at implantation, underlying co-morbidities and baseline medical therapy use. More patients with ICM had CMR-TSI \geq 110ms than those with NICM. The mean QRS duration was significantly higher in the patients with CMR-TSI \geq 110ms. However, the proportion of patients in atrial fibrillation was similar in both groups.

The CMR data show that patients with CMR-TSI \geq 110ms had significantly greater left ventricular volumes, and poorer left ventricular function. The infarct volumes were also significantly greater in the group with CMR-TSI \geq 110ms. However, there was no

significant difference between the two groups in terms of echocardiographic left ventricular volumes and ejection fraction.

4.3.2 Symptomatic response to therapy

Table 5.2 shows the baseline and last available clinical and echocardiographic follow up status. The mean follow up was 429 ± 293 days. CRT was similarly effective in reducing NYHA class and improving six minute walk distance. The patients with $\text{CMR-TSI} < 110$ ms had the greatest symptom scores on the Minnesota living with heart failure questionnaire, but both groups improve with CRT, and at the last available follow up there was no significant difference in the symptom score. Overall the group with $\text{CMR-TSI} \geq 110$ ms did not experience left ventricular remodelling with CRT, unlike those with baseline $\text{CMR-TSI} < 110$ msec.

4.3.3 Survival after CRT

Figure 4-1 shows the Kaplan-Meier curves showing the survival after CRT dichotomised by CMR-TSI group, using the same outcomes as the CARE-HF study. (J. G. Cleland et al., 2001). The long term survival, censored up to a maximum of 2250 days, shows that patients with a baseline $\text{CMR-TSI} \geq 110$ ms have a significantly worse outcome in terms of overall mortality and hospitalisation for heart failure, cardiovascular mortality, and cardiovascular death and hospitalisation for heart failure.

4.3.4 Uni-variable and multi-variable predictors of outcome

Table 5.3 shows the uni-variable and multi-variable Cox Hazard analysis for the clinical endpoints in relation to CMR variables. CMR-TSI emerged as a powerful predictor of total mortality, total mortality and cardiovascular events, sudden cardiac death, heart failure hospitalisation. Left ventricular volumes and ejection fraction were not predictors. Indeed, CMR-TSI was independent of ejection fraction, left ventricular volumes and QRS duration on multi-variable analysis. In terms of predicting cardiovascular death, those patients with a CMR-TSI ≥ 110 ms were 5 fold more likely to die than those with a CMR-TSI < 110 ms.

4.4 Discussion

The most striking finding is the confirmation of the original findings by Chalil et al. that CMR-TSI in a large group of patients as a powerful predictor of the long term outcome in patients treated with CRT. Furthermore, this finding supports the hypothesis that severe dyssynchrony is a marker of adverse outcome in patients treated with CRT, consistent with previous work. (Chalil et al., 2007d)

This finding that severe dyssynchrony is associated with poor outcome is in contrast to echocardiographic studies which suggest firstly that not all cardiac failure patients are dyssynchronous, and secondly that those with the greatest amount of dyssynchrony benefit the most from CRT. However, given that there appears to be an inverse exponential relationship between ejection fraction, left ventricular volumes and CMR-TSI, the adverse outcomes associated with increasing dyssynchrony are unsurprising, reflecting poor left

ventricular function and a greater burden of ischaemic cardiomyopathy. Hence, the CMR-TSI is a marker not only wall motion, but is also a measure of left ventricular function reflecting the heterogenous and dyscoordinate left ventricular wall motion seen in advanced left ventricular dysfunction.

The recent multi-centre PROSPECT study has cast some doubt on the general applicability of these techniques as a wide inter and intra-observer reporting of the dyssynchrony findings, such that at the present time, the echocardiographic markers of dyssynchrony could not be used to select patients for CRT in routine clinical practice. (Chung et al., 2008) One explanation for this finding is the lack of expertise in some centres, such that acquisition of the images is not ideal. (Yu et al., 2009) However, Bax et al. noted that beyond a septal to posterior delay of 100 ms measured using tissue Doppler imaging, there was no significant reduction in LVESV, suggesting there is a limit beyond which CRT will not result in reverse remodelling. (Bax et al., 2004b) We found no significant change in EF in the patients with a CMR-TSI of greater than 110 ms. In addition, the outcome of patients with CMR-TSI greater than 110 ms was worse in terms of hospitalisations for heart failure and mortality. It appears that rather than dyssynchrony being a marker of good outcome after CRT, it is a marker of poor left ventricular function. Whilst all groups improved in terms of walk distance, quality of life and NYHA class, the improvement in NYHA class did not reach statistical significance in the patients with $\text{CMR-TSI} \geq 110\text{ms}$.

Cardiac resynchronisation therapy improves symptoms and clinical outcome. Although we have found that patients with greater dyssynchrony have a poorer outcome, we did demonstrate a significant improvement in six minute walk distance, quality of life and

NYHA class even in the group with $\text{CMR-TSI} \geq 110$ ms. This is keeping with other studies which have found that clinical improvement does not always reflect survival from CRT, (C. M. Yu et al., 2005b) and the lack of correlation between clinical and echocardiographic response. (Bleeker et al., 2006a) CRT has other effects in addition to correction of dyssynchrony, including reducing mitral regurgitation (Achilli et al., 2003, Bax and Poldermans, 2006, Nunez et al., 2002), improving diastolic ventricular interaction (Bleasdale et al., 2004) and correction of prolonged AV delay. In addition, the effectiveness of CRT may be governed by other factors such as left ventricular scar (Bleeker et al., 2006c) and heart rhythm. (Gasparini, 2008, Khadjooi et al., 2008) Our observation that CMR-TSI is highest in patients with ischaemic heart disease as compared to patients with non-ischaemic cardiomyopathy, and that scar burden is associated with increasing CMR-TSI may explain these findings. Thus, patients with ischaemic heart disease are more dyssynchronous than those with dilated cardiomyopathy.

4.4.1 QRS duration and CMR-TSI

The current guidelines for CRT select patients on the basis of evidence of electrical conduction delay, currently pivoting on QRS duration of 120ms. However, studies using TDI have not found a relationship between QRS duration and intra-ventricular dyssynchrony, (Yu et al., 2003b) whilst there does appear to be a weak correlation on the basis of pulsed Doppler measuring inter-ventricular delay. (Ghio et al., 2004) Clinical response to CRT is variable, with some patients deteriorating after implantation. (Chung et al., 2008) This is most likely due to the natural history of heart failure, which is supported by

evidence from the MUSTIC study, which found that more patients deteriorated without CRT than with CRT. (Cazeau et al., 2001) An alternative is failure of adequate resynchronisation or CRT causing worsening of dyssynchrony. As a result, the search for an improved predictor of response to CRT continues, with the hope that demonstrating mechanical dyssynchrony may be a better predictor than QRS duration. (Auricchio and Yu, 2004) Interestingly, CMR-TSI increases proportionally QRS duration, although the measurement of CMR-TSI is statistically independent of QRS duration. However, we found that QRS was unable to predict outcome in this study, either as a dichotomous (120 to 149ms, or ≥ 150 ms) or continuous variable. In contrast, Gasparini et al found patients with a narrow QRS (129 – 149ms) appeared to benefit more than those with QRS (≥ 150 ms) in terms of clinical progress after CRT. (Gasparini et al., 2003)

The intra and inter-observer variability for CMR-TSI is low, (Chalil et al., 2007d) and hence has greater potential application than other methods of measuring dyssynchrony, such as echocardiography. (Chung et al., 2008)

Cardiovascular magnetic resonance imaging of heart failure patients is becoming the expected standard of care providing information of structure, function, aetiology and prognosis in a single scan,(Germans and van Rossum, 2008) making CMR-TSI readily applicable. Other advanced CMR analysis techniques are available, including myocardial tagging and other indices of dyssynchrony, such as the CURE formula. (Bilchick et al., 2008) However, clinical validation of these techniques is awaited before widespread adoption. The CMR-TSI measure requires validation by other groups, preferably against clinical events rather than another imaging parameter.

4.5 TABLE LEGENDS

Table 4-1 Baseline clinical and cardiovascular magnetic resonance imaging characteristics for patients undergoing cardiac resynchronisation therapy

Table 4-2 Clinical and echocardiographic outcome at baseline and last available follow up

Table 4-3 Uni variable and multi-variable Cox proportional hazards analyses of clinical endpoints in relation to cardiac magnetic resonance variables according to imaging modality

4.6 FIGURE LEGENDS

Figure 4-1 Kaplan-Meier estimates of the time to the death from any cause or hospitalisation for major cardiovascular events, survival from cardiovascular death or hospitalisation for heart failure, survival from cardiovascular death or survival from death from any cause. Patients were stratified according to a pre-implant CMR-TSI (<110 msec or CMR-TSI \geq 110 msec). HF=heart failure.

Table 4-1 Baseline clinical and cardiovascular magnetic resonance imaging characteristics for patients undergoing cardiac resynchronisation therapy

	<i>ALL</i>	<i>CMR-TSI<110</i>	<i>CMR-TSI≥110</i>	<i>p</i>
<i>N</i>	153	92	61	
Male (%)	76.5	72.8	82.0	ns
Age, years	66.8 ± 10.4	66.3 ± 10.8	67.5 ± 9.8	ns
Aetiology (%)				
ICM	62.1	36.6	25.5	ns
NICM	38.0	29.6	8.4	0.006
Co-morbidity (%)				
Hypertension	28.1	29.3	26.2	ns
CABG	22.2	18.5	27.9	ns
Valvular heart disease	4.8	4.9	4.3	ns
Upgrade	1.3	1.1	1.6	ns
Diabetes Mellitus	17.0	14.1	21.3	ns
Medication (%)				
Diuretic	87.6	90.2	83.6	ns
ACE/ARB	92.8	93.5	91.8	ns
Beta-blocker	56.2	53.3	60.7	ns
Amiodarone	16.3	19.7	14.1	ns
Spirolactone	43.1	44.6	41.0	ns
ECG variables				
Mean QRS (ms)	144.5 ±	140.7 ± 28	150.1 ± 26.5	0.0408

	27.9			
AF (%)	20.9	19.6	23.0	ns
CMR variables				
Myocardial mass, g	106.56 ± 36.53	104.64 ± 33.59	109.6 ± 40.9	ns
Infarct volume (%)	19.1 ± 19.1	13.68 ± 15.2	27.7 ± 21.5	<0.0001
CMR End-systolic volume (mls)	201 ± 94.5	176.3 ± 91.8	238.2 ± 86.6	<0.0001
CMR End-diastolic volume (mls)	248.1 ± 98.2	224.5 ± 95	283.8 ± 93.1	0.0002
CMR Ejection fraction (%)	22.05 ± 9.9	25.32 ± 10.57	17.13 ± 6.2	<0.0001
CMR-TSI (ms)	102.4 ± 45.5	73.08 ± 21.5	146.7 ± 41.1	<0.0001
Echo variables				
Echo end-systolic volume (mls)	192.6 ± 84.8	187.5 ± 91.1	200.2 ± 74.7	ns
Echo end-diastolic volume (mls)	249.5 ± 97.7	242.1 ± 105.5	260.4 ± 84.5	ns
Echo ejection fraction (%)	23.6 ± 9.1	23.4 ± 9.4	23.8 ± 8.7	ns

Table 4-2 Clinical and echocardiographic outcome at baseline and last available follow up

	<i>ALL</i>	<i>CMR-TSI<110</i>	<i>CMR-TSI≥110</i>	<i>p</i>
Last follow up (days)	429 ± 293	440 ± 285	413.5 ± 308	
Clinical status				
NYHA class	3.19 ± 0.52	3.2 ± 0.55	3.164 ± 0.49	ns
FUP NYHA class	2.07 ± 0.83 [¥]	2.05 ± 0.89 [*]	2.08 ± 0.71	ns
6MWD (metres)	244 ± 117	239 ± 124	252 ± 107	ns
FUP 6MWD (metres)	314.5 ± 117.9 [§]	322.46 ± 127 [§]	302.6 ± 103 [§]	ns
Quality of Life (Minnesota)	56.4 ± 20.7	61.3 ± 20.4	48.9 ± 18.9	0.001
FUP Quality of Life (Minnesota)	32.46 ± 23.5 [§]	32.56 ± 24.5 [¥]	31.6 ± 22.2 [¥]	ns
Echocardiographic data				
Echo LVESV (mls)	192.6 ± 84.8	187.5 ± 91.1	200.2 ± 74.7	ns
FUP Echo LVESV (mls)	186.97 ± 90.8 [§]	175.1 ± 95.5 [§]	204.5 ± 81.0	ns
Echo LVEDV (mls)	249.5 ± 97.7	242.1 ± 105.5	260.4 ± 84.5	ns
FUP Echo LVEDV (mls)	246.5 ± 101 [§]	234.1 ± 106.3 [§]	264.8 ± 90.8	ns
Baseline Echo EF (%)	23.6 ± 9.1	23.4 ± 9.4	23.8 ± 8.7	ns

FUP Echo EF (%)	26.09 ± 11.93 [¥]	27.6 ± 12.8 [§]	23.8 ± 10.18	ns
-----------------	-------------------------------	--------------------------	--------------	----

Significance between baseline and final measurements are shown in the table. * = $p < 0.05$,
¥ = $p \leq 0.01$, § = $p \leq 0.001$

Table 4-3 Uni variable and multi-variable Cox proportional hazards analyses of clinical endpoints in relation to cardiac magnetic resonance variables according to imaging modality

		Exp
Total mortality - single variable		
CMR-TSI (ms)	2.633 (1.38 - 5.023)	0.0033
CMR-LVESV (mls)	1.004 (1.000 - 1.008)	0.0357
CMR-LVEDV (mls)	1.003 (0.999 - 1.006)	ns
EF-CMR (%)	0.97 (0.933 - 1.008)	ns
Mean QRS (ms)	1.009 (0.998-1.020)	ns
Total Mortality - multi-variable		
EF-CMR (%)	0.985 (0.944 - 1.028)	0.4854
CMR-TSI (ms)	2.433 (1.238 - 4.785)	0.0099
CMR-LVEDV (mls)	1.002 (0.998 - 1.005)	0.4039
CMR-TSI (ms)	2.457 (1.264 - 4.776)	0.008
EF-CMR (%)	0.94 (0.909-0.973)	0.004
CMR-LVESV (%)	1.004 (1.001-1.006)	0.0017
CMR-LVEDV (%)	1.003 (1.001-1.006)	0.0088
CMR-TSI (ms)	3.945 (2.241 - 6.945)	<0.0001
Mean QRS (ms)	1.006 (0.996-1.016)	0.2253

CMR-TSI (ms)	3.417 (1.884 - 6.2)	<0.0001
CMR-LVESV (mls)	1.002 (0.999 - 1.005)	0.1279
CMR-TSI (ms)	3.59 (1.985 - 6.492)	<0.0001
CMR-LVEDV (mls)	1.001 (0.999 - 1.004)	0.2842
CMR-TSI (msec)	2.954 (1.612 - 5.413)	0.0005
EF-CMR (%)	0.961 (0.926 - 0.998)	0.367
CMR-LVESV (mls)	1.004 (1.001 - 1.006)	0.0045
CMR-LVEDV (mls)	1.003 (1.00 - 1.006)	0.0241
EF-CMR (%)	0.941 (0.908-0.975)	0.0007
mean QRS (ms)	1.009 (0.998 - 1.020)	0.1063
Sudden Cardiac Death - Cox multi-variable		
CMR-TSI (ms)	2.345 (1.2 - 4.57)	0.123
CMR-LVESV (mls)	1.003 (0.999 - 1.007)	0.1991
EF-CMR (%)	0.96 (0.923 - 0.998)	0.0391
CMR-TSI (ms)	2.718 (1.464 - 5.048)	0.0015
CMR-LVESV (mls)	1.002 (0.999 - 1.005)	0.1744
CMR-TSI (ms)	3.175 (1.724 - 5.848)	0.0002

CMR-LVEDV (mls)	1.001 (0.998-1.004)	0.3984
CMR-TSI (ms)	3.357 (1.829 - 6.161)	<0.0001

Cardiovascular mortality - uni variable

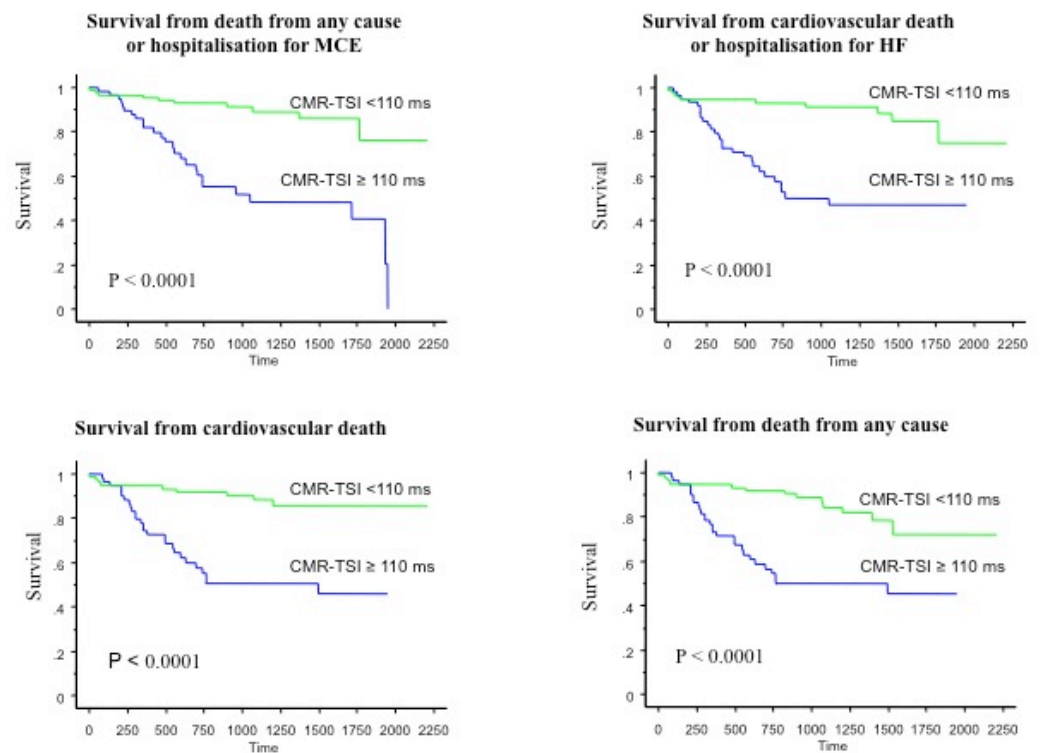
CMR-LVESV (mls)	1.004 (1.001 - 1.007)	0.0167
CMR-LVEDV (mls)	1.003 (1.000 - 1.006)	0.0703
EF-CMR (%)	0.941 (0.901 - 0.981)	0.0047
CMR-TSI (ms)	5.028 (2.425 - 10.423)	<0.0001
mean QRS (ms)	1.008 (0.997 - 1.020)	0.1537

Cardiovascular mortality - multi-variable

CMR-LVESV (mls)	1.002 (0.998 - 1.005)	0.3667
CMR-TSI (ms)	4.549 (2.127 - 9.728)	<0.0001
CMR-LVEDV (mls)	1.001 (0.997 - 1.004)	0.7068
CMR-TSI (ms)	4.832 (2.264 - 10.31)	<0.0001
EF-CMR (%)	0.967 (0.922 - 1.014)	0.1688
CMR-TSI (ms)	3.988 (1.832 - 8.681)	0.0005

Figure 4-1 Kaplan-Meier estimates of the time to the death

From any cause or hospitalisation for major cardiovascular events, survival from cardiovascular death or hospitalisation for heart failure, survival from cardiovascular death or survival from death from any cause.



CHAPTER 5. MYOCARDIAL SCAR AND OUTCOME AFTER CRT

5.1 Introduction

The main cause of death after CRT is progressive heart failure. (Cleland et al., 2005b) Until recently, the impact of aetiology of cardiomyopathy on outcome has been unclear. Patients with ICM have distinct areas of myocardial scarring due to infarction. Patients with ICM may be expected to have a worse prognosis after CRT. After myocardial infarction the prognosis is determined by left ventricular function and adverse left ventricular remodelling. Therefore, the greater the myocardial loss, the worse the expected prognosis.

The efficacy of CRT in patients with extensive scarring might be expected to be less than those with little scar. In the field of revascularisation, registry data suggests that coronary bypass grafting surgery is of benefit to patients with poor left ventricular function and jeopardised viable myocardium, but revascularisation of patients without viable myocardium results in worse outcome than medical treatment alone. (Alderman et al., 1983) As a result, AHA/ACC 2004 guidelines state that in the absence of viable myocardium these patients should not be revascularised. (Eagle et al., 2004) Recently, Zhang et al. have found that in a relatively small cohort of patients from a single centre, in contrast with the multi-centre CARE-HF study, those with ICM have a worse outcome than those with NICM. (Q. Zhang et al., 2009) This has been confirmed in re-analysis of the CARE-HF data, which also found that the absolute benefit from CRT may be greatest in those with ischaemic cardiomyopathy. (Wikstrom et al., 2009)

Postero-lateral scar appears to have particular importance in determining outcome. Bleeker et al. (Bleeker et al., 2006c) reported that patients with postero-lateral (PL) scar had a worse

outcome six months after CRT in terms of left ventricular remodeling compared with those without postero-lateral scar. It is postulated that PL scar results in failure of effective electrical stimulation of the left ventricle, as at implantation the lead is targeted towards the postero-lateral region. Additionally, there appears to be a threshold of scar, beyond which there is insufficient viable myocardium to obtain a response to CRT. (Adelstein and Saba, 2007, Ypenburg et al., 2007a)

The aim of this study is to evaluate the effect of myocardial scar on long term outcome after cardiac resynchronisation therapy. Specifically, in those patients with myocardial scar, the impact of volume and location of scar may be important in terms of survival. However, although the short term response to CRT in relation to scar has been evaluated, long term outcome has not been studied.

This study is a longer term follow up study of the cohort of patients with ICM undergoing CMR and CRT. It includes the 62 patients included in previous work, (Chalil et al., 2007a, Chalil et al., 2007c) with further long term data on clinical status, clinical events and echocardiographic follow up as well as additional patients. As such, it forms the largest long term study between CMR scar and CRT treated HF patients.

5.2 Methodology

Patients undergoing CRT underwent cardiovascular magnetic resonance imaging prior to implantation as described in chapter 2. In mid-2007, patients with estimated glomerular filtration rate of less than 30 ml per minute did not undergo administration of intravenous

gadolinium due to the potential risk of nephrogenic systemic fibrosis. (Thomsen et al., 2008) However, end stage renal failure was not common and thus this did not have a significant effect on the recruitment of subjects.

5.2.1 Volume of scar

The scans were transferred in digital imaging and communication in medicine (DICOM) format to an Apple computer running Osirix version 2.5 (Apple freeware available from www.osirix-viewer.com, downloaded 28 January 2007). The late enhanced areas, which denotes scar, on the slices were manually planimetered. The total area of scar in all the segments was calculated and multiplied by the thickness of the slices to give the volume of scar. The mass of myocardium in diastole was multiplied by 1.05 to give the volume of myocardium. The percentage of myocardial scar was calculated by dividing the volume of scar by the volume of myocardium.

5.2.2 Scar location and transmurality

The areas of scar were then segmented using the American Heart Association sixteen segment tomographic model of the heart (Lang et al., 2005). The slices were matched as closely as possible to the model. The amount of scar per segment was calculated by dividing the diameter of scar by the diameter of the myocardial wall per segment, and this was expressed as a ratio. A ratio of greater than 0.51 was designated as transmural scar in line with previous work by Kim et al (Kim et al., 1999), and less than 0.51 indicative of non-trans-mural myocardial infarction which is usually viable myocardium.

In patients who had scar, the presence was dichotomised into postero-lateral or other areas. In addition, a subset of the patients with NICM was noted to have midwall late enhancement, indicative of mid-wall myocardial fibrosis, which can be found in some patients with dilated cardiomyopathy. (Assomull et al., 2007, McCrohon et al., 2003, Moon et al., 2003, Moon et al., 2004)

5.2.3 Device follow up

Patients were followed up in a specialised device clinic post implant at approximately 6 weeks, 6 months and then six monthly thereafter. At each visit, in patients in sinus rhythm the atrio-ventricular device timings were optimised using the iterative method to achieve the longest left ventricular filling time measured from the early wave to atrial contraction wave without allowing intrinsic conduction, and avoiding diastolic mitral regurgitation. The pulsed Doppler sample cursor was placed just below the mitral valve in the apical four chamber view. (Ritter et al., 1999) The offset between left and right ventricular stimulation was changed to achieve simultaneous time from the R wave to the aortic and pulmonary ejection, termed the aortic and pulmonary pre-ejection time measured using pulsed Doppler in the aortic and pulmonary outflow tracts, respectively.

5.2.4 Echocardiographic analysis

Patients underwent a baseline echocardiogram (Vivid 5 and 7 systems, General Electric, Slough, UK) prior to pacemaker implantation, and then during pacemaker follow up. The echocardiogram was stored digitally and analysed using EchoPac.

The left ventricular dimensions were recorded in M-mode, left ventricular volumes in the apical four chamber view at end-diastole (onset of the R wave) and systole (minimum volume) were used to determine the ejection fraction using modified Simpson's methodology. (Lang et al., 2005)

5.2.5 Clinical follow up

At baseline and each visit the patients underwent a six minute hall walk test, completed a Minnesota living with heart failure questionnaire and the New York Heart Association class was recorded by an observer blinded to initial implant information (NI). In addition, medications were reviewed at each clinic follow up and adjusted appropriately as part of standard clinical care.

As in the CARE-HF study, the clinical end points which considered were the composite of death from any cause or an un-planned hospitalisation for a major coronary event, which included cardiac transplantation. Hospitalisations for worsening heart failure, myocardial infarction, unstable angina, arrhythmia, stroke, pulmonary embolism, or upgrading to an implantable cardioverter-defibrillator were included in this endpoint. The first event was included in the analysis. The second end point considered was the composite of death from

any cause and unplanned hospitalisation with worsening heart failure. The third endpoint considered was mortality from any cause. The additional endpoint of cardiovascular mortality was also considered. Sudden cardiac death was defined as “a natural, unexpected death due to cardiac causes, heralded by an abrupt loss of consciousness within one hour of the onset of acute symptoms”. (Myerburg and Castellanos, 1997) Mortality data were collected through medical records, death certificates and post-mortem data and, where appropriate, from interviews with patients’ care providers.

5.2.6 Determination of site of scar

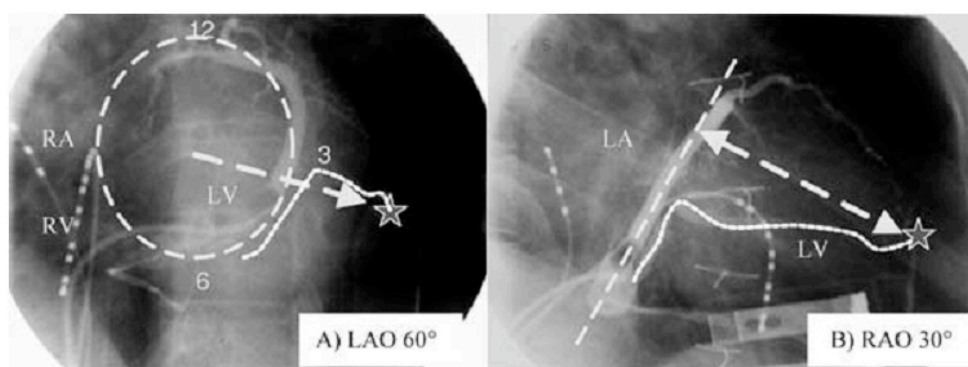
A posterolateral scar was defined as scar in the basal and mid posterior, and the basal and mid postero-lateral segments. Transmurality was defined as scar greater than 50% of the wall. (Kim et al., 1999)

5.2.7 Left ventricular lead position

Albertsen et al. described a method of recording the position of the left ventricular lead using bi-plane fluoroscopy. In the left anterior oblique view, the coronary sinus encircles the mitral valve rather like the hands upon a clock. The right anterior oblique view was used to record the position of the lead tip relative to the coronary sinus to mitral valve plane. (Albertsen et al., 2005)

In this study we determined the lead position using the stored fluoroscopy images. The venograms were viewed on Osirix 2.5 (Apple Inc). We sought to determine whether the tip of the left ventricular lead was pacing scar by examining the delayed enhanced CMR images. Where available we used the coronary sinus venogram to determine the position of the veins. At the end of the procedure, images were acquired recording the position of the left ventricular lead. The distance from the coronary sinus, running in the atrio-ventricular groove, to the tip of the left ventricular lead was measured in the right anterior-oblique view. A reference fluoroscopic acquisition of a set distance was used to calibrate the image, allowing conversion from pixels to centimetres. The position of the lead in the left anterior oblique view was then recorded using the o'clock method, as described by Mortensen (see Figure 5-1).

Figure 5-1 Determination of left ventricular lead position using fluoroscopy



The left anterior oblique view (LAO) is used for determining the left ventricular lead tip position from 12 to 6 o'clock. The right anterior oblique (RAO) view is used for determining the distance from the coronary sinus to the lead tip.²⁵

²⁵ Taken from: Albertsen, A.E., Nielsen, J.C., Pedersen, A.K., et al. (2005) Left ventricular lead performance in cardiac resynchronization therapy: impact of lead localization and complications. **Pacing Clin Electrophysiol**, 28: (6): 483-488. Permission for reproduction obtained from John Wiley & Sons.

5.2.8 Determination of effect of pacing scar via the left ventricular lead

Steady state free precision images of the 4 chamber view were used to plan the left delayed enhanced left ventricular short axis stacks, acquired from base to apex after the administration of intravenous gadolinium. The lines drawn to plan the acquisition which are perpendicular to the 4 chamber view were restored. The lines were examined to ensure that the most basal slice was acquired at the level of the aortic valve, which was assumed to be the level of the coronary sinus. If the slices were acquired below the valve, the distance from a line drawn perpendicular to the ventricle at the level of the aortic valve to the first planning line was measured. This distance was then added to the distance measured from the fluoroscopic images of the tip of the lead to the top of the coronary sinus.

The delayed enhanced image slice thickness and the gap between slices was summed. The distance from the top of the coronary sinus to the lead tip was used to determine which left ventricular delayed enhanced short axis stack would show the heart at the level of the tip of the lead. Using the o'clock method, we determined whether the myocardium at the level of the lead contained full thickness (>51% in diameter) or partial thickness infarction.

5.2.9 End points

The primary endpoint considered was the composite endpoint of cardiovascular death or unplanned hospitalization for worsening HF. The first event was included in the analysis. The secondary endpoint was cardiovascular death. Mortality data was collected through medical records, and where appropriate, from interviews with patient's carers. Information

regarding clinical outcome was collected by an investigator who was blinded to the CMR study.

5.2.10 Statistics

Continuous variables are expressed as mean \pm standard deviation (SD). Normality was tested using the Shapiro–Wilk test (the W-statistic). Comparisons between normally distributed continuous variables were made using ANOVA with Fisher’s protected least significance difference test for multiple comparisons. Serially measured variables were analyzed using repeated measures ANOVA. Categorical variables were analyzed using χ^2 tests. The effect of myocardial scarring on the various endpoints was explored using Cox proportional hazards analyses and Kaplan–Meier survival curves. Differences in survival curves between the groups were assessed using the log-rank (Mantel–Cox) test. Statistical analyses were performed using Statview (Cary, NC) and SPSS 13.0 (Chicago, Illinois). A two-tailed P value of <0.05 was considered statistically significant.

5.3 Results

The mean follow up to the clinical end-points was 862 days (range 2 to 2210). There were 33 deaths, all from cardiovascular mortality during the follow up period. At baseline, the age of the patients with posterolateral (PL) and non-PL scar were not significantly different. The medical treatment, medical history and NYHA class were similar. The proportion of males was significantly higher in those with PL scar. The QRS duration was also similar in both

cohorts. There was a trend to greater left ventricular volumes in those with PL scar. The ejection fraction was significantly lower in those with PL scar (19.2% vs 25.3%). The percentage scar volume was non-significantly greater in those with PL scar.

73/ 95 (76.8%) of patients responded to CRT, defined as a reduction of ≥ 1 NYHA class, and 25% improvement in six minute walk distance. The last available clinical and echocardiographic follow up was used for analysis in those who had died.

5.3.1 Effects of PL scar

During the follow up period, 31/51 (60.7%) of those patients with PL scar had died, where as 2/41 (4.9%) of those without postero-lateral scar had died. Kaplan-Meier survival estimates for the time to the two clinical endpoints for transmural and non-transmural PL scars are shown in Figure 5-2.

Table 5-2 shows the differences in symptomatic response between those with PL scars and those with scar in other areas. There were no differences in terms of NYHA class at baseline and follow up in those with and without PL scar. Both groups improved significantly with CRT. Again both groups improved in terms of LVEF, six minute walk distance and quality of life score. The improvement from baseline LVEF was greatest in the patients without PL scar. The symptomatic responder rate was similar in both groups. Interestingly, in terms of echocardiographic derived LVEF, the baseline values were similar, in contrast to the CMR derived LVEF.

5.3.2 Effects of PL scar transmurality

Patients with transmural PL scar did not improve significantly in terms of NYHA class and LVEF, whereas those without transmural PL scar improved significantly (see Table 5-3). However, quality of life measures and six minute walk distance improved significantly in both groups. The improvement in six minute walk distance and quality of life was greater in those without posterolateral transmural scar, but this did not reach significance. There was a trend to a greater symptomatic responder rate in patients with postero-lateral scar, but this did not reach statistical significance.

Comparison between transmural and non-transmural posterolateral scar was made, although there were only 16 patients with non-transmural PL scar (see Table 5-4). In comparison, those with non-transmural PL scar had a greater improvement in NYHA class, six minute walk distance and LVEF. All patients with PL scar improved significantly in terms of quality of life, but those with non-transmural scar had a much greater improvement.

5.3.3 Effects of pacing PL scar

Kaplan Meier survival analysis shows a significantly worse outcome in terms of cardiovascular mortality and heart failure hospitalisations in patients where the left ventricular lead is pacing left ventricular scar (see Figure 5-3). The cardiovascular mortality was 5.6 fold greater (2.7 -11.4, $p < 0.0001$). Response to CRT in terms of improvement by one NYHA class and 25% increase in six minute walking distance was worse in patients where the left ventricular lead was pacing scar (32% vs 79%, $p < 0.0001$) compared with those where the lead was not pacing scar. However, it cannot be stated that placing the lead

outside the scar would have resulted in a difference in outcome, as this was purely an observational study, not a randomised controlled trial.

5.4 Discussion

The key finding from this observational study is that the presence of posterolateral scar predicts death and adverse events after CRT in comparison to patients without posterolateral scar. Furthermore, patients with trans-mural scar fared worse than those with non-transmural scar both in terms of clinical response and outcome. The observation that placing the left ventricular pacing lead on myocardial scar resulted in worse outcome than pacing outside the scar in terms of mortality and hospitalisations is of clinical significance, suggesting that avoidance of scar could improve the outcome of patients undergoing CRT.

Bleeker et al. noted that the response to CRT was lower in patients with PL scar in comparison to those without PL scar. This raises the hypothesis that resynchronisation is reduced in these patients. (Bleeker et al., 2006c) Our findings are consistent with Bleeker et al.'s results, showing a worse outcome in those with PL scar. The adverse events, cardiovascular death and heart failure hospitalisations were predicted by the presence of postero-lateral myocardial scar, and were independent of the volume of scarred myocardium. Furthermore, this was independent of LVEF, LVEDV, LVESV and QRS duration. Postero-lateral myocardial scar is a powerful predictor of adverse outcome after CRT.

We have found that the extent of PL myocardial scar has less prognostic impact than whether the scar is transmural or subendocardial. Whilst symptomatic benefit can be achieved in patients with PL scar, the benefit is lower in comparison to those without transmural scarring. As a result the response rate is lower for transmural PL scar (66.6% vs. 83%) when compared with subendocardial scar. This is in keeping with the findings of Bleeker et al, where a transmural scar was associated with a responder rate of 47%, compared with 83% for non-PL scar. (Bleeker et al., 2006c) Nevertheless, CRT results in symptomatic benefit in patients with transmural PL scar. The extent of scarring was less important than the trans-murality of scarring, suggesting that myocardial viability increases the benefit gained from CRT.

5.4.1 Pacing PL scar

Implantation of the LV lead over the site of scar is associated with a higher risk of cardiovascular death and hospitalisations. Furthermore, pacing over the scar results in a lower response rate to CRT, suggesting that resynchronisation is reduced. One mechanism by which the effectiveness of CRT is reduced is that pacing scar increases duration and fragmentation of QRS complexes. (Reddy et al., 2003, Schwartzman et al., 1999) Furthermore, scar tissue slows the conduction of the pacing stimulus. (Lambiase et al., 2004) Pacing outside the area of slowed conduction increases the effectiveness of electrical resynchronisation when measured acutely using non-contact mapping. (Lambiase et al., 2004) The observed mortality rate is admittedly high, as is the absence of reverse remodeling. This may be due to the inclusion of patients with, exclusively, ischaemic cardiomyopathy. The

CARE-HF study, in which 40% of patients in the paced group had ischaemic cardiomyopathy has shown a significantly higher mortality in patients with ICM, and lower uptake of medical therapy, as these patients were sicker. (Wikstrom et al., 2009) Moreover, our study involves a greater proportion of patients in NYHA class IV (22%) than the CRT arms of the Multicenter InSync Randomized Clinical Evaluation (MIRACLE) (9.9%) (Abraham et al., 2002) and the Multisite Stimulation in Cardiomyopathies (MUSTIC) (Cazeau et al., 2001) studies. Patients in this study also had lower 6-min walking distance (275 m) than in the MIRACLE (307.2 m) and the MUSTIC (399 m) studies.

5.4.2 Limitations of the study

The presence of myocardial scarring does not take into account the effects of myocardial thinning. If thinning has occurred, the planimetered area of myocardial scar is likely to be an underestimation of the original scar size. Our finding of 33% as a cut-off for clinical response following CRT is the result of a retrospective analysis. Clearly, this threshold would be different if patients were not selected on the basis of QRS duration. These findings therefore require confirmation in a validation series.

This observational study generates the hypothesis that pacing scar results in a worse outcome, and patients with PL myocardial scarring have reduced benefit from CRT. Confirmation of this finding would require randomised studies, although the strength of effect is so great that there would be concern as to whether deliberately pacing scar would be ethical. Whilst we have demonstrated that patients with PL scar have worse outcome than

patients without PL scar, we have not shown that patients with PL scar do not benefit from CRT.

This study was exclusively comprised of patients with ICM, but some patients with DCM demonstrate mid-wall enhancement, (Assomull et al., 2006, McCrohon et al., 2003) which may also have prognostic impact.

Recent attempts to improve selection of patients for CRT have largely focussed on pre-implant dyssynchrony echocardiography. This study did not measure dyssynchrony. However, the use of TDI in addition to CMR to assess dyssynchrony and scar, respectively, found little additive benefit from TDI when assessed in terms of clinical response and reverse remodelling assessed using echocardiography. (Bleeker et al., 2006c)

The presence of PL scar in patients with ICM identifies a group with a higher risk of cardiovascular death. In addition, pacing left ventricular scar is associated with a worse outcome than pacing outside scar. It is reasonable to avoid pacing scar wherever possible, and pre-implant CMR will make this achievable.

5.5 Table legends:

Table 5-1 Baseline clinical and cardiovascular magnetic resonance characteristics of the study group

Table 5-2 Baseline and last available follow up clinical and echocardiographic characteristics of the study group according to presence or absence of posterolateral scar.

Table 5-3 Baseline and last available follow up clinical and echocardiographic characteristics of the study group according to presence or absence of trans-mural posterolateral scar.

Table 5-4 Baseline and last available follow up clinical and echocardiographic characteristics of the study group according to transmurality of posterolateral scar.

Table 5-5 Cox proportional hazard analyses of clinical magnetic resonance variables in relation to clinical endpoints

5.6 Figure legends

Figure 5-2 Kaplan Meier outcome transmural PL scar vs non-transmural PL

Figure 5-3 Kaplan-Meier outcome of pacing scar vs not pacing scar

Table 5-1 Baseline clinical and cardiovascular magnetic resonance characteristics of the study group

	All	Non-PL scar	PL scar	P
Number	95	43	52	
Age, yrs	68.0 ± 10.0	67.6 ± 9.4	68.3 ± 9.96	0.97
Sex, male (%)	81 (85.2)	33 (76.7)	48 (92.0)	0.03
NYHA Class, n (%)	3.2 ± 0.55	3.07 ± 0.55	3.23 ± 0.55	0.1876
Co-morbidity, n (%)				
Diabetes mellitus	18 (18.9)	8 (18.6)	10 (19.2)	0.9382
Hypertension	28 (29.4)	15 (34)	13 (25)	0.29
CABG	33 (34.7)	10 (23.2)	23 (44.3)	0.032
Medication, n (%)				
Loop diuretics	85 (89.4)	40 (93.0)	45 (86.5)	0.3
ACEI or AIIIB	89 (93.6)	40 (93.0)	49 (94.2)	0.39

β-blockers	56 (58.9)	29 (67.4)	27 (51.9)	0.45
Spirolactone	38 (40)	18 (41.8)	20 (38.4)	0.73
ECG variables				
Sinus rhythm, n (%)	75 (78.9)	33 (76.7)	42 (80.7)	0.63
Atrial fibrillation, n (%)	20 (21.1)	10 (23.3)	10 (19.3)	0.63
QRS duration, ms	143.9 ± 28.5	144.5 ± 28.2	143.5 ± 29.1	0.86
CMR variables				
LVEDV, cm ³	252.3 ± 96.5	242.6 ± 109.7	260.4 ± 84.4	0.12
LVESV, cm ³	203.8 ± 91.4	188.2 ± 101.6	216.8 ± 80.8	0.37
LVEF, %	22.0 ± 9.7	25.3 ± 10.8	19.2 ± 7.8	0.0019
Total scar volume, %	31.0 ± 18.3	27.6 ± 17.6	33.5 ± 18.6	0.1285

Table 5-2 Baseline and last available clinical and echocardiographic parameters according to presence or absence of posterolateral scar.

	Non-PL	PL scar	p
n	52	43	
NYHA class			
baseline	3.07 ± 0.55	3.23 ± 0.55	0.1581
FUP	2.0 ± 0.89	2.27 ± 0.87	0.1083
p	0.3387	0.0029	
Quality of Life			
baseline	52.1 ± 18.5	53.1 ± 19.7	0.8251
FUP	28.4 ± 22.0	35.3 ± 26.4	0.217
p	0.0034	0.0058	
6 minute walk distance			
baseline	251.3 ± 129.0	233.6 ± 107.6	0.5189
FUP	324.2 ± 137.6	305.7 ± 99.6	0.5031
	<0.0001	0.0001	

P			
LVEF (%)			
Baseline	24.1 ± 7.3	24.0 ± 8.4	0.9266
FUP	30.5 ± 11.3	27.4 ± 10.9	0.2362
p	0.4029	0.0619	
Responder (%)	75	79	0.6927

FUP = follow up. LVEF = left ventricular ejection fraction. The significance value of changes from baseline to follow up is presented beneath the change.

Table 5-3 Baseline and last available clinical and echocardiographic parameters according to presence or absence of PL scar.

	Non-PL scar	Transmural PL scar	p
	59	36	
NYHA class			
Baseline	3.119 ± 0.53	3.22 ± 0.6	0.377
Follow-up	1.96 ± 0.89	2.42 ± 0.8	0.015
P	p=0.0086	p=0.1975	
Quality of life			
Baseline	52.2 ± 18.7	53.4 ± 18.7	0.7868
Follow-up	28.3 ± 22.7	38.9 ± 26.6	0.0653
P	p=0.0011	p=0.0001	
6 minute walk distance			
Baseline	268.3 ± 121.4	197.5 ± 95.5	0.0093
Follow-up	332.4 ± 126.4	281.6 ± 94.4	0.0726
P	p<0.0001	p=0.0014	
Symptomatic responders (%)	83	66.6	0.068
LVEF, %			
Baseline	23.2 ± 8.0	25.3 ± 8.9	0.2681
Follow-up	29.5 ± 12.0	27.6 ± 9.0	0.8177
p	p=0.7032	p=0.0352	

Table 5-4 Baseline and last available clinical and echocardiographic parameters according to either non-transmural or transmural posterolateral scar

	PL-non transmural	Transmural PL scar	p
n	16	36	
NYHA class			
Baseline	3.25 ± 0.5	3.3 ± 0.5	ns
Follow-up	1.9 ± 0.9	2.4 ± 0.8	ns
p	p=0.0138	p=ns	
Quality of life			
Baseline	52.8 ± 22.5	53.2 ± 18.5	ns
Follow-up	24.1 ± 21	41.4 ± 27.2	0.0385
p	p=0.001	p=0.0002	
6 minute walk distance			
Baseline	280.5 ± 119	208.6 ± 94.0	0.035
Follow-up	343.8 ± 103	283.8 ± 92.4	ns
P	p=0.0071	p=0.0173	
Symptomatic responders			
LVEF, %			
Baseline	22.3 ± 7.4	24.8 ± 9.9	ns
Follow-up	28.1 ± 11.9	26.9 ± 10.6	ns
	p=ns	p=0.0171	

Table 5-5 Univariate Cox proportional hazard analyses of clinical magnetic resonance variables in relation to clinical endpoints

	HR (95% CI)	P
Cardiovascular death		
PL scar	3.5 (1.9 - 6.4)	<0.0001
Transmural PL scar	5.2 (2.5 - 10.9)	<0.0001
Total scar volume (%)	1.01 (0.99 - 1.03)	0.1775
LVEF, %	0.93 - 0.97)	0.0949
LVEDV	1.00 (1.00-1.01)	0.0249
LVESV	1.01 (1.00 - 1.01)	0.0138
QRS duration (ms)	0.99 - 1.02)	0.3578
Cardiovascular death or hospitalisation for HF		
	HR (95% CI)	P
PL scar	2.42 (1.6 - 3.8)	<0.0001
Transmural PL scar	2.29 (1.49 - 3.55)	0.0002
Total scar volume (%)	1.01 (0.99 - 1.02)	0.2766
LVEF, %	1.0 (0.97 - 1.02)	0.6464
LVEDV	1.00 (1.00 - 1.01)	0.7829
LVESV	1.00 (1.00 - 1.01)	0.9504
QRS duration		

1.00 (0.99 - 1.00) 0.1705

HR (95% CI) PL = posterolateral, LVESV = left ventricular end systolic volume, LVEDV = left ventricular end diastolic volume, LVEF = left ventricular ejection fraction

Figure 5-2 Kaplan-Meier survival graphs of outcome of transmural PL scar vs non-transmural PL scar

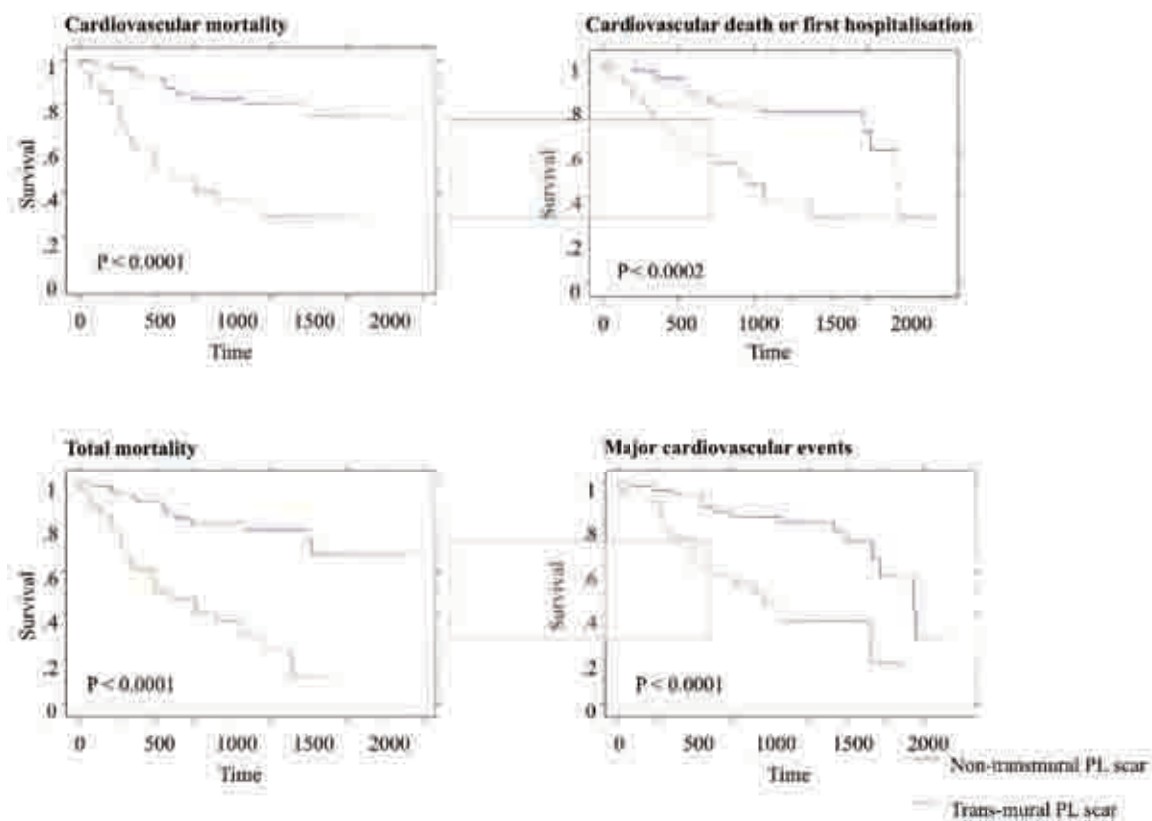
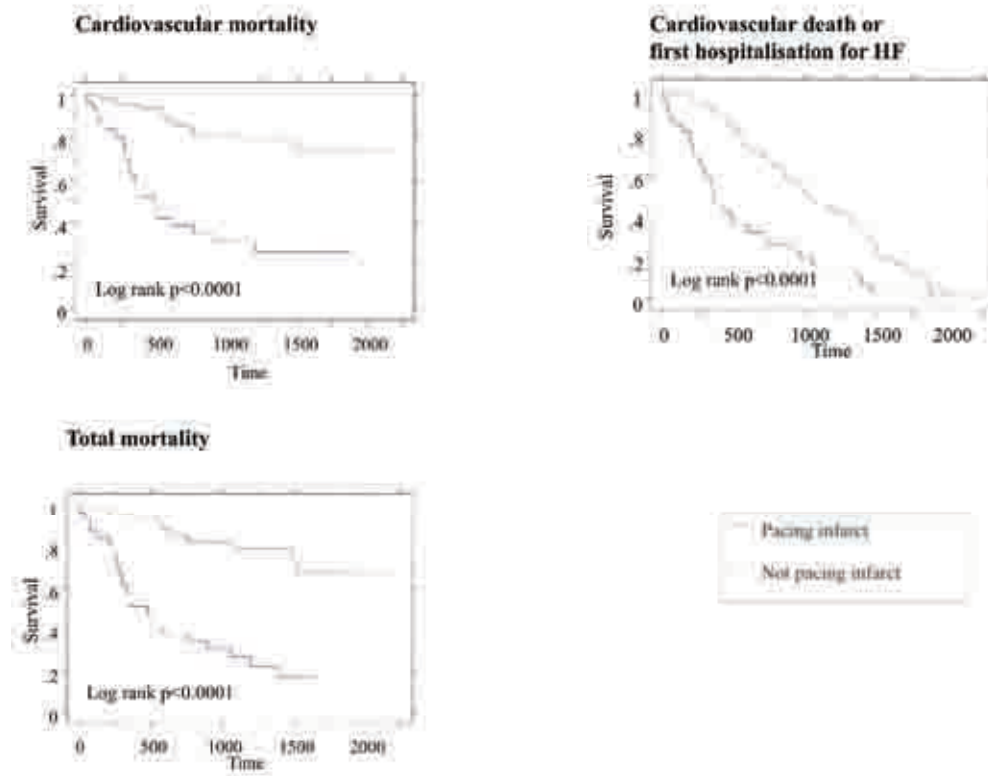


Figure 5-3 Kaplan-Meier survival graph of effect of pacing myocardial scar on outcome



CHAPTER 6. CMR-TSI AND SCAR

6.1 Introduction

Pre-implant imaging with cardiovascular magnetic resonance identifies two variables which predict outcome in patients undergoing CRT implantation. Firstly, dyssynchrony can be assessed with CMR-TSI and additionally, posterolateral scar can be visualised.

The role of dyssynchrony in relation to outcome appears central to the current paradigm of CRT that dyssynchrony is a major contributor to systolic heart failure and its correction with CRT results in clinical benefit. Quantification of dyssynchrony has been explored using different techniques in an attempt to predict patients who derive symptomatic benefit. Echocardiography has a high temporal resolution, and sophisticated advances in technology have facilitated detection of myocardial velocity and motion. A number of single centre studies had found that tissue velocity imaging could predict the outcome, in terms of response, from CRT. (Bleeker et al., 2005, Van de Veire et al., 2007, Yu et al., 2002)

The only multicentre study to explore the predictive value of echocardiographic measures of dyssynchrony found that no single echocardiographic measure reliably predicted outcome. (Chung et al., 2008) Others have reported difficulties in the reliability of assessment of dyssynchrony with tissue velocity imaging (Conca et al., 2009, De Boeck et al., 2008, Miyazaki et al., 2008), which may relate to technological difficulties with the methodology. (Kirn et al., 2008) In the light of these disappointing results, the current American Society of Echocardiography guidelines recommend that dyssynchrony measured with echocardiography should not be used to exclude or select patients for CRT, (Gorcsan et al., 2008) a position statement which has been supported by Cleland et al. (Cleland et al., 2008b) Never the less, it may be the case that methodological issues

within the PROSPECT study resulted in the outcome that no single echocardiographic measure predicts outcome after CRT. (Yu et al., 2009) In contrast, we have found that the cardiovascular magnetic resonance imaging based tissue synchronisation index (CMR-TSI) predicts outcome after CRT. (Chalil et al., 2007d)

Myocardial viability influences the outcome after CRT. Bleeker et al. found that patients with transmural myocardial scar in the postero-lateral region, demonstrated with gadolinium enhanced cardiovascular magnetic resonance, did not improve symptomatically or demonstrate reverse remodelling at six months post implant. (Bleeker et al., 2006c) It has been shown that both short term (Ypenburg et al., 2007a) and long term outcome (Chalil et al., 2007a, Chalil et al., 2007b) are affected by both volume of scar and location. Transmural posterolateral scar results in the worst prognostic outcome after CRT relative to other groups.

The aim of this chapter is to explore the value of pre-implant cardiovascular magnetic resonance imaging in patients undergoing CRT, combining the assessment of dyssynchrony with CMR-TSI and myocardial scar. The advantage of these two techniques is their simplicity, allowing assessment to be carried out without the need for specialised technology or complicated algorithms.

6.2 Methods

141 patients were prospectively enrolled in this prospective observational study. CRT was implanted for standard clinical indications (NYHA 3 or 4, left ventricular ejection fraction $\leq 35\%$, QRS duration $\geq 120\text{ms}$) as approved by the National Institute for Clinical Excellence Healthcare Technology Appraisal. (Healthcare Technology Appraisal 120: Cardiac resynchronisation therapy for the treatment of heart failure, 2007) The patients

were treated with CRT without implantable defibrillator back up because implantable defibrillators were not funded for primary prevention at that time.

6.2.1 Study Design

All patients underwent clinical assessment at baseline, 6 weeks and then at six monthly intervals thereafter. A CMR study was performed at baseline, prior to pacemaker implantation. Clinical assessment included NYHA class, a six minute walk distance test (Guyatt et al., 1985) and Minnesota living with heart failure questionnaire. (Rector et al., 1987) All patients provided written informed consent and the study was approved by the North Birmingham Research Ethics Committee.

6.2.2 Device Therapy

Biventricular pacemaker implantation was carried out after written informed consent under conscious sedation and local anaesthesia. Follow up took place in a dedicated device clinic where the pacemaker was checked by cardiac physiologists, the device optimised with echocardiography and medications adjusted by cardiac research fellows or the specialised heart failure and device nurse. Patients in atrial fibrillation did not undergo AV node ablation. (Khadjooi et al., 2008) Patients in sinus rhythm (n = 118) were optimised using echocardiography to prolong AV filling time whilst avoiding diastolic mitral regurgitation. (Ritter et al., 1999) The AV delay was optimised at each follow up visit thereafter. The back up atrial rate was set to 60 beats per minute, and the pacing mode set to DDD with rate response switched on, with a baseline inter-ventricular delay of 0 to 4 ms (nominal settings varied according to device manufacturer). In patients in atrial fibrillation (n = 23), the atrial port was plugged and the device was programmed to a minimum base rate with ventricular triggered pacing such that sensed right

ventricular activity would result in left ventricular stimulation. All patients had functional leads and generators during the study period.

The position of the left ventricular lead was chosen by the implanting physician, who was blinded to the CMR study. Lead placement was determined using the o'clock method, which uses bi-plane fluoroscopy. (Albertsen et al., 2005)

6.2.3 Cardiovascular Magnetic Resonance

Imaging was performed using a 1.5 Tesla magnetic resonance imaging scanner as described earlier.

6.2.4 Tissue Synchronization Index.

The CMR-TSI was derived as previously described.

6.2.5 Scar Imaging

The CMR study was carried out as described earlier. Scar volume was calculated in cm^3 by multiplying the planimetric area of late gadolinium enhancement in each slice by the slice thickness. Scar volume was expressed as a % of LV myocardial volume in the diastolic phase. Areas of scar were then segmented using a 17 segment model. (Lang et al., 2005) A posterolateral (PL) scar was defined as a scar in ≥ 1 of the following segments: basal posterior, mid posterior, basal-PL and mid-PL.

6.2.6 Echocardiography

ECG gated two dimensional echocardiograms were acquired using standard protocols.

The images were stored digitally for off line analysis. The left ventricular volumes were measured using planimetry and the left ventricular ejection fraction calculated using the modified Simpson's technique in the apical four chamber view (EchoPac, GE, Slough).

6.2.7 Follow up and Endpoints

The clinical endpoints considered were the composite of heart failure hospitalisation and cardiovascular mortality, and the composite of total mortality or heart failure hospitalisation for a major cardiovascular event. The latter endpoint included myocardial infarction, pulmonary embolism, upgrading to implantable defibrillator, cardiac transplantation or admission with worsening heart failure. The other endpoints were cardiovascular mortality and total mortality. Sudden cardiac death was defined as “a natural, unexpected death due to cardiac causes, heralded by an abrupt loss of consciousness within one hour of the onset of acute symptoms”. (Myerburg and Castellanos, 1997) Mortality was collected through medical records and, where appropriate, from interviews with patient’s caregivers, and was not confirmed by post mortem. Sudden death during sleep was assigned to sudden cardiac death. Clinical outcomes were collected by an investigator who was blinded to other clinical and imaging data.

6.2.8 Statistical analysis

Continuous variables are expressed as mean \pm standard deviation (SD). Normality was tested using the Shapiro-Wilk test. Variables which were not normally distributed were log-transformed before statistical analyses. Comparisons between normally distributed continuous variables were made using ANOVA with Scheffe’s F procedure for multiple comparisons. Categorical variables were analysed using chi-squared tests and Scheffe’s post-hoc test. Changes in variables from baseline to follow-up were analyzed using paired Students’ t-tests. Variables showing significant group differences at baseline were entered into Cox proportional hazards analyses.

As in a previous study, (Chalil et al., 2007d) the value of CMR-TSI with the optimum sensitivity and specificity was 110 msec for all endpoints. The ability of CMR-TSI to discriminate between patients in the various risk categories at this cut-off value was assessed using Cox proportional hazards analyses and Kaplan-Meier survival curves. Differences in survival curves between the groups were assessed using the log-rank (Mantel-Cox) test. Statistical analyses were performed using Statview (Cary, NC) and SPSS 15.0 (Chicago, Illinois). A two-tailed p value of <0.05 was considered statistically significant. In a previous study, (Chalil et al., 2007d) intra-observer and interobserver variabilities for CMR-TSI were 3.0% and 8.8%, respectively.

Analysis of wall motion was performed using the R statistical language. The non-linear least square fit function implemented by Bates and DebRoy into the 'nls' packet of R was used for the sine fit. (Bates and Watts, 1988)

6.3 Results

6.3.1 Baseline characteristics

The patients were grouped according to the CMR-TSI and the presence of posterolateral scar, as shown in table 1. Patients without posterolateral scar included patients with non-ischaemic cardiomyopathy as well as patients with ischaemic cardiomyopathy who had scar in other locations. Furthermore, the groups with posterolateral scar only included patients with ischaemic cardiomyopathy, as well as a greater proportion of patients who had undergone coronary bypass surgery. The patients were well matched for age, but there were significantly more males in the patients with a CMR-TSI \geq 110 ms with posterolateral scar. There were no significant differences in the numbers of patients who

had hypertension or diabetes mellitus at baseline. All the patients with posterolateral scar and $\text{CMR-TSI} \geq 110\text{ms}$ were in sinus rhythm, which was significantly greater than seen in other groups. There were no significant differences in the baseline pre-implant medications between the groups. The pre-implant use of beta blockers was lower than other studies such as CARE-HF, but the proportion of patients in NYHA class IV was greater, reflecting a sicker population, with a greater proportion of patients with ischaemic heart disease. (J. G. Cleland et al., 2005a, Wikstrom et al., 2009) In the CARE-HF study patients with ICM were prescribed less medical therapy in comparison with those with NICM. (Wikstrom et al., 2009)

There were no significant differences in the baseline QRS duration between the groups, although there was a trend to a greater QRS duration in the $\text{CMR-TSI} \geq 110\text{ ms}$ with posterolateral scar group. The ventricular volumes were greater in the group with $\text{CMR-TSI} \geq 110\text{ ms}$, and significantly greater in the $\text{CMR-TSI} \geq 110\text{ ms}$ without posterolateral scar group for LVEDV alone, and for both groups with $\text{CMR-TSI} \geq 110\text{ms}$ for LVESV. The latter was also the case for both groups which had significantly lower LVEF. The scar volume was significantly greater in both the groups which had postero-lateral scar relating to the higher proportion of patients with ischaemic heart disease.

The baseline characteristics of the participants are shown in Table 6-1. The maximum follow up of the participants was 1936 days (5.3 years) for events, there were 3 non-cardiovascular deaths and 30 cardiovascular deaths. 24 were due to pump failure and 6 due to sudden cardiac death. There were 5/91 (5.5%) sudden cardiac deaths in patients with ischaemic cardiomyopathy and 1/50 (2%) in patients with non-ischaemic cardiomyopathy ($p = \text{NS}$). One patient underwent cardiac transplantation. The risk of reaching all endpoints was greatest in the group with the $\text{CMR-TSI} \geq 110\text{ ms}$ with

posterolateral scar, amounting to approximately 10 times as many events as in the CMR < 110 ms and no PL scar group (all $P < 0.001$). In the CMR ≥ 110 msec and PL scar group, 14/15 (93%) of the cardiovascular deaths were due to pump failure. In the CMR-TSI ≤ 110 ms and no PL scar group, 4/7 (57%) of the cardiovascular deaths were due to pump failure. See Table 6-2

In terms of the risk of the composite endpoint of cardiovascular mortality and heart failure hospitalisation, this was higher in the CMR-TSI ≤ 110 ms and PL scar than in the CMR-TSI ≥ 110 msec and no PL scar group ($P=0.026$), although no other differences emerged in terms of the other end points. As the risk of reaching the endpoints was similar in both groups, the groups were amalgamated. Using Kaplan-Meier survival analysis, curves were drawn for 3 risk groups: 1) CMR-TSI ≤ 110 ms and no PL scar, 2) CMR-TSI ≥ 110 ms *and* no PL scar *or* CMR-TSI ≤ 110 ms and PL scar, and 3) CMR-TSI ≥ 110 ms and PL scar. As shown in Figure 6-1, the group with CMR-TSI ≥ 110 ms and PL scar emerged as the highest risk group with respect to all endpoints (log-rank $P < 0.001$). Kaplan-Meier survival analysis for ICM and NICM are presented in Figure 6-2.

Uni-variable Cox proportional hazard analyses were used to explore the value of assessing CMR-TSI alone, scar location alone, or the combination of both. As shown in Table 6-3, both the CMR-TSI and PL scar location emerge as the strongest predictor of all endpoints when considered separately in uni-variable models. The highest difference between low and high risk groups, however was observed when both CMR-TSI and PL scar were combined. Patients with a CMR-TSI ≥ 110 ms and PL scar were identified as a particularly high risk group for all endpoints (all $p < 0.01$), compared to patients with CMR-TSI ≤ 110 msec and no PL scar. Although other CMR variables, such as LV volumes, LVEF and scar volume, reached statistical significance in univariate Cox

models, all had $HR \leq 1.0$. Age and gender failed to emerge as predictors of the various endpoints in univariate analyses. In multi-variable Cox proportional analyses, the finding of $CMR-TSI \geq 110$ msec and PL scar or the finding of either $CMR-TSI \geq 110$ msec or a PL scar emerged as strong predictors of all the endpoints, independent of LVEF and scar size.

6.3.2 Clinical and echocardiographic data

As shown in Table 6-4 similar changes in NYHA class, 6 minute walking distance and quality of life scores were observed across the groups. Significant reductions in LVEDV ($p = 0.049$) and LVESV ($p = 0.0007$) were only observed in the $CMR-TSI \leq 110$ msec and no PL scar group. Similarly, an increase in LVEF was only observed in this group ($p < 0.001$).

6.4 Discussion

Cardiovascular magnetic resonance provides unique information with regard to diagnosis, aetiology, function and outcome in patients with cardiomyopathy (Assomull et al., 2006, McCrohon et al., 2003). The key finding from this study is that CMR can provide unique information regarding risk stratification in terms of morbidity and mortality of patients undergoing CRT pacing. This study demonstrates that the morbidity and mortality after CRT was lowest in patients with $CMR-TSI < 110$ ms and absence of posterolateral scar. In contrast, the highest risk group were identified as those with $CMR-TSI \geq 110$ msec and the presence of PL scar, and this group were twelve fold more likely to experience cardiovascular death or hospitalisation with heart failure. Strikingly, all groups benefit from CRT in terms of symptomatic improvement, although the patients with $CMR-TSI \geq 110$ msec and PL scar did not improve in terms of left ventricular ejection fraction at follow up.

6.4.1 Dyssynchrony and outcome

The finding that dyssynchrony is associated with worse outcome after CRT is not surprising given the relationship between CMR-TSI and other measures of myocardial performance and electrical dyssynchrony. We have demonstrated that CMR-TSI is greatest in patients with ischaemic heart disease when compared to non-ischaemic cardiomyopathy (see Chapter 3). Outcome from CRT is worst in patients with ischaemic cardiomyopathy. (Wikstrom et al., 2009, Q. Zhang et al., 2009) Furthermore, we have shown that dyssynchrony is inversely related to left ventricular ejection fraction, governed by an exponential relationship, so that the greatest CMR-TSI is seen in patients with the lowest LVEF. This is in line with findings from observational studies which show that NT-pro-BNP, a marker of left ventricular dysfunction and neurohumoral activation, predicts outcome after CRT, with those with the highest levels experiencing the worst outcome. (Cleland et al., 2008a, Fruhwald et al., 2007) Dyssynchrony and BNP has not been evaluated in many studies, but Lellouche et al. found that BNP was related to the presence of dyssynchrony on tissue Doppler imaging in patients undergoing CRT implantation. (Lellouche et al., 2007)

Myocardial viability is essential to gain benefit from revascularisation in the field of ischaemic cardiomyopathy, (Dakik et al., 1997, Pagley et al., 1997, Schwartzman et al., 2003) It would seem logical that viable myocardium is required to gain benefit from CRT, as pacing scar and attempting to stimulate myocardium which has little residual viability is likely to be futile. Recent work has suggested that stress echocardiography could aid patient selection for CRT, identifying those patients with sufficient contractile reserve to benefit. (Da et al., 2006)

6.4.2 CMR dyssynchrony and outcome – contrast with echocardiographic dyssynchrony

The relationship identified between CMR-TSI and both left ventricular volume and QRS duration, lies in contrast to findings which emerge predominantly from echocardiographic studies. (Bax et al., 2004b, Van de Veire et al., 2007, Yu et al., 2003a) Although QRS duration has not been shown to predict outcome after CRT, this may be because it is too insensitive as a marker. (Bristow et al., 2004, Cleland et al., 2005b) The COMPANION study suggested patients with the broadest QRS duration gained the greatest absolute benefit from CRT in terms of reduced mortality and hospitalisations, but the study was not powered for subgroup analysis. A longer follow up may determine if there is a benefit to starting CRT in those with a narrower QRS, who may be at an earlier stage in the disease process. (Bristow et al., 2004) The worst outcome in our study was seen in patients with the most dyssynchrony and the presence of posterolateral scar, and these patients were at greatest risk of pump failure. This finding is consistent with the observation that these patients had the worst left ventricular function pre-implantation.

6.4.3 Effect of posterolateral scar

The presence of PL scar may have prevented adequate resynchronisation. The finding of a better outcome in patients with CMR-TSI ≥ 110 msec but without PL scar is consistent with this hypothesis. This study suggests that those patients with the most damaged and dyssynchronous ventricles benefit the least from CRT. An interesting finding from studies using septal to lateral delay to predict outcome after CRT found that beyond a septal to lateral delay of 100 msec, there was no benefit from CRT, suggesting that

beyond a certain threshold beyond which there is little benefit from CRT.(Bax et al., 2004b)

The advantage to this technique of risk stratification is the simplicity of the technique. This application of CMR demonstrates the ability to determine outcome in terms of morbidity and mortality after CRT pacing, which has so far eluded other imaging and neuro-hormonal techniques. (Chung et al., 2008, Cleland et al., 2008a) There are a number of other CMR techniques which are under development, such as tissue velocity imaging, myocardial tagging (Curry et al., 1998, Helm et al., 2005), strain encoding (Kuijjer et al., 2006) and velocity-encoding (Westenberg et al., 2006). However, these techniques have not yet been applied to determine whether they have the ability to predict outcome after CRT.

The basis of measurement of CMR-TSI is the use of steady state free precession (SSFP) short axis stacks available on a routine LV perfusion study, which are straightforward to acquire and do not require specialised sequences or analysis. The very low inter-observer and intra-observer variabilities of CMR-TSI (< 9%) (Chalil et al., 2007d) and scar quantification (Bülow et al., 2005, Thiele et al., 2006) make these techniques readily applicable clinically. The disadvantage to measurement of CMR-TSI is that it is time consuming, taking up to 2 hours per scan, although in the future this could become automated.

Pacing left ventricular scar is associated with worse outcome after CRT. This may simply relate to lack of myocardial viability at the pacing site, making the scar less excitable in response to the pacing stimulus. (Tedrow et al., 2004) The presence of scar is associated with delayed conduction of the stimulus through the myocardium (Lambiase et al., 2004),

which may in turn result in delayed contraction of the postero-lateral wall, which is crucial in CRT. (Breithardt et al., 2002) Furthermore, we have shown that posterolateral scar is associated with worse reverse remodelling after CRT implantation. (Chalil et al., 2007c)

The unique application of CMR-TSI coupled with the assessment of postero-lateral scar is a powerful risk-stratifier of patients with symptomatic moderate to severe heart failure undergoing CRT. Patients with marked dyssynchrony and the presence of posterolateral scar are 12 fold more at risk of cardiovascular death or heart failure hospitalisation. Furthermore, pacing left ventricular scar results in worse outcome after CRT. The findings demonstrate the value of a CMR scar prior to CRT implantation.

6.5 TABLE LEGENDS

Table 6-1 Baseline clinical and cardiovascular magnetic resonance imaging characteristics for patients undergoing cardiac resynchronisation therapy, grouped according to degree of dyssynchrony and presence or absence of posterolateral scar

Table 6-2 Clinical endpoints for patients undergoing cardiac resynchronisation therapy, grouped according to degree of dyssynchrony and presence or absence of posterolateral scar

Table 6-3 Uni-variable Cox proportional hazards analyses of clinical endpoints in relation to cardiovascular magnetic resonance variables according to imaging modality

Table 6-4 Clinical and echocardiographic variables during follow-up in patients undergoing cardiac resynchronisation therapy, grouped according to degree of dyssynchrony and presence of posterolateral scar at baseline

6.6 FIGURE LEGENDS

Figure 6-1 Kaplan-Meier estimates of the time to the various clinical endpoints. Patients were stratified according to a pre-implant CMR-TSI (<110 msec or CMR-TSI \geq 110 msec) as well as presence or absence of a posterolateral (PL) scar. MCE=major cardiovascular events; HF=heart failure.

Figure 6-2 Kaplan-Meier estimates of the time to the various clinical endpoints in patients with ischemic (ICM) or non-ischaemic (NICM) cardiomyopathy. MCE=major cardiovascular events; HF=heart failure.

Table 6-1 Baseline clinical and cardiovascular magnetic resonance imaging characteristics

Grouped by dyssynchrony and presence or absence of posterolateral scar.

	All	CMR-TSI<110	CMR-TSI≥110	CMR TSI<110	CMR TSI≥110
		No PL scar	No PL scar	+ PL scar	+ PL scar
<i>N</i>	141	62	28	24	27
Age, yrs	66.8 ± 10.1	65.4 ± 10.4	68.1 ± 9.6	68.4 ± 9.6	67.0 ± 10.2
Male sex %	76	68	75	88	85 *
Aetiology %					
ICM	65	39	57	100	100 ***
NICM	35	61	43	0	0 ***
Co-morbidity %					
Diabetes mellitus	15	11	25	17	11
Hypertension	28	29	29	29	22
CABG	23	16	7	33 *	48 ***
Medication %					
Loop diuretics	88	94	86	88	78
ACE-I or ARB	92	94	89	92	93
Beta-blockers	58	56	61	58	59
Spironolactone	47	53	36	33	56
ECG variables					
Sinus rhythm					

(n=118) %	84	82	71	83	100 *
QRS duration	145.0	143.9	146.9	135.0	156.8
, msec	±27.2	± 28.1	± 26.1	± 20.8	± 28.5
CMR variables					
LVEDV, cm ³	243.0	217.8	288.1	220.2	276.9
	± 98.3	± 94.5	± 102.3 *	± 99.6	± 79.6
LVESV, cm ³	195.8	168.9	244.1	172.7	230.8
	± 95.7	± 92.2	± 98.0 **	± 95.3	± 74.5 *
LVEF, %	23.2	27.2	17.0	26.3	17.4
	± 11.0	± 12.3	± 6.0 ***	± 10.6	± 6.6 ***
CMR-TSI, msec	101.4	69.8	134.2	76.2	161.4
	± 48.8	± 23.8	± 20.5 ***	± 16.1	± 53.8 ***
Scar volume, %	20.0	11.1	19.7	26.9	35.1
	± 20.0	± 16.5	± 22.6	± 14.5 **	± 18.2 ***

P values refer to differences between the groups and the group with a CMR-TSI < 110msec and no posterolateral (PL) scar. *, p<0.05, **, p<0.01, ***, p<0.001.

Table 6-2 Clinical endpoints for patients undergoing CRT in relation to PL scar

	All	CMR-TSI			
		<110 - PL	≥110 - PL	<110msec + PL	≥110msec + PL
<i>N</i>	141	62	28	24	27
Follow-up period, days	794 ± 483	854 ± 471	676 ± 570	777 ± 443	792 ± 448
Endpoints %					
Total mortality or Hospitalisation for MCE (n=43)	30	8	25 *	46 ***	74 ***
Cardiovascular mortality or hospitalisation for HF (n=36)	26	6	14	42 ***	67 ***
Cardiovascular mortality (n=30)	21	5	18 *	29 **	56 ***
Total mortality (n=33)	23	6	21 *	33 **	56 ***
Mode of death %					
Pump failure (n=23)	16	3	11 †	17 *	52 ***
Sudden cardiac death (n=7)	5	2	7	13 *	4
Non-cardiac death (n=3)	2	2	4	4	0

Variables are expressed as n (% of total patients in the group). Follow-up period is expressed as mean ± p values refer to differences between the groups and the group with a CMR-TSI < 110 msec and no posterolateral (PL) scar. MCE = major cardiovascular events; HF = heart failure. †, includes 1 heart transplant.

Table 6-3 Uni-variable Cox proportional hazards analyses of clinical endpoints**Cardiovascular death or hospitalization for HF**

Comparator	HR (95% CI)	p
<i>Assessment of CMR-TSI or scar</i>		
CMR-TSI \geq 110 msec CMR-TSI < 110 msec	2.86 (1.46 - 5.59)	0.0022
PL scar No PL scar	6.26 (3.00 -13.1)	<0.0001
<i>Assessment of CMR-TSI and scar</i>		
CMR-TSI \geq 110 msec and PL scar CMR-TSI <110 msec/No PL scar	11.8 (3.99 - 35.0)	<0.0001
CMR-TSI \geq 110 msec or PL scar	4.77 (1.57 - 14.5)	0.0059
<i>Continuous variables</i>		
LVEF	0.94 (0.91 - 0.98)	0.003
LVEDV	1.00 (1.00 - 1.01)	NS
LVESV	1.00 (1.00 - 1.01)	NS
Scar volume	1.02 (1.01 - 1.04)	0.0029

Death from any cause or hospitalisation for MCE

<i>Assessment of CMR-TSI or scar</i>		
CMR-TSI \geq 110 msec CMR-TSI < 110 msec	3.70 (1.96 - 6.99)	<0.0001
PL scar No PL scar	5.07 (2.65 - 9.69)	<0.0001
CMR-TSI \geq 110 msec/+PL scar CMR-TSI \geq 110 msec or PL scar <i>or</i> neither	4.71 (2.52 - 8.78)	<0.0001

Assessment of CMR-TSI and scar

CMR-TSI \geq 110 msec and PL scar CMR-TSI <110 msec/No PL scar	12.6 (4.69 - 33.7)	<0.0001
CMR-TSI \geq 110 msec or PL scar	5.07 (1.88 - 13.7)	0.0013

Continuous variables

LVEF	0.94 (0.90 - 0.97)	0.0006
LVEDV	1.00 (1.00 - 1.01)	0.0405
LVESV	1.00 (1.00 - 1.01)	0.0076
Scar volume	1.02 (1.00 - 1.03)	0.0066

Cardiovascular Death*Assessment of CMR-TSI or scar*

CMR-TSI \geq 110 msec CMR-TSI < 110 msec	3.55 (1.66 - 7.60)	0.0011
PL scar No PL scar	4.38 (2.03 - 9.46)	0.0002
CMR-TSI \geq 110 msec/+PL scar CMR-TSI \geq 110 msec or PL scar <i>or</i> neither	3.74 (1.81 - 7.71)	0.0004

Assessment of CMR-TSI and scar

CMR-TSI \geq 110 msec and PL scar CMR-TSI <110 msec/No PL scar	12.2 (3.54 - 42.3)	<0.0001
CMR-TSI \geq 110 msec or PL scar	5.29 (1.49 - 18.8)	0.0099

Continuous variables

LVEF	0.94 (0.90 - 0.99)	0.0086
LVEDV	1.00 (1.00 - 1.01)	NS

LVESV	1.00 (1.00 - 1.01)	0.0147
Scar volume	1.02 (1.01 - 1.04)	0.0124

Death from any cause

Assessment of CMR-TSI or scar

CMR-TSI \geq 110 msec CMR-TSI $<$ 110 msec	3.37 (1.62 - 7.01)	0.0011
PL scar No PL scar	3.39 (1.67 - 6.89)	0.0007
CMR-TSI \geq 110 msec/+PL scar CMR-TSI \geq 110 msec or PL scar <i>or</i> neither	3.28 (1.62 - 6.65)	0.0010

Assessment of CMR-TSI and scar

CMR-TSI \geq 110 msec and PL scar CMR-TSI $<$ 110 msec/No PL scar	8.91 (2.95 - 26.9)	0.0001
CMR-TSI \geq 110 msec or PL scar	4.64 (1.53 - 14.1)	0.0068

Continuous variables

LVEF	0.94 (0.89 - 0.98)	0.0036
LVEDV	1.00 (1.00 - 1.01)	NS
LVESV	1.00 (1.00 - 1.00)	0.0146
Scar volume	1.02 (1.01 - 1.03)	0.0098

The comparator is the lowest risk group category in each model. HF = heart failure; HR (95% CI) = hazard ratio and 95% confidence intervals; CMR-TSI = cardiovascular magnetic resonance tissue synchronisation imaging score; PL = postero-lateral; MCE = major cardiovascular events; LVESV = left ventricular end-systolic volume; LVEDV = left ventricular end-diastolic volume; LVEF = left ventricular ejection fraction.

Table 6-4 Clinical and echocardiographic variables during follow-up in patients undergoing cardiac resynchronisation therapy, grouped according to degree of dyssynchrony and presence of posterolateral scar at baseline

	All	<110 msec -PL scar	≥110msec -PL scar	<110msec + PL scar	≥110msec + PL scar
<i>N</i>	141	62	28	24	27
Clinical variables					
NYHA class					
Baseline	3.18 ± 0.54	3.19 ± 0.51	3.21 ± 0.42	3.21 ± 0.72	3.07 ± 0.54
Follow-up	1.98 ± 0.77 ***	1.93 ± 0.76 ***	2.09 ± 0.68 ***	2.0 ± 1.0 ***	1.96 ± 0.66 ***
6-min walk test, metres					
Baseline	252.9 ± 111.2	259.4 ± 111.9	221.5 ± 115.8	235.8 ± 119.9	282.7 ± 93.6
Follow-up	323.5 ± 116.4 ***	338.2 ± 129.9 ***	287.6 ± 116.8*	334.9 ± 113.1**	319.0 ± 93.8 **
Quality of life score					
Baseline	56.7 ± 20.1	62.9 ± 20.4	54.9 ± 20.1	58.2 ± 18.3	44.7 ± 16.5
Follow-up	32.5 ± 23.7 ***	30.0 ± 22.1 ***	36.1 ± 20.4 *	37.5 ± 29.9 **	29.5 ± 23.1*
Echocardiography					
LVEDV, mL					
Baseline	231.4 ± 86.4	225.0 ± 95.9	257.3 ± 82.5	215.3 ± 70.0	232.5 ± 77.7
Follow-up	209.6 ± 92.2 *	202.4 ± 115.7 *	225.2 ± 56.4	202.0 ± 64.5	218.5 ± 78.6
LVESV, mL					
Baseline	175.4 ± 75.7	172.0 ± 82.5	200.0 ± 73.5	159.4 ± 66.0	171.3 ± 68.0
Follow-up	148.0 ± 82.7 **	139.5 ± 98.2 ***	148.3 ± 56.4	146.4 ± 72.3	166.9 ± 72.2
LVEF, %					

Baseline	25.2 ± 10.7	24.3 ± 10.7	23.1 ± 10.2	27.2 ± 11.5	27.4 ± 10.4
Follow-up	30.4 ± 11.5 ***	33.4 ± 10.2 ***	29.1 ± 11.1	30.4 ± 14.6	25.2 ± 10.2

LVESV = left ventricular end-systolic volume; LVEDV = left ventricular end-diastolic volume; LVEF = left ventricular ejection fraction. P values refer to differences from baseline values within the group. *, p<0.05; **, p<0.01; ***, p<0.001.

Figure 6-1 Kaplan-Meier estimates of the time to the various clinical endpoints

Patients were stratified according to a pre-implant CMR-TSI (<110 msec or CMR-TSI \geq 110 msec) as well as presence or absence of a posterolateral (PL) scar.

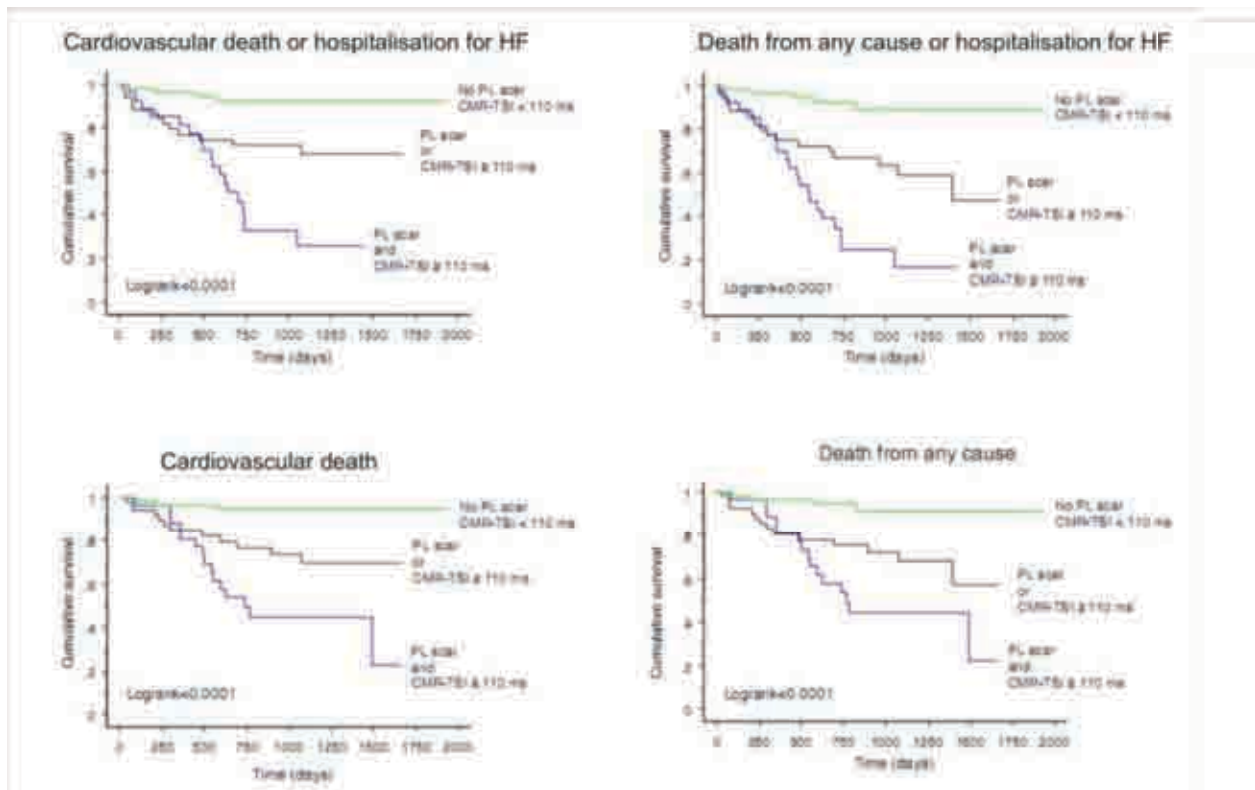
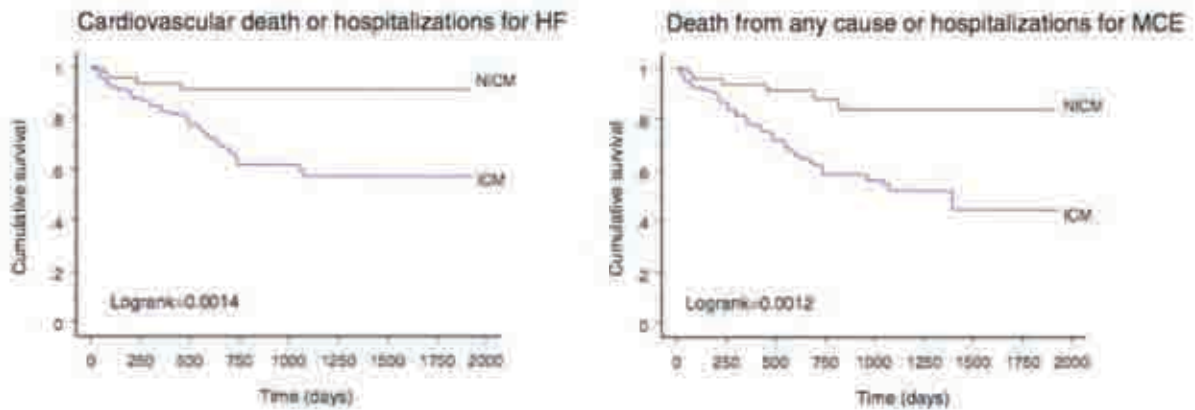


Figure 6-2 Kaplan Meier stratified according to ICM vs NICM

Kaplan-Meier estimates of the time to the various clinical endpoints in patients with ischemic (ICM) or non-ischaemic (NICM) cardiomyopathy. MCE=major cardiovascular events; HF=heart failure.



**CHAPTER 7. DEVELOPMENT AND VALIDATION OF A
CLINICAL INDEX TO PREDICT SURVIVAL AFTER CARDIAC
RESYNCHRONISATION THERAPY**

7.1 Introduction

Outcome in patients with moderate to severe heart failure is improved by CRT, but cannot be predicted in an individual patient. Various pre-implant factors have been shown in multicentre controlled clinical trials to affect the long term outcome, for instance, patients in class IV heart failure do not survive as long as patients in class III heart failure. (Lindenfeld et al., 2007) Despite this, there are a number of case series of patients in cardiogenic shock at the time of implantation, who survived for long periods after being implanted with CRT. (Herweg et al., 2007)

It is widely recognised that the effect of CRT is variable. As many as 20-30% of patients fail to gain symptomatic improvement (Abraham et al., 2002, Molhoek et al., 2002) and the survival benefit varies between patients. (Chalil et al., 2007a, Chalil et al., 2007b)

Identifying a pre-implant measure that robustly predicts mortality in patients undergoing CRT is, therefore, desirable. In many other fields of medicine, it has been considered desirable to determine which patients benefit from particular interventions, for instance reperfusion treatment in acute myocardial infarction. This allows efficacious treatment to be directed at those most likely to gain benefit, which is particularly important for relatively high cost interventions.

Cardiovascular magnetic resonance (CMR) is becoming a routine investigation for patients with heart failure, being the gold standard for the *in vivo* assessment of cardiac structure, function, and dyssynchrony. (Lardo et al., 2005) In this thesis, CMR tissue synchronisation index (CMR-TSI), derived from a routine CMR scan, has been found to be a powerful predictor of mortality and morbidity after CRT. In addition, CMR also

allows visualisation and quantification of myocardial scarring. (Chalil et al., 2007c, White et al., 2006) Importantly, the size (burden), trans-murality and location of a myocardial scar in the LV free wall, the target location for the left ventricular lead in CRT, have been linked to a poor outcome after CRT. (Bleeker et al., 2006c, Chalil et al., 2007c, Chalil et al., 2007d, White et al., 2006)

Having shown that CMR-TSI and posterolateral scar are important determinants of outcome, we sought to develop a risk score to enable prediction of outcome after CRT. We have explored the value of pre-implant CMR measures of dyssynchrony and myocardial scarring, as well as more conventional heart failure risk factors, (Aaronson et al., 1997) in predicting cardiovascular mortality after CRT. This study focuses on the derivation and validation of a clinical risk index based on a combination of such non-invasive measures.

7.2 Methods

7.2.1 Patients

A total of 148 consecutive heart failure patients were prospectively enrolled from January 2001 to April 2008 at a single centre (Good Hope Hospital). Patients were selected if they were due to undergo CRT for standard indications (ischaemic or non-ischaemic cardiomyopathy, New York Heart Association [NYHA] class III or IV, LV ejection fraction [LVEF] <35%, QRS duration \geq 120 ms). The majority of patients were recruited prior to the publication of the guidelines on implantable cardioverter-defibrillator therapy in the United Kingdom. (Implantable cardioverter defibrillators for

arrhythmias. Review of Technology Appraisal 11. Technology Appraisal 95, 2006) All patients had undergone coronary angiography. The clinical diagnosis of systolic heart failure was based on clinical criteria and evidence of systolic dysfunction on echocardiography. The diagnosis of ischaemic cardiomyopathy was made if systolic dysfunction was associated with a history of myocardial infarction, (Alpert et al., 2000) the findings of coronary angiography, or if the pattern of late-gadolinium hyperenhancement was characteristic of a myocardial infarction. (Assomull et al., 2006) The study was approved by the North Birmingham Ethics Committee.

7.2.2 Study design

A CMR study was performed at baseline. For validation of the DSC risk index, the clinical endpoint considered was cardiovascular death. For qualitative comparisons with the CARE-HF study, we also considered the composite endpoint of death from any cause or hospitalizations for major cardiovascular events, as defined in the CARE-HF study protocol. (Cleland et al., 2005b) Mortality data was collected through medical records and, where appropriate, from interviews with patient's caregivers. Clinical outcome data were collected on a 2-monthly basis by an investigator who was blinded to other clinical and imaging data. Sudden cardiac death was defined as "a natural, unexpected death due to cardiac causes, heralded by an abrupt loss of consciousness within one hour of the onset of acute symptoms". (Myerburg and Castellanos, 1997)

7.2.3 Device therapy

Biventricular pacemaker (CRT-P) implantation was undertaken as previously described.

7.2.4 Cardiovascular magnetic resonance

The CMR-TSI and scar imaging was measured as previously described.

7.2.5 Statistical analysis

Continuous variables are expressed as mean \pm standard deviation (SD). Normality was tested using the Shapiro-Wilk test. Variables which were not normally distributed were log-transformed before statistical analyses. Comparisons between normally distributed continuous variables were made using ANOVA with Scheffe's F procedure for multiple comparisons. Categorical variables were analyzed using chi-squared tests and Scheffe's post-hoc test. Changes in variables from baseline to follow-up were analyzed using paired Students' t-tests. Variables showing significant group differences at baseline were entered into Cox proportional hazards analyses.

Differences in Kaplan-Meier survival curves between the risk groups were assessed using the log-rank (Mantel-Cox) test. Areas under the receiver-operating characteristic curves (AUC) were used to derive optimal cut-off points for the DSC index. Statistical analyses were performed using Statview (Cary, NC) and SPSS 13.0 (Chicago, Illinois). A two-tailed p value of <0.05 was considered statistically significant. Analysis of wall motion was performed using the R statistical language.

7.2.6 Development of the risk index

This was developed on the basis of the data presented in this chapter. In line with Harrell's recommendations on multivariate prognostic modelling, (Harrell et al., 1984,

Harrell et al., 1996) candidate variables were selected on the basis of their proven clinical, pathophysiological and epidemiological relevance to the endpoint in question.

Accordingly, studies of patients with heart failure treated (Chalil et al., 2007a, Chalil et al., 2007b, Chalil et al., 2007c, Chalil et al., 2007d) and not treated (Aaronson et al., 1997, Anker et al., 2003, Lee et al., 2003) with CRT were used to guide data reduction. Continuous rather than dichotomous variables were used wherever possible. (Harrell et al., 1996) The aim throughout the data reduction process was to identify a small number of variables which, on the basis of their biological relevance to heart failure and CRT, explained survival. (Harrell et al., 1984) Interactions between variables were extensively explored using interaction terms in Cox proportional hazards models. Linearity assumptions were checked using Martingale residuals. Cross-product terms were added to check for additivity assumptions. The proportional hazards assumption was checked using Schoenfeld residuals. (Schoenfeld, 1982)

Variables achieving a $p < 0.10$ in univariate Cox proportional hazards analyses were entered in a stepwise multivariate model using Akaike's information criterion as a stopping rule (χ^2 for a set of variables > 2 degrees of freedom), implemented using the Harrell 'Design' package version 2.1-1 in R. (Harrell, 2007)

7.2.7 Validation

Validation was implemented using bootstrapping. (Harrell et al., 1984) (Efron, 1979, Harrell et al., 1996) This nonparametric method, which estimates sampling distributions of a predictor variable by resampling with replacement from the original sample, is, in effect, an impression of the validity of predictions in new but similar patients. For each

group of 200 bootstrap samples, the model was refitted and tested against the observed sample in order to derive an estimate of the predictive accuracy and bias. This was used to select 148 ‘new’ patients from the original cohort, one at a time with replacement, 200 times over.

For each of these 200 samples, the following parameters were derived: 1) the β coefficients from Cox proportional hazards models; 2) Somer’s D rank correlation index and 3) an estimate of the slope shrinkage. (Harrell et al., 1984) The apparent Somer’s D (D_{app}) was derived using stepwise Cox proportional analyses. The bootstrap-corrected performance of the predictor equation, or ‘optimism’, (Harrell et al., 1996) was quantified by assessing the difference between Somer’s D in the original sample (D_{orig}) and D in the bootstrap sample (D_{boot}). The average optimism, termed O, was derived by repeating the above steps 200 times over. The bootstrap-corrected performance of the original stepwise model, $D_{app} - O$, is, effectively, an honest estimate of internal validity. (Harrell et al., 1996) Actual survival was plotted against apparent estimated survival and bootstrap-corrected estimated survival.

7.2.8 Calculation of the risk index

The risk prediction index was expressed as the absolute value of the sum of the products of these variables and their β coefficients [ie.weights] from the final stepwise multivariate Cox proportional hazards model, identified by Harrell’s routine (Harrell et al., 1984) (Harrell et al., 1996): $\sum \beta_i x_i = |\beta_1 x_1 + \beta_2 x_2 + \dots + \beta_n x_n|$, where x_1, x_2, \dots, x_n are the values for the variables and $\beta_1, \beta_2, \dots, \beta_n$ are the coefficients for each variable. For categorical variables, presence was computed as the β coefficient and absence as zero.

7.3 Results

The characteristics of the study group are shown in Table 7-1.

7.3.1 Predictor variables

There were 20 cardiovascular deaths by 1 year and 28 by 2 yrs. After a median follow-up of 913 (interquartile range 967) days for events, there were 37 cardiovascular deaths. Of these, 28 were due to pump failure, 8 were sudden and one patient underwent cardiac transplantation. Table 7-2 shows the candidate variables, ranked according to the likelihood ratio (LR) χ^2 . With respect to imaging variables, posterolateral scar location, CMR-TSI, scar size and LVEF emerged as the most significant predictors (all $p < 0.0001$). Amongst circulating markers, sodium and creatinine were significant predictors (both $p < 0.01$), uric acid only reached borderline significance ($p = 0.0808$) and haemoglobin failed to reach significance. Male gender was also a predictor ($p = 0.0417$). Age, NYHA class, QRS duration, presence of atrial fibrillation, as well as diagnosis of diabetes or a previous CABG failed to reach statistical significance. Similarly, use of loop diuretics, angiotensin converting enzyme inhibitors (ACE)/angiotensin-receptor blockers, beta-blockers or spironolactone failed emerge as predictors of cardiovascular mortality (data not shown).

Although ischaemic aetiology did emerge as a significant predictor of cardiovascular mortality in univariate analysis, addition of scar burden to this model rendered aetiology non-significant (data not shown). The decision not to include ischaemic aetiology in the multivariate model was taken in view of its expected interaction with scar burden and scar location (non-ischaemic cardiomyopathy is associated with little or no scar). In

addition, the diagnoses of ischaemic and non-ischaemic cardiomyopathy were made on the basis of size, transmural and location of scar in the CMR scan.

7.3.2 Derivation

Variables that reached a $p < 0.10$ on univariate Cox proportional hazards analyses were entered into stepwise models. These variables included gender, sodium, creatinine, scar burden, scar transmural, CMR-LVEF, CMR-TSI and posterolateral scar location. As shown in Table 7-3, the variables identified in the final stepwise model were:

Dyssynchrony, Scar location (posterolateral) and Creatinine. Therefore, the DSC index was calculated as follows: (2.5039 if posterolateral scar present; 0 if absent) + 0.0107. CMR-TSI [ms]) + (0.0132 * plasma creatinine [$\mu\text{mol/L}$]).

7.3.3 The DSC index

Strata of the DSC index were designated as low, intermediate or high risk, with cut-offs of <3 , between 3 and 5 and ≥ 5 . These were chosen arbitrarily for ease of use in clinical practice. Kaplan-Meier analyses were used to assess survival according strata of the DSC index (Figure 7-1). The Cox proportional hazards analyses adopting cardiovascular mortality as the dependent variable and strata of the DSC index as an independent variable were LR χ^2 : 59.1, $p < 0.0001$. The AUC for the DSC index in relation to cardiovascular mortality at various time points is shown in Figure 7-3.

7.3.4 Validation

Amongst the statistics derived from Harrell's routine (Harrell, 2007, Harrell et al., 1996) was a bias-corrected slope of the model of 0.93, indicating an excellent model calibration, taking into account over fitting (Figure 7-2). Somer's D_{app} was -0.70 and the optimism (O) was -0.01. The bias-corrected performance of the stepwise model ($D_{app} - O$) was acceptable, at -0.69, indicating excellent internal validity. The optimism-corrected discrimination index was 0.91; the optimism-corrected unreliability index U was 0.01 and the overall quality index was 0.85.

7.4 Discussion

These findings have been derived on the basis of the previous chapters demonstrating that dyssynchrony and postero-lateral scar imply an adverse outcome after CRT. We sought to develop a predictive index of mortality in patients prior to pacemaker implantation. This index is based on CMR variables as we have shown these to predict outcome after CRT. Echocardiographic variables may in future robustly determine outcome, but the methodology still requires further evaluation. (Yu et al., 2009)

In deriving an index for the prediction of cardiovascular mortality after CRT, 16 non-invasive variables have been considered which have been shown to be of prognostic value in patients with heart failure treated (Chalil et al., 2007c, White et al., 2006) and not treated (Aaronson et al., 1997, Anker et al., 2003, Lee et al., 2003) with CRT.

The aim was to identify a non-invasive predictive index, derived from a small number of variables. The DSC index, which combines pre-implant measures of Dyssynchrony and location of myocardial Scar as well as Creatinine, is a novel, powerful predictor of

cardiovascular mortality in patients treated with CRT. Compared to patients in the lowest risk stratum, cardiovascular mortality in the intermediate and high risk strata of the DSC index were 11.1 and 30.5 times higher by the end of the follow-up period, respectively. This index may be useful in tailoring follow-up strategies and device selection in CRT patients.

The collection of variables from which the DSC was derived included those which have previously been linked to a poor outcome in patients with heart failure. (Aaronson et al., 1997, Anker et al., 2003, Lee et al., 2003) Of particular mechanistic relevance to CRT is scar burden and scar location.

7.4.1 Role of posterolateral scar

This study confirms our findings showing that the presence of myocardial scar over the posterolateral LV wall is a powerful predictor of cardiovascular mortality. The precise pathophysiological mechanism is still unclear, but several factors may contribute to this observation. Firstly, myocardial scars are not readily excitable. (Tedrow et al., 2004) A posterolateral scar reduces the volume of excitable myocardium in the vicinity of the LV pacing stimulus and delays activation of potentially recruitable myocardium, which is crucial for CRT. (Breithardt et al., 2002, Lambiase et al., 2004) Secondly, a posterolateral scar also reduces the amount of myocardium available for contraction in CRT, thereby leading to suboptimal reverse LV remodelling following CRT. (Bleeker et al., 2006c) Thirdly, posterolateral scarring may also preclude proper papillary muscle function, which is essential for competence of the mitral valve. The posterolateral region is commonly targeted for placement of the left ventricular lead.

7.4.2 Role of dyssynchrony

This study is consistent with the previous chapters which found that dyssynchrony, assessed using CMR-TSI, predicts of a relatively poor outcome after CRT. These findings are in contrast to numerous echocardiographic studies showing that increasing dyssynchrony relates to increasing benefit from CRT. In other words, our findings point towards a ‘dyssynchrony is bad’ paradigm, whereas echocardiographic studies support a ‘dyssynchrony is good’ paradigm of CRT.

Our finding that ‘dyssynchrony is bad’ is, however, consistent with echocardiographic studies in non-paced patients with heart failure. (Bader et al., 2004) Bax et al. found that beyond a limit of dyssynchrony (a septal-to posterior wall motion delay of 100 ms), CRT does not result in reverse LV remodelling. (Bax et al., 2004b) The finding that dyssynchrony is an adverse prognostic marker is consistent with the non-paced data, and makes biological sense.

7.4.3 Role of renal function in outcome

The emergence of plasma creatinine in the final model is not surprising. Renal dysfunction is an important determinant of adverse prognosis in heart failure. (Dries et al., 2000, Hillege et al., 2000, Smilde et al., 2004) and it is on this basis that plasma creatinine has been included in risk prediction models for patients with heart failure. (Lee et al., 2003, Levy et al., 2006) We have shown that the inverse relationship between plasma creatinine and survival still holds in patients with heart failure undergoing CRT. The strength of this influence is reflected by the fact that it remained significant in final stepwise Cox proportional hazard models.

As our study did not include a control group, one cannot be certain the CRT-P led to a prognostic benefit. This, however, seems likely in view of the similarity between the prognostic risk profile of the present cohort and that of the CRT-P arm of the CARE-HF study (Figure 7-4).

7.4.4 Limitations of the Study

All patients in this study underwent implantation of a CRT device without defibrillator backup. Therefore, the DSC index may not be generalisable to a population of patients treated with defibrillator back-up (CRT-D). Ideally, external validation of the DSC index in a cohort of patients undergoing CRT-D would be desirable. The DSC index could be used to risk-stratify patients to CRT-P or the more costly CRT-D, which is more appropriate for patients at high risk of cardiovascular events. Importantly, however, the principal cause of cardiovascular death in this study was pump failure, rather than sudden, presumed arrhythmic death.

As a further limitation, the use of beta blockers and spironolactone were relatively low. Whilst drug therapy failed to emerge as a predictor of cardiovascular mortality, we cannot discount the possibility that the relationship between the DSC score and cardiovascular mortality might be influenced by better optimised medical therapy. However, the proportion of patients in NYHA class IV heart failure was greater than randomised in contemporary studies, suggesting that these patients were sicker and possibly less able to tolerate medical therapy.

The presence of posterolateral scar implies such an adverse prognosis that it carries a proportionate weight. In terms of the model, as this is a dichotomous variable rather than a continuous variable, it makes the presence of posterolateral scar the dominant factor in the model.

NT-pro-BNP was not included in this model, as it was not systematically available pre-implant. NT-pro-BNP has been shown to be an important prognostic marker in patients treated with CRT and future work should be directed to studied the effect of this biomarker on the risk index.

7.5 Summary

This study comprised patients with heart failure in NYHA class III and IV, such as those included in the CARE-HF study. We conclude that, in such patients, the DSC index is a powerful risk-stratifier for cardiovascular mortality. Patients in the highest risk stratum were more than 30 times more likely to die from cardiovascular causes than those in the low risk group. These findings underline the value of a standard CMR LV study in the risk-stratification of patients undergoing CRT. Such risk stratification may be helpful in tailoring follow-up and further therapy.

7.6 Table legends

Table 7-1 Clinical characteristics of the study patients, grouped according to survival status at the end of the study period Clinical characteristics of the study patients, grouped according to survival status at the end of the study period.

Table 7-2 Univariate Cox proportional hazard analyses of predictors of mortality Univariate Cox proportional hazard analyses of predictors of mortality.

Table 7-3 Final model from bootstrapped stepwise multivariate Cox proportional hazard analyses of predictors of mortality Final model from bootstrapped stepwise multivariate Cox proportional hazard analyses of predictors of mortality.

7.7 Figure legend

Figure 7-1 Kaplan-Meier estimates of the time to cardiovascular death. Patients were stratified according to pre-implant DSC index.

Figure 7-2 Calibration of predictions of mortality after cardiac resynchronisation therapy.

Figure 7-3 Receiver-operator characteristic curves of the DSC index against cardiovascular mortality at 1 and 2 years, and at the end of the follow-up period.

Figure 7-4 Comparison of events in the present cohort and in the CARE-HF study.

Table 7-1 Clinical characteristics of the study patients, grouped according to survival status at the end of the study period

	All
<i>N</i>	148
Age, yrs	66.7 ((10.4)
Men, No. (%)	114 (77)
Ischaemic aetiology, No. (%)	92 (62)
NYHA class	3.2 ((0.43)
Creatinine, µmol/L	119.8 ((38.3)
Sodium, mmol/L	139.0 ((5.8)
Haemoglobin, g/dL	14.1 ((7.9)
Co-morbidity, No. (%)	
Diabetes mellitus	24 (16)
Hypertension	40 (27)
CABG	31 (21)
Medication, No. (%)	
Loop diuretics	129 (87)
ACE-I or ARB	136 (92)
Beta-blockers	81 (55)
Spironolactone	66 (45)
ECG variables	
Atrial fibrillation, No. (%)	23 (16)
QRS duration (ms)	145.9 ((26.5)
CMR variables	
LVEDV, mL	247.8 ((99.5)

LVESV, mL	200.2 ((96.6)
LVEF, %	22.5 ((10.6)
CMR-TSI, ms	100.7 ((47.8)
Scar †	
Volume, %	19.5 ((20.1)
Transmural, No. (%)	62 (42)
Posterolateral, No. (%)	48 (32)

Abbreviations:

NYHA, New York Heart Association; CABG, coronary artery bypass graft; ACE-I, angiotensin-converting enzyme inhibitors; ARB, angiotensin receptor blockers; LVEDV, left ventricular end-diastolic volume; LVESV, left ventricular end-systolic volume; LVEF, left ventricular ejection fraction; CMR-TSI, cardiovascular magnetic resonance tissue synchronization index.

† Transmural scars were those with $\geq 51\%$ transmural. Continuous variables are expressed as mean (SD).

Table 7-2 Univariate Cox proportional hazard analyses of predictors of mortality

	β coefficient (95% CI)	HR (95% CI)	LR χ^2	p
PL scar location	2.82 (1.94 to 3.70)	16.8 (6.94 to 40.5)	58.6	<0.0001
CMR-TSI, ms*	0.015 (0.01 to 0.02)	1.01 (1.01 to 1.02)	22.5	<0.0001
Scar burden, %	0.03 (0.01 to 0.04)	1.03 (1.01 to 1.04)	13.3	0.0001
CMR-LVEF, %	-0.06 (-0.10 to -0.02)	0.94 (0.90 to 0.98)	11.1	0.0032
Sodium, mmol/L	-0.13 (0.04 to -0.04)	0.88 (0.81 to 0.96)	8.2	0.0031
Creatinine, μmol/L	0.01 (0.00 to 0.02)	1.01 (1.00 to 1.02)	7.92	0.0049
Transmurality	0.92 (0.26 to 1.58)	2.51 (1.29 to 4.84)	7.64	0.0057
Male gender	0.95 (-0.08 to 1.99)	2.59 (0.92 to 7.32)	4.15	0.0417
Uric acid, μmol/L	0.00 (-0.00 to 0.00)	1.00 (1.00 to 1.00)	2.33	0.1265
NYHA class	0.54 (-0.17 to 1.21)	1.73 (0.84 to 3.37)	2.24	0.1343
CABG	-0.28 (0.18 to -0.62)	0.75 (0.53 to 1.08)	2.42	0.1196
QRS duration, ms	0.01 (-0.00 to 0.02)	1.01 (1.00 to 1.02)	1.01	0.2202
Age, yrs	0.01 (0.02 to -0.01)	1.01 (0.98 to 1.05)	0.78	0.3765
Atrial fibrillation	0.15 (-0.23 to 0.49)	1.16 (0.80 to 1.63)	0.64	0.4220
Diabetes mellitus	-0.17 (-0.55 to 0.28)	0.84 (0.57 to 1.33)	0.61	0.4324
Haemoglobin, g/dL	-0.02 (-0.19 to 0.02)	0.98 (0.83 to 1.02)	0.51	0.4763

Abbreviations: HR, hazard ratio; CI, confidence interval; CMR-TSI, cardiovascular magnetic resonance tissue synchronization index ; CMR-LVEF, cardiovascular magnetic resonance left ventricular ejection fraction; NYHA, New York Heart Association; CABG, coronary artery bypass graft.

Variables are listed in order of statistical significance and likelihood ratio (LR) (χ^2).

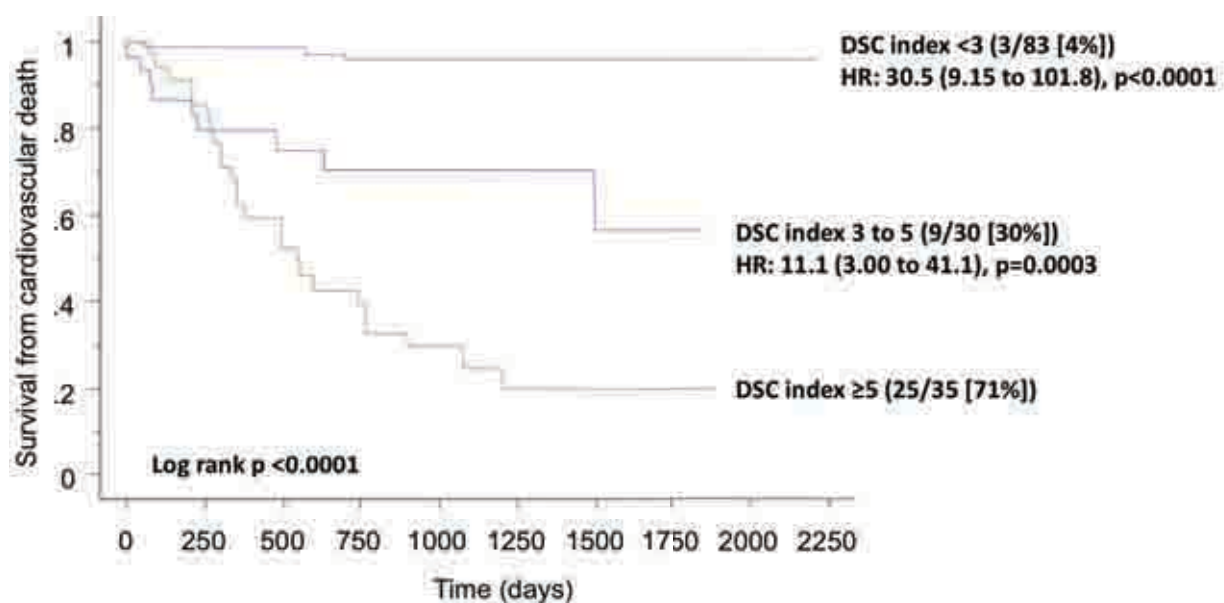
* Log transformed value used for statistical analysis.

Table 7-3 Final model from bootstrapped stepwise multivariate Cox proportional hazard analyses of predictors of mortality

	β coefficient (95% CI)	HR (95% CI)	Z-score	<i>p</i>
Posterolateral scar location	2.50 (1.60 to 3.40)	12.2 (4.97 to 30.1)	5.46	<0.0001
CMR-TSI , ms*	0.01 (0.00 to 0.02)	1.01 (1.00 to 1.02)	3.26	0.0011
Creatinine, $\mu\text{mol/L}$	0.01 (0.00 to 0.02)	1.01 (1.00 to 1.02)	2.83	0.0046
Model LR χ^2 : 73.4, $p < 0.0001$				

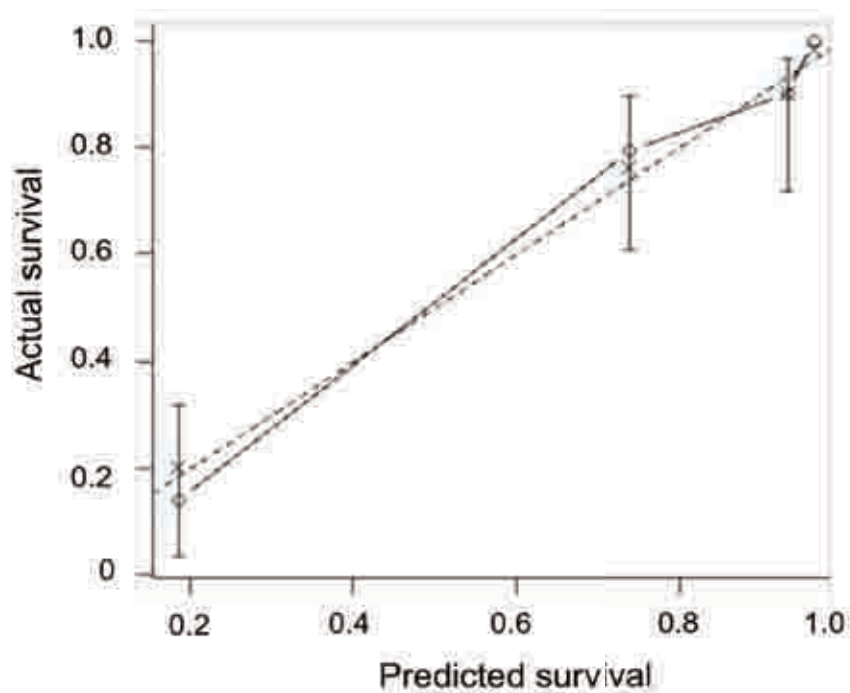
Abbreviations: HR, hazard ratio; CI, confidence interval; LR, likelihood ratio.

Figure 7-1 Kaplan-Meier estimates of the time to cardiovascular death.²⁶



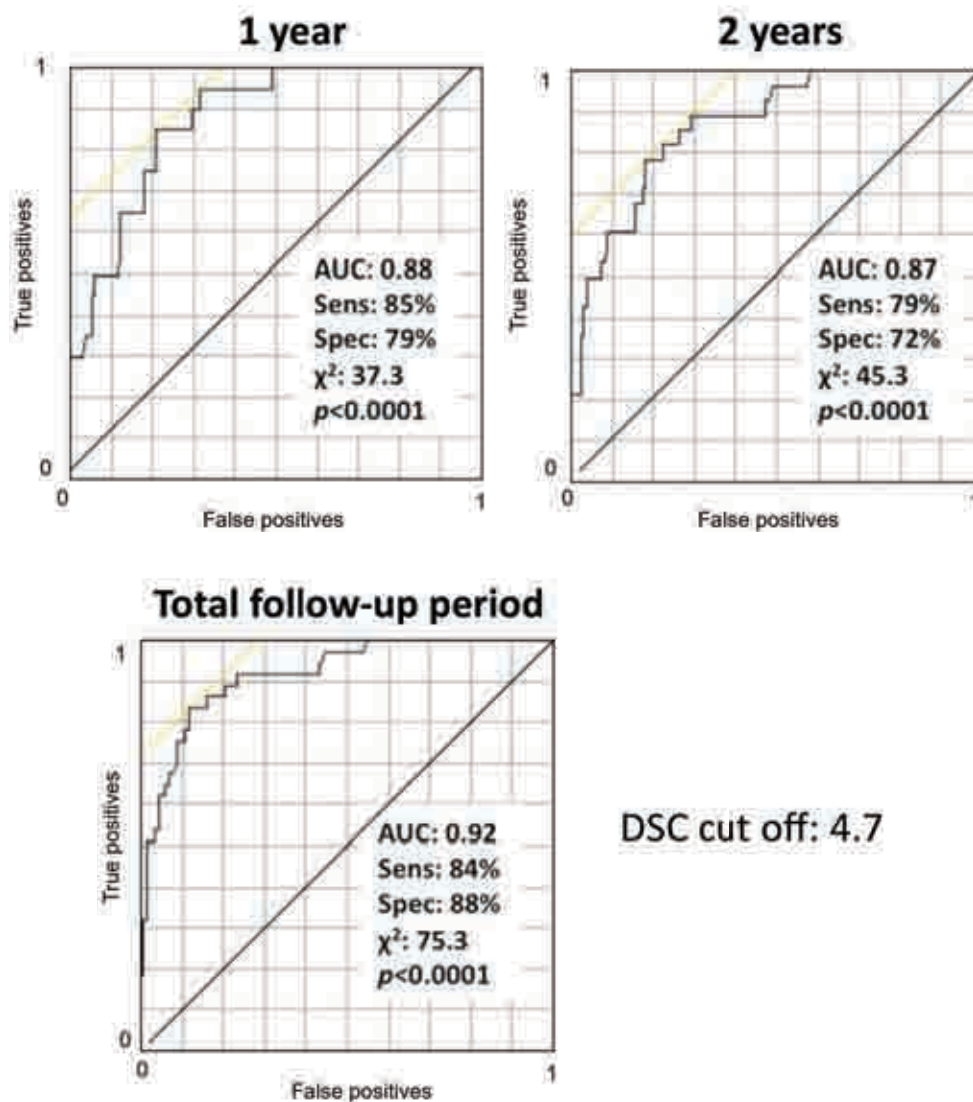
²⁶ Patients were stratified according to pre-implant DSC index. The event rate, number of patients in the DSC risk stratum and the percentage event rate are shown in brackets. The hazard ratio (HR) and 95% confidence intervals are also shown

Figure 7-2 Calibration of predictions of mortality after cardiac resynchronisation therapy²⁷



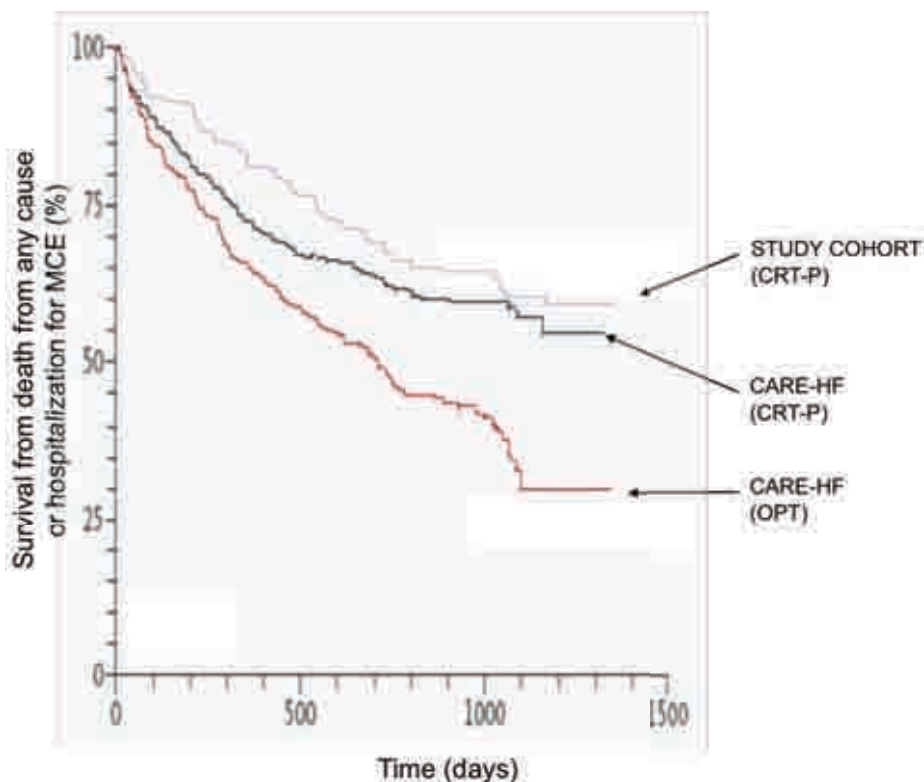
²⁷ Graph shows actual versus bootstrap-corrected predicted survival

Figure 7-3 Receiver-operator characteristic curves of the DSC index against cardiovascular mortality at 1 and 2 years, and at the end of the follow-up period²⁸



²⁸ AUC, area under the curve; sens, sensitivity, spec, specificity. Values refer to a DSC cut-off of 4.7

Figure 7-4 Comparison of events in the present cohort and in the CARE-HF study²⁹



²⁹ Qualitative comparison of Kaplan-Meier survival estimates for the combined endpoint of death from any cause or hospitalisations for major cardiovascular events (MCE) for patients included in this study as well as those in the CRT-P and the optimum medical treatment (OPT) arms the CARE-HF study. Follow-up time in the present cohort has been truncated to 1500 days.

CHAPTER 8. CONCLUSIONS

The studies included in this thesis were undertaken in the context that the prediction of the long term outcome in patients with HF treated with CRT remains problematic. It is widely recognised that patient selection for CRT treatment is difficult as patients selected with the current criteria do not always gain a symptomatic benefit. Whilst CMR remains the gold standard imaging technique in patients with systolic heart failure, systematic evaluation for dyssynchrony using CMR has not been widely available.

A study of a large cohort of patients with systolic heart failure revealed that dyssynchrony, measured with CMR-TSI, was highly prevalent regardless of QRS duration. We found that CMR-TSI was able to discriminate between normal patients and patients with systolic heart failure accurately. As might be expected, the CMR-TSI value was higher in patients with a broader QRS, and highest in those with the largest left ventricular volumes. Potentially, CMR-TSI may provide a global measure of left ventricular function. Further research comparing CMR-TSI with LVEF would demonstrate the prognostic value of this measure in other cohort, such as those undergoing revascularisation.

Myocardial scarring strongly influences dyssynchrony. The greater the myocardial scar the worse the dyssynchrony measured with CMR-TSI. The presence of greater dyssynchrony may contribute to the lower response rate seen in ICM patients, and the poorer prognosis compared with NICM patients. Thus, patients with extreme dyssynchrony may have extremely scarred ventricles, and hence are less likely to gain benefit from CRT due to failure to resynchronise and less viable myocardium. Patchiness of dyssynchrony was seen to increase in line with QRS duration, and the relationship

between the patchiness of the LV and the LV lead position may be crucial to understanding about the correct placement of the LV lead.

Septal to lateral wall motion delay measurement appeared less robust when compared with CMR-TSI in the heart failure cohort. CMR-TSI is a global measure of the LV motion, and hence contains a greater number of measurements compared with the septal to lateral delay, reducing the signal to noise ratio. An alternative explanation for the greater discrimination between HF patients and controls with CMR-TSI, is that a global measurement is more accurate than examining the difference between two regions of the left ventricle. This finding has implications for further research into predictors of response from CRT which has largely focussed on examining the difference in time to peak contraction in the septal to lateral region. Global measures of dyssynchrony, such as CMR-TSI and three dimensional echocardiography may be greater predictors of outcome.

The aim of pre-implant imaging is to predict the likely outcome from CRT, and we examined this in an observational study of large cohort of patients. We have shown that CMR-TSI is a powerful predictor of long term clinical outcome. However, in contrast to echocardiographic findings, we have found that the patients with the severest dyssynchrony fair the worst from CRT. This raises the hypothesis that patients with severe dyssynchrony do not gain significant life expectancy from CRT.

The role of QRS duration in selection of patients for CRT remains problematic.

Interestingly, QRS duration did not predict outcome in our cohort of patients undergoing CRT implantation. In addition, we found that patients with heart failure and narrow QRS (<120 ms) had significant dyssynchrony measured with CMR-TSI. This finding, coupled

with the failure of QRS duration to predict outcome, suggests that further long term study of CRT in this group is worthwhile, examining long term outcome and clinical evaluation with proven prognostic measures.

The visualisation of myocardial scar is straightforward with CMR, and this allows accurate measurement of the volume and distribution of scar. In a large cohort of patients with PL scar we found that transmural scar prevented significant long term symptomatic improvement. Furthermore, pacing left ventricular scar was associated with a worse symptomatic response and mortality and it is reasonable to suggest that pacing scar is detrimental.

Analysis of our cohort had identified two major predictors of adverse outcome in our cohort, and in Chapter 6 we found that the combination of both PL scar and CMR-TSI emerged as powerful predictors of events. Combining both measures allowed the CRT cohort to be divided into 2 major risk groups, with those patients who did not have either PL scar or a CMR-TSI > 110ms having the lowest risk. This supports the use of CMR as a pre-implant measure, and suggests the examination of dyssynchrony or scar alone will not be sufficient to accurately risk stratify patients.

The addition of standard parameters to CMR measures could potentially further risk stratify patients undergoing CRT, and this was examined in the final study of our cohort. We examined the importance of factors known to influence outcome, and sought to determine whether these factors independently predicted outcome. Based on three factors, the CMR-TSI, the presence of PL scar and the creatinine we developed a risk score which was then validated with bootstrapping. Unlike other heart failure scores, we found that the predictive impact of CMR was sufficient such that we required only three

markers to predict outcome. This study confirms the major role that CMR has in predicting outcome in HF patients.

A number of limitations arise from this work. Most importantly, this is purely observational data, and has not been confirmed in clinical trials. Our cohort is relatively unusual as the majority of patients underwent CRT pacing and we did not study patients undergoing CRT with defibrillator (CRT-D) backup. Potentially, the outcomes may differ in patients treated with CRT-D. A major criticism of the CMR-TSI technique is the lack of validation in another centre, by different researchers. The technique itself is not suitable for clinical use in its current form due to the labour intensity involved in demarcating the left ventricular borders, although potentially this could be automated.

A further major limitation of this observational study is that patients were entered when their clinical condition was recognised to merit further treatment by their treating physician. As a result, patients will have been implanted with CRT at variable lengths of time remote from their myocardial infarct. The development of heart failure could be more insidious in patients with PL scar compared with other locations, which could result in lead time bias in this type of observational study. Although the medical treatment of HF patients is implemented, inevitably the maximum tolerated HF medication will vary between patients depending on their condition. We have seen that pre-implant beta blockade appears to strongly influence outcome, and controlling for medical factors is difficult in this type of study. Further development of the risk model in a larger cohort could examine the role of medication in the prediction of outcome.

The position of the left ventricular lead influences outcome in observational series, and in this cohort in relation to scar. We did not include the left ventricular lead position in our

risk score, and this may weaken the model. However, designing a study to look into this would need to take into account both anatomical position and the tributary which had been selected. This is likely to require greater numbers to ensure that a valid result was obtained. The position of the right ventricular lead may be important, and this has not been examined and is a further limitation of this work.

The importance of mitral regurgitation as a predictor of outcome is now well appreciated. We did not examine the importance of pre-implant mitral regurgitation on the CMR scans, and this is an additional parameter which requires investigation to determine whether it should be in the risk score. Assessment of mitral regurgitation on echocardiography is recognised to be difficult, but the importance of residual MR on outcome could be studied in relation to the other identified factors.

Further work should investigate the importance of the patchiness of dyssynchrony and outcome. The development of CMR safe CRT or the use of computed tomography of the left ventricle could allow pre and post implant patch maps to be developed. The role of multi-site left ventricular pacing is unclear, but potentially this could be deployed in patients who had multiple patches of dyssynchrony despite left ventricular lead implantation.

We have shown that CMR-TSI predicts outcome in paced patients with symptomatic heart failure, but we do not have data about un-paced patients. Furthermore, we do not know if patients with dyssynchrony on CMR-TSI but $EF > 35\%$ who are asymptomatic could benefit from prophylactic medication or even CRT.

We observed that pacing left ventricular scar was associated with a worse outcome from CRT. These observational findings could be examined with an experimental study, possibly in an animal model, accepting the potential weaknesses of animal work.

This thesis has confirmed the prognostic importance of CMR-TSI in patients undergoing CRT, calculated a reference range for normality and demonstrated the use of three dimensional polar maps showing the patchiness of dyssynchrony. Furthermore, we have explored the relationship between CMR-TSI, QRS duration and measures of left ventricular function. The combination of scar and CMR-TSI has good prognostic discrimination between groups, and combined with creatinine provides a powerful risk score for determining cardiovascular mortality.

**APPENDIX I. CMR-TSI CALCULATION - WRITTEN BY
BERTHOLD STEGEMANN**

```

t.wma.max <- t.wta.max <- as.data.frame (matrix (nrow=0, ncol=5)); #PatID, Slice,
Segment, Value names (t.wma.max) <- names(t.wta.max) <- c('nr', 'slice', 'seg', 'val',
'file');

disp.t.wma.max <- disp.t.wta.max <- as.data.frame (matrix (nrow=0, ncol=3)); #Patid,
Value names (disp.t.wma.max) <- names(disp.t.wta.max) <- c('nr', 'val', 'file');

for (filenr in 1:length(files)){

# analyse file and extract data

file <- files[filenr];

print(file);

t <- NULL;

t <- toupper(readLines(file));

# obtain number of phase points from file

idx <- grep("^NUMBER OF PHASES:",t);

if (length(idx)==0){print('Line Error: Number of Phases')};

phasenr <- read.table(file,header=F,sep='\t',nrows=1,skip=idx-
1,colClasses=c("NULL","double"));

phasenr <- as.double(phasenr);

Obtain number of slices from file

idx <- grep("^NUMBER OF SLICES:",t);

if (length(idx)==0){print('Line Error: Number of Slices')};

slnr <- read.table (file, header=F, sep='\t', nrows = 1, skip = idx-1, colClasses = c
("NULL", "double"));

slnr <- as.double(slnr);

Obtain phase time and volume table from file

idx <- grep ("^PHASE\t", t);

if (length(idx)==0){print('Line Error: Volumes')};

```

```
time <- read.table (file, header = F, sep='\t', nrows = phasenr, skip = idx, col Classes =
c(rep("double",4)), na. strings="NA");
```

```
time <- as.data.frame(time);
```

```
names (time) <- c("Phase", "Time", "LVendo", "LVepi");
```

Obtain rr-interval

```
idx <- grep ("^HEART RATE:",t) ;
```

```
if (length(idx)==0){print('Line Error: Heart Rate')};
```

```
rr <- read.table (file,header=F, sep='\t',nrows = 1 , skip = idx-1, col Classes = c ("NULL",
"double"));
```

```
rr <- as.integer (60000/rr);
```

Add on final time measurement to the t0 dataframe

```
#time [nrow (time)+1,] <- time[1,] # add final one time measurement
```

```
#time$Time [nrow(time)] <- t1; # RR + 10 msec
```

```
# obtain the slice index pointing at the start of the slices
```

```
idx <- NULL;
```

```
idx <- grep ("^SLICE NUMBER [1-9]*", t); # finds start of slices
```

```
if (length (idx) == 0){print ('Line Error: Slice Number')};
```

```
slidx <- idx;
```

Calculate number of slices (number taken from MASS file may be incorrect)

```
slnr <- length(slidx)/3;
```

```
# set number of segments (constant 6)
```

```
sgnr <- 6 # number of segments
```

```
# create NA data matrix with number of expected rows and columns
```

```
d <- as.data.frame (matrix (nrow = sgnr*3*slnr, ncol = phasenr))
```

```

names (d) <- time$Time;
linect <- 1;
for (i in 1:length(slidx)){ # run i over all elements of the slideidx
sgidx <- (slidx[i] - 1 + grep("^ *S[1-6]\\t",t[slidx[i]:(slidx[i]+10)])); # find start of
segments in each slice
if (diag==T){print(sgidx)}; # Just to show what is happening

```

Obtain phases contained in this slice

```

tphase <- t[sgidx[1]-1] ;
tphase <- strsplit(tphase,'\t');
tphase <- as.double(tphase[[1]][-1]);
if (diag==T) {print(tphase)};

```

Obtain (data) lines

```

For (j in 1:6) { # cycle through all 6 segment lines
line <- t[sgidx[j]];
line <- strsplit(line,'\t');
line <- as.double(line[[1]][-1]);
if (diag==T){print(line)};
# copy (data) lines into dataframe d
For (k in 1:length(tphase))
d [linect,tphase[k]] <- line[k];
linect <- linect + 1;
wta <- d[(1*(slnr*sgnr)+1):(2*(slnr*sgnr)),]; # dataframe for wall thickening
wma <- d[(2*(slnr*sgnr)+1):(3*(slnr*sgnr)),]; # dataframe for wall motion absolute

```

Create extended format with slice and segment indices

```

slice <- rep(1:slnr, each = 6, times = 1);

```

```
segment <- rep(seq(1:6), slnr);
wma.x <- cbind(sli, seg, wma);
wta.x <- cbind(sli, seg, wta);
```

Calculate the time of maximal systolic excursion for each segment

```
xx <- time$Time;
xr <- xx/rr*2*pi;
for (i in 1: (slice number *segment number))
t.wma.max <- rbind(t.wma.max, NA);
y <- as.double (wma[i,]);
yy <- subset (y ,!is.na(y));
xx <- subset (xr,!is.na(y));
s0 <- list(a = mean(yy), b=max(yy)-min(yy), c = xx[sort (yy, decreasing = T, index =
T)$ix[1]]);
f <- nls (yy ~ a + b * cos(xx - c) ,start = s0,na.action = na.omit);
a0 <- coef (f)[1]; # Offset
b0 <- coef (f)[2]; # Amplitude
pt0 <- summary (f)$parameters[3,4];
pb0 <- summary (f)$parameters[2,4];

if( pt0 < 1.0){ # p-value
  if (b0 >= 0){c0 <- (coef(f)[3])%%(2*pi);}
  else
    {c0 <- (coef(f)[3]-pi)%%(2*pi);} n0 <- 1;
  else
    c0 <- NA;
  if(diag==T){print(c(a0,b0,c0,c0/(2*pi)*rr))};
```

```

t.wma.max [nrow(t.wma.max),5] <- file;           # filename
t.wma.max [nrow(t.wma.max),4] <- c0/(2*pi)*rr;   # time to maximum
t.wma.max [nrow(t.wma.max),3] <- ((i-1)%6)+1    # segment
t.wma.max [nrow(t.wma.max),2] <- ((i-1)%6)+1    # slice
t.wma.max [nrow(t.wma.max),1] <- filenr         # filenr
} #for(i in 1:lines)

```

Output the data per file, if wanted

```

If (export == T){
write.table ( time, paste(file,'.vol', '.tab',sep=""), sep="\t",row.names=F, col.names=T,
append=F);
write.table (wma.x, paste(file,'.wma', '.tab',sep=""), sep="\t",row.names=F, col.names=T,
append=F);
write.table (wta.x, paste(file,'.wta', '.tab', sep=""), sep="\t",row.names=F, col.names=T,
append=F);
for (filenr in 1:length (files))

```

Calculate the global dispersion (TSI)

```

For (filenr in unique(t.wma.max$nr)){ # for each file
y <- sd(subset(t.wma.max, nr == filenr, select=c(val)),na.rm=T);
disp.t.wma.max <- rbind (disp.t.wma.max, NA);
disp.t.wma.max [nrow (disp.t.wma.max), 3] <- files[filenr];
disp.t.wma.max [nrow (disp.t.wma.max), 2] <- y;
disp.t.wma.max [nrow (disp.t.wma.max), 1] <- filenr;
} # for (filenr in pats)

```

Write dispersion results into file

```

write.table (disp.t.wma.max,paste ('tsi', '.global', '.t.wma', '.tab', sep=""), sep="\t", row.
Names = T, col.names=F, append=F);

```

APPENDIX 2: PUBLICATIONS ARISING FROM THESIS

Leyva F., Foley P.W. (2011) Current and future role of cardiovascular magnetic resonance in cardiac resynchronization therapy. **Heart Fail Rev.**16: (3): 251-62.

Foley P.W., Khadjooi K, Ward J.A., et al. (2009) Radial dyssynchrony assessed by cardiovascular magnetic resonance in relation to left ventricular function, myocardial scarring and QRS duration in patients with heart failure. **J Cardiovasc Magn Reson.** 24: (11): 50.

Foley P.W., Leyva F., Frenneaux M.P. (2009) What is treatment success in cardiac resynchronization therapy? **Europace.** 11: (5): 58-65.

Leyva F., Foley P.W., Stegemann B., et al. (2009) Development and validation of a clinical index to predict survival after cardiac resynchronisation therapy. **Heart.** 95: (19): 1619-2

LIST OF REFERENCES

Aaronson, K.D., Schwartz, J.S., Chen, T.M., et al. (1997) Development and prospective validation of a clinical index to predict survival in ambulatory patients referred for cardiac transplant evaluation. **Circulation**, 95: (12): 2660-2667.

Abraham, W.T., Fisher, W.G., Smith, A.L., et al. (2002) Cardiac Resynchronization in Chronic Heart Failure. **N Engl J Med**, 346: (24): 1845-1853.

Achilli, A., Sassara, M., Ficili, S., et al. (2003) Long-term effectiveness of cardiac resynchronization therapy in patients with refractory heart failure and "narrow" QRS. **J Am Coll Cardiol**, 42: (12): 2117-2124.

Adelstein, E.C. and Saba, S. (2007) Scar burden by myocardial perfusion imaging predicts echocardiographic response to cardiac resynchronization therapy in ischemic cardiomyopathy. **Am Heart J**, 153: (1): 105-112.

Albertsen, A.E., Nielsen, J.C., Pedersen, A.K., et al. (2005) Left ventricular lead performance in cardiac resynchronization therapy: impact of lead localization and complications. **Pacing Clin Electrophysiol**, 28: (6): 483-488.

Alderman, E.L., Fisher, L.D., Litwin, P., et al. (1983) Results of coronary artery surgery in patients with poor left ventricular function (CASS). **Circulation**, 68: (4): 785-795.

Alpert, J.S., Thygesen, K., Antman, E., et al. (2000) Myocardial infarction redefined--a consensus document of The Joint European Society of Cardiology/American College of Cardiology Committee for the redefinition of myocardial infarction. **J Am Coll Cardiol**, 36: (3): 959-969.

Amundsen, B.H., Helle-Valle, T., Edvardsen, T., et al. (2006) Noninvasive myocardial strain measurement by speckle tracking echocardiography: validation against sonomicrometry and tagged magnetic resonance imaging. **J Am Coll Cardiol**, 47: (4): 789-793.

Anker, S.D., Doehner, W., Rauchhaus, M., et al. (2003) Uric acid and survival in chronic heart failure: validation and application in metabolic, functional, and hemodynamic staging. **Circulation**, 107: (15): 1991-1997.

Ansalone, G., Giannantoni, P., Ricci, R., et al. (2001) Doppler myocardial imaging in patients with heart failure receiving biventricular pacing treatment. **Am Heart J**, 142: (5): 881-896.

Assomull, R.G., Lyne, J.C., Keenan, N., et al. (2007) The role of cardiovascular magnetic resonance in patients presenting with chest pain, raised troponin, and unobstructed coronary arteries. **Eur Heart J**, 28: (10): 1242-1249.

Assomull, R.G., Prasad, S.K., Lyne, J., et al. (2006) Cardiovascular magnetic resonance, fibrosis, and prognosis in dilated cardiomyopathy. **J Am Coll Cardiol**, 48: (10): 1977 - 1985.

Auricchio, A., Fantoni, C., Regoli, F., et al. (2004) Characterization of left ventricular activation in patients with heart failure and left bundle-branch block. **Circulation**, 109: (9): 1133-1139.

Auricchio, A., Stellbrink, C., Sack, S., et al. (2002) Long-term effect of hemodynamically optimized cardiac resynchronization therapy in patients with heart failure and ventricular conduction delay. **J Am Coll Cardiol**, 39: (12): 2026-2033.

Auricchio, A. and Yu, C.M. (2004) Beyond the measurement of QRS complex toward mechanical dyssynchrony: cardiac resynchronisation therapy in heart failure patients with a normal QRS duration. **Heart**, 90: (5): 479-481.

Azevedo, C.F., Amado, L.C., Kraitchman, D.L., et al. (2004) Persistent diastolic dysfunction despite complete systolic functional recovery after reperfused acute myocardial infarction demonstrated by tagged magnetic resonance imaging. **Eur Heart J**, 25: (16): 1419-1427.

Bader, H., Garrigue, S., Lafitte, S., et al. (2004) Intra-left ventricular electromechanical asynchrony: a new predictor of severe cardiac events in heart failure patients. **J Am Coll Cardiol**, 43: (2): 248-256.

Baldasseroni, S., Opasich, C., Gorini, M., et al. (2002) Left bundle-branch block is associated with increased 1-year sudden and total mortality rate in 5517 outpatients with congestive heart failure: a report from the Italian network on congestive heart failure. **Am Heart J**, 143: (3): 398-405.

Bates, D.M. and Watts, D.G. (1988) **Nonlinear regression analysis and its applications**. New York: Wiley.

Bax, J.J., Abraham, T., Barold, S.S., et al. (2005) Cardiac Resynchronization Therapy: Part 1--Issues Before Device Implantation. **J Am Coll Cardiol**, 46: (12): 2153-2167.

Bax, J.J., Ansalone, G., Breithardt, O.A., et al. (2004a) Echocardiographic evaluation of cardiac resynchronization therapy: ready for routine clinical use? A critical appraisal. **J Am Coll Cardiol**, 44: (1): 1-9.

Bax, J.J., Bleeker, G.B., Marwick, T.H., et al. (2004b) Left ventricular dyssynchrony predicts response and prognosis after cardiac resynchronization therapy. **J Am Coll Cardiol**, 44: (9): 1834 - 1840.

Bax, J.J., Marwick, T.H., Molhoek, S.G., et al. (2003a) Left ventricular dyssynchrony predicts benefit of cardiac resynchronization therapy in patients with end-stage heart failure before pacemaker implantation. **Am J Cardiol**, 92: (10): 1238-1240.

Bax, J.J., Molhoek, S.G., van, E.L., et al. (2003b) Usefulness of myocardial tissue Doppler echocardiography to evaluate left ventricular dyssynchrony before and after biventricular pacing in patients with idiopathic dilated cardiomyopathy. **Am J Cardiol**, 91: (1): 94-97.

- Bax, J.J. and Poldermans, D. (2006) Mitral regurgitation and left ventricular dyssynchrony: implications for treatment. **Heart**, 92: (10): 1363-1364.
- Becker, M., Franke, A., Breithardt, O.E., et al. (2007) Impact of Left Ventricular Lead Position on the Efficacy of Cardiac Resynchronization Therapy. A Two-Dimensional Strain Echocardiography Study. **Heart**, 93: (10): 1197-1203.
- Bellenger, N.G., Rajappan, K., Rahman, S.L., et al. (2004) Effects of carvedilol on left ventricular remodelling in chronic stable heart failure: a cardiovascular magnetic resonance study. **Heart**, 90: (7): 760-764.
- Bello, D., Shah, D.J., Farah, G.M., et al. (2003) Gadolinium cardiovascular magnetic resonance predicts reversible myocardial dysfunction and remodeling in patients with heart failure undergoing beta-blocker therapy. **Circulation**, 108: (16): 1945-1953.
- Beshai, J.F., Grimm, R.A., Nagueh, S.F., et al. (2007) Cardiac-Resynchronization Therapy in Heart Failure with Narrow QRS Complexes. **N Engl J Med**, 357: (24): 2461-2471.
- Bilchick, K.C., Dimaano, V., Wu, K.C., et al. (2008) Cardiac Magnetic Resonance Assessment of Dyssynchrony and Myocardial Scar Predicts Function Class Improvement Following Cardiac Resynchronization Therapy. **J Am Coll Cardiol Img**, 1: (5): 561-568.
- Bleasdale, R.A., Turner, M.S., Mumford, C.E., et al. (2004) Left ventricular pacing minimizes diastolic ventricular interaction, allowing improved preload-dependent systolic performance. **Circulation**, 110: (16): 2395-2400.
- Bleeker, G.B., Bax, J.J., Fung, J.W.-H., et al. (2006a) Clinical Versus Echocardiographic Parameters to Assess Response to Cardiac Resynchronization Therapy. **Am J Cardiol**, 97: (2): 260-263.
- Bleeker, G.B., Bax, J.J., Schalij, M.J., et al. (2005) Tissue Doppler imaging to assess left ventricular dyssynchrony and resynchronization therapy. **Eur J Echocardiogr**, 6: (5): 382-384.
- Bleeker, G.B., Holman, E.R., Steendijk, P., et al. (2006b) Cardiac resynchronization therapy in patients with a narrow QRS complex. **J Am Coll Cardiol**, 48: (11): 2243-2250.
- Bleeker, G.B., Kaandorp, T.A., Lamb, H.J., et al. (2006c) Effect of posterolateral scar tissue on clinical and echocardiographic improvement after cardiac resynchronization therapy. **Circulation**, 113: (7): 969-976.
- Bleeker, G.B., Schalij, M.J., Molhoek, S.G., et al. (2004) Relationship between QRS duration and left ventricular dyssynchrony in patients with end-stage heart failure. **J Cardiovasc Electrophysiol**, 15: (5): 544-549.
- Breithardt, O.A., Stellbrink, C., Herbots, L., et al. (2003) Cardiac resynchronization therapy can reverse abnormal myocardial strain distribution in patients with heart failure and left bundle branch block. **J Am Coll Cardiol**, 42: (3): 486-494.

- Breithardt, O.A., Stellbrink, C., Kramer, A.P., et al. (2002) Echocardiographic quantification of left ventricular asynchrony predicts an acute hemodynamic benefit of cardiac resynchronization therapy. **J Am Coll Cardiol**, 40: (3): 536-545.
- Bristow, M.R., Saxon, L.A., Boehmer, J., et al. (2004) Cardiac-Resynchronization Therapy with or without an Implantable Defibrillator in Advanced Chronic Heart Failure. **N Engl J Med**, 350: (21): 2140-2150.
- Bülow, H., Klein, C., Kuehn, I., et al. (2005) Cardiac magnetic resonance imaging: long term reproducibility of the late enhancement signal in patients with chronic coronary artery disease. **Heart**, 91: (9): 1158-1163.
- Burgess, M.I., Jenkins, C., Chan, J., et al. (2007) Measurement of left ventricular dyssynchrony in patients with ischaemic cardiomyopathy: A comparison of real-time three-dimensional and tissue doppler echocardiography. **Heart**, 93: (10): 1191-1196.
- Burkhoff, D., Oikawa, R.Y. and Sagawa, K. (1986) Influence of pacing site on canine left ventricular contraction. **Am J Physiol**, 251: (2 Pt 2): H428-435.
- Caro, J.J., Guo, S., Ward, A., et al. (2006) Modeling the economic and health consequences of cardiac resynchronization therapy in the UK. **Curr Med Res Opin**, 22: (6): 1171-1179.
- Cazeau, S., Leclercq, C., Lavergne, T., et al. (2001) Effects of Multisite Biventricular Pacing in Patients with Heart Failure and Intraventricular Conduction Delay. **N Engl J Med**, 344: (12): 873-880.
- Cazeau, S., Ritter, P., Bakdach, S., et al. (1994) Four chamber pacing in dilated cardiomyopathy. **Pacing Clin Electrophysiol**, 17: (11 Pt 2): 1974-1979.
- Chalil, S., Foley, P.W.X., Muhyaldeen, S.A., et al. (2007a) Late gadolinium enhancement-cardiovascular magnetic resonance as a predictor of response to cardiac resynchronization therapy in patients with ischaemic cardiomyopathy. **Europace**, 9: (11): 1031-1037.
- Chalil, S., Muhyaldeen, S.A., Khadjooi, K., et al. (2007b) Effect of posterolateral left ventricular scar on mortality and morbidity following cardiac resynchronisation therapy: a late gadolinium enhancement cardiovascular magnetic resonance study. **Heart**, 93 (Sppl D): A87.
- Chalil, S., Stegemann, B., Muhyaldeen, S., et al. (2007c) Effect of posterolateral left ventricular scar on mortality and morbidity following cardiac resynchronization therapy. **Pacing Clin Electrophysiol**, 30: (10): 1201-1209.
- Chalil, S., Stegemann, B., Muhyaldeen, S., et al. (2007d) Intraventricular Dyssynchrony Predicts Mortality and Morbidity After Cardiac Resynchronization Therapy: A Study Using Cardiovascular Magnetic Resonance Tissue Synchronization Imaging. **J Am Coll Cardiol**, 50: (3): 243-252.

Cho, G.Y., Song, J.K., Park, W.J., et al. (2005) Mechanical dyssynchrony assessed by tissue Doppler imaging is a powerful predictor of mortality in congestive heart failure with normal QRS duration. **J Am Coll Cardiol**, 46: (12): 2237-2243.

Chung, E.S., Leon, A.R., Tavazzi, L., et al. (2008) Results of the Predictors of Response to CRT (PROSPECT) Trial. **Circulation**, 117: (20): 2608-2616.

Cleland, J., Freemantle, N., Ghio, S., et al. (2008a) Predicting the Long-Term Effects of Cardiac Resynchronization Therapy on Mortality From Baseline Variables and the Early Response: A Report From the CARE-HF (Cardiac Resynchronization in Heart Failure) Trial. **J Am Coll Cardiol**, 52: (6): 438-445.

Cleland, J.G., Daubert, J.C., Erdmann, E., et al. (2001) The CARE-HF study (CARDiac RESynchronisation in Heart Failure study): rationale, design and end-points. **Eur J Heart Fail**, 3: (4): 481-489.

Cleland, J.G., Daubert, J.C., Erdmann, E., et al. (2005a) Baseline characteristics of patients recruited into the CARE-HF study. **Eur J Heart Fail**, 7: (2): 205-214.

Cleland, J.G.F., Cullington, D., Khaleva, O., et al. (2008b) Cardiac resynchronization therapy: dyssynchrony imaging from a heart failure perspective. **Curr Opin Cardiol**, 23: (6): 634-645.

Cleland, J.G.F., Daubert, J.C., Erdmann, E., et al. (2005b) The Effect of Cardiac Resynchronization on Morbidity and Mortality in Heart Failure. **N Engl J Med**, 352: (15): 1539-1549.

Cleland, J.G.F., Tavazzi, L., Daubert, J.-C., et al. (2009) Cardiac Resynchronization Therapy: Are Modern Myths Preventing Appropriate Use? **J Am Coll Cardiol**, 53: (7): 608-611.

Conca, C., Faletra, F.F., Miyazaki, C., et al. (2009) Echocardiographic Parameters of Mechanical Synchrony in Healthy Individuals. **Am J Cardiol**, 103: (1): 136-142.

Curry, C., Fetts, B., Wyman, B., et al. (1998) Mechanical dyssynchrony at rest and with adrenergic stimulation in patients with dilated cardiomyopathy studied by MRI-tagging: Can it help identify candidates for chronic VDD pacing therapy? **Circulation**, 98: (17): I-302 (abstract).

Da, C.A., Thevenin, J., Roche, F., et al. (2006) Prospective validation of stress echocardiography as an identifier of cardiac resynchronization therapy responders. **Heart Rhythm**, 3: (4): 406-413.

Dakik, H.A., Howell, J.F., Lawrie, G.M., et al. (1997) Assessment of Myocardial Viability With 99mTc-Sestamibi Tomography Before Coronary Bypass Graft Surgery : Correlation With Histopathology and Postoperative Improvement in Cardiac Function. **Circulation**, 96: (9): 2892-2898.

- De Boeck, B.W.L., Meine, M., Leenders, G.E., et al. (2008) Practical and conceptual limitations of tissue Doppler imaging to predict reverse remodelling in cardiac resynchronisation therapy. **Eur J Heart Fail**, 10: (3): 281-290.
- Dohi, K., Pinsky, M.R., Kanzaki, H., et al. (2006) Effects of radial left ventricular dyssynchrony on cardiac performance using quantitative tissue Doppler radial strain imaging. **J AM Soc Echocardiogr**, 19: (5): 475-482.
- Dohi, K., Suffoletto, M., Ganz, L., et al. (2005a) Utility of echocardiographic tissue synchronization imaging to redirect left ventricular lead placement for improved cardiac resynchronization therapy. **Pacing Clin Electrophysiol**, 28: (5): 461-465.
- Dohi, K., Suffoletto, M.S., Schwartzman, D., et al. (2005b) Utility of echocardiographic radial strain imaging to quantify left ventricular dyssynchrony and predict acute response to cardiac resynchronization therapy. **Am J Cardiol**, 96: (1): 112-116.
- Donal, E., Tournoux, F., Leclercq, C., et al. (2008) Assessment of Longitudinal and Radial Ventricular Dyssynchrony in Ischemic and Nonischemic Chronic Systolic Heart Failure: A Two-Dimensional Echocardiographic Speckle-Tracking Strain Study. **J AM Soc Echocardiogr**, 21: (1): 58-65.
- Dose Schwarz, J., Bader, M., Jenicke, L., et al. (2005) Early Prediction of Response to Chemotherapy in Metastatic Breast Cancer Using Sequential 18F-FDG PET. **J Nucl Med**, 46: (7): 1144-1150.
- Doughty, R., Whalley, B.A., Gamble, M.S., et al. (1997) Left Ventricular Remodeling With Carvedilol in Patients With Congestive Heart Failure Due to Ischemic Heart Disease. **J Am Coll Cardiol**, 29: (5): 1060-1066.
- Dries, D.L., Exner, D.V., Domanski, M.J., et al. (2000) The prognostic implications of renal insufficiency in asymptomatic and symptomatic patients with left ventricular systolic dysfunction. **J Am Coll Cardiol**, 35: (3): 681-689.
- Duncan, A., Wait, D., Gibson, D., et al. (2003) Left ventricular remodelling and haemodynamic effects of multisite biventricular pacing in patients with left ventricular systolic dysfunction and activation disturbances in sinus rhythm: sub-study of the MUSTIC (Multisite Stimulation in Cardiomyopathies) trial. **Eur Heart J**, 24: (5): 430-441.
- Duncan, A.M., Lim, E., Clague, J., et al. (2006) Comparison of segmental and global markers of dyssynchrony in predicting clinical response to cardiac resynchronization. **Eur Heart J**, 27: (20): 2426-2432.
- Eagle, K.A., Guyton, R.A., Davidoff, R., et al. (2004) ACC/AHA 2004 Guideline Update for Coronary Artery Bypass Graft Surgery. **Circulation**, 110: (14): e340-437.
- Efron, B. (1979) Bootstrap method: another look at the jackknife. **Ann Stat**, 7: (1): 1-26.
- Fauchier, L., Marie, O., Casset-Senon, D., et al. (2002) Interventricular and intraventricular dyssynchrony in idiopathic dilated cardiomyopathy. A prognostic study

with Fourier phase analysis of radionuclide angioscintigraphy. **J Am Coll Cardiol**, 40: (11): 2022-2030.

Fauchier, L., Marie, O., Casset-Senon, D., et al. (2003) Reliability of QRS duration and morphology on surface electrocardiogram to identify ventricular dyssynchrony in patients with idiopathic dilated cardiomyopathy. **Am J Cardiol**, 92: (3): 341-344.

Foley, P.W.X., Chalil, S., Khadjooi, K., et al. (2008) Relationship between prognostic, symptomatic and echocardiographic outcomes after cardiac resynchronisation therapy. **Heart**, 94: (Suppl 2): A17.

Fried, A.G., Parker, A.B., Newton, G.E., et al. (1999) Electrical and hemodynamic correlates of the maximal rate of pressure increase in the human left ventricle. **J Card Fail**, 5: (1): 8-16.

Fruhwald, F.M., Fahrleitner-Pammer, A., Berger, R., et al. (2007) Early and sustained effects of cardiac resynchronization therapy on N-terminal pro-B-type natriuretic peptide in patients with moderate to severe heart failure and cardiac dyssynchrony. **Eur Heart J**, 28: (13): 1592-1597.

Gabriel, R.S., Bakshi, T.K., Scott, A.G., et al. (2007) Reliability of echocardiographic indices of dyssynchrony. **Echocardiography**, 24: (1): 40-46.

Garrigue, S., Efimov, I.R., Jais, P., et al. (2001) Voltage-sensitive dye mapping technique applied to biventricular pacing during ischemia: role of the voltage output, the interventricular delay, pacing sites on ventricular arrhythmias occurrence. **Pacing Clin Electrophysiol**, 24: (Suppl): 539.

Gasparini, M. (2008) Long-term survival in patients undergoing cardiac resynchronization therapy: the importance of atrio-ventricular junction ablation in patients with permanent atrial fibrillation: reply. **Eur Heart J**, 29: (17): 2182-2183.

Gasparini, M., Mantica, M., Galimberti, P., et al. (2003) Beneficial effects of biventricular pacing in patients with a "narrow" QRS. **Pacing Clin Electrophysiol**, 26: (1 Pt 2): 169-174.

Germans, T. and van Rossum, A.C. (2008) The use of cardiac magnetic resonance imaging to determine the aetiology of left ventricular disease and cardiomyopathy. **Heart**, 94: (4): 510-518.

Ghio, S., Constantin, C., Klersy, C., et al. (2004) Interventricular and intraventricular dyssynchrony are common in heart failure patients, regardless of QRS duration. **Eur Heart J**, 25: (7): 571-578.

Gorcsan, J., III, Abraham, T., Agler, D.A., et al. (2008) Echocardiography for Cardiac Resynchronization Therapy: Recommendations for Performance and Reporting-A Report from the American Society of Echocardiography Dyssynchrony Writing Group Endorsed by the Heart Rhythm Society. **J AM Soc Echocardiogr**, 21: (3): 191-213.

Gorcsan, J., III, Kanzaki, H., Bazaz, R., et al. (2004) Usefulness of echocardiographic tissue synchronization imaging to predict acute response to cardiac resynchronization therapy. **Am J Cardiol**, 93: (9): 1178-1181.

Gras, D., Mabo, P., Tang, T., et al. (1998) Multisite pacing as a supplemental treatment of congestive heart failure: preliminary results of the Medtronic Inc. InSync Study. **Pacing Clin Electrophysiol**, 21: (11 Pt 2): 2249-2255.

Grines, C.L., Bashore, T.M., Boudoulas, H., et al. (1989) Functional abnormalities in isolated left bundle branch block. The effect of interventricular asynchrony. **Circulation**, 79: (4): 845-853.

Grothues, F., Smith, G.C., Moon, J.C., et al. (2002) Comparison of interstudy reproducibility of cardiovascular magnetic resonance with two-dimensional echocardiography in normal subjects and in patients with heart failure or left ventricular hypertrophy. **Am J Cardiol**, 90: (1): 29-34.

Guyatt, G.H., Sullivan, M.J. and Thompson, P.J. (1985) The 6-minute walk: a new measure of exercise capacity in patients with chronic heart failure. **Can Med Assoc J**, 132: (8): 919-923.

Haghjoo, M., Bagherzadeh, A., Fazelifar, A.F., et al. (2007) Prevalence of Mechanical Dyssynchrony in Heart Failure Patients with Different QRS Durations. **Pacing Clin Electrophysiol**, 30: (5): 616-622.

Harrell, F.J. (2007) **The Design Package** [online]. <http://CRAN.R-project.org/package=Design> [Accessed March 1st 2009]

Harrell, F.J., Lee, K., Califf, R., et al. (1984) Regression modelling strategies for improved prognostic prediction. **Stat Med**, 3: (2): 143-152.

Harrell, F.J., Lee, K. and Mark, D. (1996) Multivariate prognostic models: issues in developing models, evaluating assumptions and adequacy, and measuring and reducing errors. **Stat Med**, 15: (4): 361-387.

Healthcare Technology Appraisal 120: Cardiac resynchronisation therapy for the treatment of heart failure (2007) [online].

<http://www.nice.org.uk/Guidance/TA120/NiceGuidance/pdf/English> [Accessed November 1st 2008]

Helm, R.H., Byrne, M., Helm, P.A., et al. (2007) Three-dimensional mapping of optimal left ventricular pacing site for cardiac resynchronization. **Circulation**, 115: (8): 953-961.

Helm, R.H., Lecquerq, C., Faris, Q., et al. (2005) Cardiac dyssynchrony analysis using circumferential versus longitudinal strain: Implications for assessing cardiac resynchronization. **Circulation**, 111: (21): 2760-2767.

Herweg, B., Ilercil, A., Cutro, R., et al. (2007) Cardiac Resynchronization Therapy in Patients With End-Stage Inotrope-Dependent Class IV Heart Failure. **Am J Cardiol**, 100: (1): 90-93.

Higgins, S.L., Hummel, J.D., Niazi, I.K., et al. (2003) Cardiac resynchronization therapy for the treatment of heart failure in patients with intraventricular conduction delay and malignant ventricular tachyarrhythmias. **J Am Coll Cardiol**, 42: (8): 1454-1459.

Hillege, H.L., Girbes, A.R.J., de Kam, P.J., et al. (2000) Renal Function, Neurohormonal Activation, and Survival in Patients With Chronic Heart Failure. **Circulation**, 102: (2): 203-210.

Hummel, J.P., Lindner, J.R., Belcik, J.T., et al. (2005) Extent of myocardial viability predicts response to biventricular pacing in ischemic cardiomyopathy. **Heart Rhythm**, 2: (11): 1211-1217.

Implantable cardioverter defibrillators for arrhythmias. Review of Technology Appraisal 11. Technology Appraisal 95. (2006) [Accessed January 20th 2007].

Jenkins, C., Moir, S., Chan, J., et al. (2008) Left ventricular volume measurement with echocardiography: a comparison of left ventricular opacification, three-dimensional echocardiography, or both with magnetic resonance imaging. **Eur Heart J**, 30: (1): 98-106.

Kanzaki, H., Bazaz, R., Schwartzman, D., et al. (2004) A mechanism for immediate reduction in mitral regurgitation after cardiac resynchronization therapy: Insights from mechanical activation strain mapping. **J Am Coll Cardiol**, 44: (8): 1619-1625.

Kapetanakis, S., Kearney, M.T., Siva, A., et al. (2005) Real-time three-dimensional echocardiography: a novel technique to quantify global left ventricular mechanical dyssynchrony. **Circulation**, 112: (7): 992-1000.

Kass, D.A. (2003) Ventricular resynchronization: pathophysiology and identification of responders. **Rev Cardiovasc Med**, 4: (Suppl 2): S3-S13.

Kass, D.A. (2008) An Epidemic of Dyssynchrony: But What Does It Mean? **J Am Coll Cardiol**, 51: (1): 12-17.

Kawaguchi, M., Murabayashi, T., Fetcs, B.J., et al. (2002) Quantitation of basal dyssynchrony and acute resynchronization from left or biventricular pacing by novel echo-contrast variability imaging. **J Am Col Cardiol**, 39: (12): 2052-2058.

Kayano, H., Ueda, H., Kawamata, T., et al. (2006) Improved septal contraction and coronary flow velocity after cardiac resynchronization therapy elucidated by strain imaging and pulsed wave Doppler echocardiography. **J Cardiol**, 47: (2): 51-61.

Khadjooi, K., Foley, P., Anthony, J., et al. (2008) Long-term effects of cardiac resynchronisation therapy in patients with atrial fibrillation. **Heart**, 94: (7): 879-883.

- Kim, R.J., Fieno, D.S., Parrish, T.B., et al. (1999) Relationship of MRI Delayed Contrast Enhancement to Irreversible Injury, Infarct Age, and Contractile Function. **Circulation**, 100: (19): 1992-2002.
- Kim, R.J., Wu, E., Rafael, A., et al. (2000) The use of contrast-enhanced magnetic resonance imaging to identify reversible myocardial dysfunction. **N Engl J Med**, 343: (20): 1445-1453.
- Kirn, B., Jansen, A., Bracke, F., et al. (2008) Mechanical discoordination rather than dyssynchrony predicts reverse remodeling upon cardiac resynchronization. **Am J Physiol Heart Circ Physiol**, 295: (2): H640-646.
- Knebel, F., Schattke, S., Bondke, H., et al. (2007) Evaluation of longitudinal and radial two-dimensional strain imaging versus Doppler tissue echocardiography in predicting long-term response to cardiac resynchronization therapy. **J AM Soc Echocardiogr**, 20: (4): 335-341.
- Konstam, M.A., Rousseau, M.F., Kronenberg, M.W., et al. (1992) Effects of the angiotensin converting enzyme inhibitor enalapril on the long-term progression of left ventricular dysfunction in patients with heart failure: SOLVD investigators. **Circulation**, 86: (2): 431-438.
- Kramer, C.M., Rogers, W.J., Theobald, T.M., et al. (1996) Remote Noninfarcted Region Dysfunction Soon After First Anterior Myocardial Infarction: A Magnetic Resonance Tagging Study. **Circulation**, 94: (4): 660-666.
- Kuijjer, J.P., Hofman, M.B., Zwanenburg, J.J., et al. (2006) DENSE and HARP: two views on the same technique of phase-based strain imaging. **J Magn Reson Imaging**, 24: (6): 1432-1438.
- Kvitting, J.P., Wigstrom, L., Strotmann, J.M., et al. (1999) How accurate is visual assessment of synchronicity in myocardial motion? An In vitro study with computer-simulated regional delay in myocardial motion: clinical implications for rest and stress echocardiography studies. **J AM Soc Echocardiogr**, 12: (9): 698-705.
- Kwong, R.Y., Chan, A.K., Brown, K.A., et al. (2006) Impact of unrecognized myocardial scar detected by cardiac magnetic resonance imaging on event-free survival in patients presenting with signs or symptoms of coronary artery disease. **Circulation**, 113: (23): 2733-2743.
- Lambiase, P.D., Rinaldi, A., Hauck, J., et al. (2004) Non-contact left ventricular endocardial mapping in cardiac resynchronisation therapy. **Heart**, 90: (1): 44-51.
- Lang, R.M., Bierig, M., Devereux, R.B., et al. (2005) Recommendations for Chamber Quantification: A Report from the American Society of Echocardiography's Guidelines and Standards Committee and the Chamber Quantification Writing Group, Developed in Conjunction with the European Association of Echocardiography, a Branch of the European Society of Cardiology **J AM Soc Echocardiogr**, 18: (12): 1440-1463.

- Lardo, A.C., Abraham, T.P. and Kass, D.A. (2005) Magnetic Resonance Imaging Assessment of Ventricular Dyssynchrony: Current and Emerging Concepts. **J Am Coll Cardiol**, 46: (12): 2223-2228.
- Leclercq, C., Faris, O., Tunin, R., et al. (2002) Systolic Improvement and Mechanical Resynchronization Does Not Require Electrical Synchrony in the Dilated Failing Heart With Left Bundle-Branch Block. **Circulation**, 106: (14): 1760-1763.
- Lee, D.S., Austin, P.C., Rouleau, J.L., et al. (2003) Predicting mortality among patients hospitalized for heart failure: derivation and validation of a clinical model. **JAMA**, 290: (19): 2581-2587.
- Lellouche, N., De Diego, C., Cesario, D.A., et al. (2007) Usefulness of Preimplantation B-Type Natriuretic Peptide Level for Predicting Response to Cardiac Resynchronization Therapy. **Am J Cardiol**, 99: (2): 242-246.
- Levy, W.C., Mozaffarian, D., Linker, D.T., et al. (2006) The Seattle Heart Failure Model: Prediction of Survival in Heart Failure. **Circulation**, 113: (11): 1424-1433.
- Lindenfeld, J., Feldman, A.M., Saxon, L.A., et al. (2007) Effects of Cardiac Resynchronization Therapy With or Without a Defibrillator on Survival and Hospitalizations in Patients With New York Heart Association Class IV Heart Failure. **Circulation**, 115: (2): 204-212.
- Makaryus, A.N., Arduini, A.D., Mallin, J., et al. (2003) Echocardiographic features of patients with heart failure who may benefit from biventricular pacing. **Echocardiography**, 20: (3): 217-223.
- Mann, D.L. and Bristow, M.R. (2005) Mechanisms and models in heart failure: the biomechanical model and beyond. **Circulation**, 111: (21): 2837-2849.
- Marcassa, C., Campini, R., Verna, E., et al. (2007) Assessment of cardiac asynchrony by radionuclide phase analysis: Correlation with ventricular function in patients with narrow or prolonged QRS interval **Eur J Heart Fail**, 9: (5): 484-490.
- Marcus, G.M., Rose, E., Vilorio, E.M., et al. (2005) Septal to posterior wall motion delay fails to predict reverse remodeling or clinical improvement in patients undergoing cardiac resynchronization therapy. **J Am Coll Cardiol**, 46: (12): 2208-2214.
- Markis, J.E., Malagold, M., Parker, J.A., et al. (1981) Myocardial salvage after intracoronary thrombolysis with streptokinase in acute myocardial infarction. **N Engl J Med**, 305: (14): 777-782.
- Marwick, T.H. (2006) Measurement of Strain and Strain Rate by Echocardiography: Ready for Prime Time? **J Am Coll Cardiol**, 47: (7): 1313-1327.
- Marwick, T.H. (2008) Hype and Hope in the Use of Echocardiography for Selection for Cardiac Resynchronization Therapy: The Tower of Babel Revisited. **Circulation**, 117: (20): 2573-2576.

McCrohon, J.A., Moon, J.J.C., Prasad, S.K., et al. (2003) Differentiation of heart failure related to dilated cardiomyopathy and coronary artery disease using gadolinium-enhanced cardiovascular magnetic resonance. **Circulation**, 108: (1): 54-59.

Miyazaki, C., Powell, B.D., Bruce, C.J., et al. (2008) Comparison of Echocardiographic Dyssynchrony Assessment by Tissue Velocity and Strain Imaging in Subjects With or Without Systolic Dysfunction and With or Without Left Bundle-Branch Block. **Circulation**, 117: (20): 2617-2625.

Molhoek, S.G., Bax, J.J., van Erven, L., et al. (2002) Effectiveness of resynchronization therapy in patients with end-stage heart failure. **Am J Cardiol**, 90: (4): 379-383.

Molhoek, S.G., van, E.L., Bootsma, M., et al. (2004) QRS duration and shortening to predict clinical response to cardiac resynchronization therapy in patients with end-stage heart failure. **Pacing Clin Electrophysiol**, 27: (3): 308-313.

Moon, J.C.C., McKenna, W.J., McCrohon, J.A., et al. (2003) Toward clinical risk assessment in hypertrophic cardiomyopathy with gadolinium cardiovascular magnetic resonance. **J Am Coll Cardiol**, 41: (9): 1561-1567.

Moon, J.C.C., Reed, E., Sheppard, M.N., et al. (2004) The histologic basis of late gadolinium enhancement cardiovascular magnetic resonance in hypertrophic cardiomyopathy. **J Am Coll Cardiol**, 43: (12): 2260-2264.

Moore, C.C., Lugo-Olivieri, C.H., McVeigh, E.R., et al. (2000) Three-dimensional systolic strain patterns in the normal human left ventricle: characterization with tagged MR imaging. **Radiology**, 214: (2): 453-466.

Morris-Thurgood, J.A., Turner, M.S., Nightingale, A.K., et al. (2000) Pacing in heart failure: improved ventricular interaction in diastole rather than systolic re-synchronization. **Europace**, 2: (4): 271-275.

Myerburg, R.J. and Castellanos, A. (1997) "Cardiac arrest and sudden cardiac death". In Braunwald, E. (Ed.) **Heart disease: a textbook of cardiovascular medicine**. New York:, WB Saunders Publishing Co. pp. 742-779.

Nelson, G.S., Curry, C.W., Wyman, B.T., et al. (2000) Predictors of systolic augmentation from left ventricular pre excitation in patients with dilated cardiomyopathy and intraventricular conduction delay. **Circulation**, 101: (23): 2703-2709.

Notabartolo, D., Merlino, J.D., Smith, A.L., et al. (2004) Usefulness of the peak velocity difference by tissue Doppler imaging technique as an effective predictor of response to cardiac resynchronization therapy. **Am J Cardiol**, 94: (6): 817-820.

Notomi, Y., Setser, R.M., Shiota, T., et al. (2005) Assessment of Left Ventricular Torsional Deformation by Doppler Tissue Imaging: Validation Study With Tagged Magnetic Resonance Imaging. **Circulation**, 111: (9): 1141-1147.

- Nunez, A., Alberca, M.T., Francisco, G., et al. (2002) Severe mitral regurgitation with right ventricular pacing, successfully treated with left ventricular pacing. **Pacing Clin Electrophysiol**, 25: (2): 226-230.
- Packer, M., Carver, J.R., Rodeheffer, R.J., et al. (1991) Effect of oral milrinone on mortality in severe chronic heart failure. The PROMISE Study Research Group. **N Engl J Med**, 325: (21): 1468-1475.
- Paetsch, I., Foll, D., Kaluza, A., et al. (2005) Magnetic resonance stress tagging in ischemic heart disease. **Am J Physiol Heart Circ Physiol**, 288: (6): H2708-2714.
- Pagley, P.R., Beller, G.A., Watson, D.D., et al. (1997) Improved outcome after coronary bypass surgery in patients with ischemic cardiomyopathy and residual myocardial viability. **Circulation**, 96: (3): 793-800.
- Pak, P.H., Maughan, W.L., Baughman, K.L., et al. (1998) Mechanism of acute mechanical benefit from VDD pacing in hypertrophied heart: similarity of responses in hypertrophic cardiomyopathy and hypertensive heart disease. **Circulation**, 98: (3): 242-248.
- Park, R.C., Little, W.C. and O'Rourke, R.A. (1985) Effect of alteration of left ventricular activation sequence on the left ventricular end-systolic pressure-volume relation in closed-chest dogs. **Circ Res**, 57: (5): 706-717.
- Penicka, M., Bartunek, J., De Bruyne, B., et al. (2004) Improvement of Left Ventricular Function After Cardiac Resynchronization Therapy Is Predicted by Tissue Doppler Imaging Echocardiography. **Circulation**, 109: (8): 978-983.
- Penicka, M., Vanderheyden, M., Geelen, P., et al. (2007) Tissue Doppler predicts long-term clinical outcome after cardiac resynchronization therapy. **Int J Cardiol**, 124: (1): 40-46.
- Perez de Isla, L., Florit, J., Garcia-Fernandez, M.A., et al. (2005) Prevalence of echocardiographically detected ventricular asynchrony in patients with left ventricular systolic dysfunction. **J AM Soc Echocardiogr**, 18: (8): 850 - 859.
- Perry, R., De Pasquale, C.G., Chew, D.P., et al. (2006) QRS duration alone misses cardiac dyssynchrony in a substantial proportion of patients with chronic heart failure. **J AM Soc Echocardiogr**, 19: (10): 1257-1263.
- Pitzalis, M.V., Iacoviello, M., Di Serio, F., et al. (2006) Prognostic value of brain natriuretic peptide in the management of patients receiving cardiac resynchronization therapy. **Eur J Heart Fail**, 8: (5): 509-514.
- Pitzalis, M.V., Iacoviello, M., Romito, R., et al. (2005) Ventricular asynchrony predicts a better outcome in patients with chronic heart failure receiving cardiac resynchronization therapy. **J Am Coll Cardiol**, 45: (1): 65-69.

Pitzalis, M.V., Iacoviello, M., Romito, R., et al. (2002) Cardiac resynchronization therapy tailored by echocardiographic evaluation of ventricular asynchrony. **J Am Coll Cardiol**, 40: (9): 1615-1622.

Prinzen, F.W., Hunter, W.C., Wyman, B.T., et al. (1999) Mapping of regional myocardial strain and work during ventricular pacing: experimental study using magnetic resonance imaging tagging. **J Am Coll Cardiol**, 33: (6): 1735-1742.

R Development Core Team (2005) **R: A language and environment for statistical computing** [online]. <http://www.R-project.org> [Accessed January 1st 2007]

Rector, T.S. (2005) **Overview of The Minnesota Living with Heart Failure Questionnaire** [online]. http://www.mlhfq.org/dnld/mlhfq_overview.pdf [Accessed March 6th 2007]

Rector, T.S., Kubo, S.H. and Cohn, J.N. (1987) Patients' self-assessment of their congestive heart failure. Part 2: Content, reliability and validity of a new measure, the Minnesota Living with Heart Failure questionnaire. **Heart Failure**, 198-207.

Reddy, V.Y., Wroblewski, D., Houghtaling, C., et al. (2003) Combined Epicardial and Endocardial Electroanatomic Mapping in a Porcine Model of Healed Myocardial Infarction. **Circulation**, 107: (25): 3236-3242.

Reuter, S., Garrigue, S., Barold, S.S., et al. (2002) Comparison of characteristics in responders versus nonresponders with biventricular pacing for drug-resistant congestive heart failure. **Am J Cardiol.**, 89: (3): 346-350.

Ritter, P., Padeletti, L., Gillio-Meina, L., et al. (1999) Determination of the optimal atrioventricular delay in DDD pacing : Comparison between echo and peak endocardial acceleration measurements. **Europace**, 1: (2): 126-130.

Saba, M.M., Ventura, H.O., Saleh, M., et al. (2006) Ancient Egyptian Medicine and the Concept of Heart Failure. **J Card Fail**, 12: (6): 416-421.

Saeed, M., Wendland, M.F., Takehara, Y., et al. (1990) Reversible and irreversible injury in the reperfused myocardium: differentiation with contrast material-enhanced MR imaging. **Radiology**, 175: (3): 633-637.

Sanderson, J.E. (2009) Echocardiography for Cardiac Resynchronization Therapy Selection: Fatally Flawed or Misjudged? **J Am Coll Cardiol**, 53: (21): 1960-1964.

Schoenfeld, D. (1982) Partial residuals for the proportional hazards regression model. **Biometrika**, 69: (1): 239-241.

Schwartzman, P.R., Srichai, M.B., Grimm, R.A., et al. (2003) Nonstress delayed-enhancement magnetic resonance imaging of the myocardium predicts improvement of function after revascularization for chronic ischemic heart disease with left ventricular dysfunction. **Am Heart J**, 146: (3): 535-541.

- Schwartzman, D., Chang, I., Michele, J.J., et al. (1999) Electrical impedance properties of normal and chronically infarcted ventricular myocardium. **J Interv Card Electrophysiol**, 3: (3): 213-224.
- Sciagra, R., Giaccardi, M., Porciani, M.C., et al. (2004) Myocardial perfusion imaging using gated SPECT in heart failure patients undergoing cardiac resynchronization therapy. **J Nucl Med**, 45: (2): 164-168.
- Smilde, T.D.J., Hillege, H.L., Voors, A.A., et al. (2004) Prognostic importance of renal function in patients with early heart failure and mild left ventricular dysfunction. **Am J Cardiol**, 94: (2): 240-243.
- Søgaard, P., Egeblad, H., Kim, W.Y., et al. (2002a) Tissue Doppler imaging predicts improved systolic performance and reversed left ventricular remodeling during long-term cardiac resynchronization therapy. **J Am Coll Cardiol**, 40: (4): 723-730.
- Søgaard, P., Egeblad, H., Pedersen, A.K., et al. (2002b) Sequential versus simultaneous biventricular resynchronization for severe heart failure: evaluation by tissue Doppler imaging. **Circulation**, 106: (16): 2078-2084.
- Søgaard, P., Kim, W.K., Jensen, H.K., et al. (2001) Impact of acute biventricular pacing on left ventricular performance and volumes in patients with severe heart failure. A tissue Doppler and three dimensional echocardiographic study. **Cardiology**, 95: (4): 173-182.
- Suffoletto, M.S., Dohi, K., Cannesson, M., et al. (2006) Novel Speckle-Tracking Radial Strain From Routine Black-and-White Echocardiographic Images to Quantify Dyssynchrony and Predict Response to Cardiac Resynchronization Therapy. **Circulation**, 113: (7): 960-968.
- Tecelao, S.R., Zwanenburg, J.J., Kuijper, J.P., et al. (2007) Quantitative comparison of 2D and 3D circumferential strain using MRI tagging in normal and LBBB hearts. **Magn Reson Med**, 57: (3): 485-493.
- Tedrow, U., Maisel, W., Epstein, L., et al. (2004) Feasibility of adjusting paced left ventricular activation by manipulating stimulus strength. **J Am Coll Cardiol**, 44: (11): 2249-2251.
- Thiele, H., Kappl, M.J.E., Conradi, S., et al. (2006) Reproducibility of Chronic and Acute Infarct Size Measurement by Delayed Enhancement-Magnetic Resonance Imaging. **J Am Coll Cardiol**, 47: (8): 1641-1645.
- Thomsen, H.S., Marckmann, P. and Logager, V.B. (2008) Update on Nephrogenic Systemic Fibrosis. **Magn Reson Imaging Clin N Am**, 16: (4): 551-560.
- Turner, M.S., Bleasdale, R.A., Mumford, C.E., et al. (2004) Left ventricular pacing improves haemodynamic variables in patients with heart failure with a normal QRS duration. **Heart**, 90: (5): 502-505.

- Uchiyama, T., Matsumoto, K., Suga, C., et al. (2005) QRS width does not reflect ventricular dyssynchrony in patients with heart failure. **J Artif Organs**, 8: (2): 100-103.
- Van de Veire, N., Bleeker, G., De Sutter, J., et al. (2007) Tissue synchronization imaging accurately measures left ventricular dyssynchrony and predicts response to cardiac resynchronization therapy. **Heart**, 93: (9): 1034-1039.
- Vanagt, W.Y., Verbeek, X.A., Delhaas, T., et al. (2005) Acute hemodynamic benefit of left ventricular apex pacing in children. **Ann Thorac Surg**, 79: (3): 932-936.
- Vanagt, W.Y., Verbeek, X.A., Delhaas, T., et al. (2004) The left ventricular apex is the optimal site for pediatric pacing: correlation with animal experience. **Pacing Clin Electrophysiol**, 27: (6 Pt 2): 837-843.
- Vonk-Noordegraaf, A., Marcus, J.T., Gan, C.T., et al. (2005) Interventricular mechanical asynchrony due to right ventricular pressure overload in pulmonary hypertension plays an important role in impaired left ventricular filling. **Chest**, 128: (6 Suppl): S628-630.
- Waldman, L.K. and Covell, J.W. (1987) Effects of ventricular pacing on finite deformation in canine left ventricles. **Am J Physiol**, 252: (5 Pt 2): H1023-1030.
- Waldman, L.K., Nosan, D., Villarreal, F., et al. (1988) Relation between transmural deformation and local myofiber direction in canine left ventricle. **Circ Res**, 63: (3): 550-562.
- Westenberg, J.J., Lamb, H.J., van der Geest, R.J., et al. (2006) Assessment of left ventricular dyssynchrony in patients with conduction delay and idiopathic dilated cardiomyopathy: head-to-head comparison between tissue Doppler imaging and velocity-encoded magnetic resonance imaging. **J Am Coll Cardiol**, 47: (10): 2042-2048.
- White, H.D., Norris, R.M., Brown, M.A., et al. (1987) Left ventricular end-systolic volume as the major determinant of survival after recovery from myocardial infarction. **Circulation**, 76: (1): 44-51.
- White, J.A., Yee, R., Yuan, X., et al. (2006) Delayed enhancement magnetic resonance imaging predicts response to cardiac resynchronization therapy in patients with intraventricular dyssynchrony. **J Am Coll Cardiol**, 48: (10): 1953-1960.
- Wikstrom, G., Lundqvist, C.B., Andren, B., et al. (2009) The effects of aetiology on outcome in patients treated with cardiac resynchronization therapy in the CARE-HF trial. **Eur Heart J**, 30: (7): 782-788.
- Williams, L.K., Ellery, S., Patel, K., et al. (2009) Short-Term Hemodynamic Effects of Cardiac Resynchronization Therapy in Patients With Heart Failure, a Narrow QRS Duration, and No Dyssynchrony. **Circulation**, 120: (17): 1687-1694.
- Xiao, H.B., Roy, C., Fujimoto, S., et al. (1996) Natural history of abnormal conduction and its relation to prognosis in patients with dilated cardiomyopathy. **Int J Cardiol**, 53: (2): 163-170.

- Xiao, H.B., Roy, C. and Gibson, D.G. (1994) Nature of ventricular activation in patients with dilated cardiomyopathy: evidence for bilateral bundle branch block. **Br Heart J**, 72: (2): 167-174.
- Young, J.B., Abraham, W.T., Smith, A.L., et al. (2003) Combined Cardiac Resynchronization and Implantable Cardioversion Defibrillation in Advanced Chronic Heart Failure: The MIRACLE ICD Trial. **JAMA**, 289: (20): 2685-2694.
- Ypenburg, C., Roes, S.D., Bleeker, G.B., et al. (2007a) Effect of total scar burden on contrast-enhanced magnetic resonance imaging on response to cardiac resynchronization therapy. **Am J Cardiol**, 99: (5): 657-660.
- Ypenburg, C., Schalij, M.J., Bleeker, G.B., et al. (2007b) Impact of viability and scar tissue on response to cardiac resynchronization therapy in ischaemic heart failure patients. **Eur Heart J**, 28: (1): 33-41.
- Ypenburg, C., van Bommel, R.J., Delgado, V., et al. (2008) Optimal Left Ventricular Lead Position Predicts Reverse Remodeling and Survival After Cardiac Resynchronization Therapy. **J Am Coll Cardiol**, 52: (17): 1402-1409.
- Yu, C.M., Abraham, W.T., Bax, J., et al. (2005a) Predictors of response to cardiac resynchronization therapy (PROSPECT)--study design. **Am Heart J**, 149: (4): 600-605.
- Yu, C.M., Bax, J.J. and Gorcsan III, J. (2009) Critical appraisal of methods to assess mechanical dyssynchrony. **Curr Opin Cardiol**, 24: (1): 18-28.
- Yu, C.M., Bax, J.J., Monaghan, M., et al. (2004a) Echocardiographic evaluation of cardiac dyssynchrony for predicting a favourable response to cardiac resynchronisation therapy. **Heart**, 90: (Suppl 6): 17-22.
- Yu, C.M., Bleeker, G.B., Fung, J.W., et al. (2005b) Left ventricular reverse remodeling but not clinical improvement predicts long-term survival after cardiac resynchronization therapy. **Circulation**, 112: (11): 1580-1586.
- Yu, C.M., Chan, Y.S., Zhang, Q., et al. (2006) Benefits of cardiac resynchronization therapy for heart failure patients with narrow QRS complexes and coexisting systolic asynchrony by echocardiography. **J Am Coll Cardiol**, 48: (11): 2251-2257.
- Yu, C.M., Chau, E., Sanderson, J.E., et al. (2002) Tissue Doppler echocardiographic evidence of reverse remodeling and improved synchronicity by simultaneously delaying regional contraction after biventricular pacing therapy in heart failure. **Circulation**, 105: (4): 438-445.
- Yu, C.M., Fung, J.W., Zhang, Q., et al. (2004b) Tissue Doppler imaging is superior to strain rate imaging and postsystolic shortening on the prediction of reverse remodeling in both ischemic and nonischemic heart failure after cardiac resynchronization therapy. **Circulation**, 110: (1): 66-73.

Yu, C.M., Fung, J.W.H., Zhang, Q., et al. (2005c) Improvement of Serum NT-ProBNP Predicts Improvement in Cardiac Function and Favorable Prognosis After Cardiac Resynchronization Therapy for Heart Failure. **J Card Fail**, 11: (5): S42-S46.

Yu, C.M., Fung, W.H., Lin, H., et al. (2003a) Predictors of left ventricular reverse remodeling after cardiac resynchronization therapy for heart failure secondary to idiopathic dilated or ischemic cardiomyopathy. **Am J Cardiol**, 91: ((6)): 684-688.

Yu, C.M., Lin, H., Zhang, Q., et al. (2003b) High prevalence of left ventricular systolic and diastolic asynchrony in patients with congestive heart failure and normal QRS duration. **Heart**, 89: 54-60.

Yu, C.M., Zhang, Q., Fung, J.W., et al. (2005c) A novel tool to assess systolic asynchrony and identify responders of cardiac resynchronization therapy by tissue synchronization imaging. **J Am Coll Cardiol**, 45: (5): 677-684.

Zhang, Q., Fung, J.W.H., Chan, J.Y.S., et al. (2009) Difference in long-term clinical outcome after cardiac resynchronisation therapy between ischaemic and non-ischaemic aetiologies of heart failure. **Heart**, 95: (2): 113-118.

Zhang, Y., Chan, A.K., Yu, C.M., et al. (2005) Strain rate imaging differentiates transmural from non-transmural myocardial infarction: a validation study using delayed-enhancement magnetic resonance imaging. **J Am Coll Cardiol**, 46: (5): 864-871.

Zwanenburg, J.J., Gotte, M.J., Marcus, J.T., et al. (2005) Propagation of onset and peak time of myocardial shortening in time of myocardial shortening in ischemic versus nonischemic cardiomyopathy: assessment by magnetic resonance imaging myocardial tagging. **J Am Coll Cardiol**, 46: (12): 2215-2222.